

**MSK Activity and H3 Phosphorylation Mediate Chromatin
Remodeling Required for Expression of Immediate-Early Genes**

by

Bojan Drobic

A Thesis submitted to the Faculty of Graduate Studies of

The University of Manitoba

in partial fulfilment of the requirements of the degree of

Doctor of Philosophy

Department of Biochemistry and Medical Genetics

University of Manitoba

Winnipeg, Manitoba, Canada

Copyright © 2010 by Bojan Drobic

ACKNOWLEDGEMENTS

I would like to thank my supervisor, Dr. Jim Davie for providing me with a great and exciting project. He has been a great source of advice and information throughout my Ph.D. studies. His enthusiastic support and guidance has provided a very rewarding experience during my graduate studies. An excellent professor and scientist, I am grateful to have had the opportunity to learn from one of the leaders in the chromatin field.

Also, I would like to thank all my committee members: Dr. David Eisenstat, Dr. Spencer Gibson and Dr. John Wilkins for helpful advice in regards to my project. They have been very supportive and their technical advice has pushed my project further.

I would like to thank all past and present members of Dr. Davie's lab for all the fun times in the lab. Specifically, I would like to acknowledge Paula Espino, who has helped me tremendously from the very beginning. She has truly enriched my experience in graduate studies. I feel fortunate for her friendship, humour and words of wisdom over the years. Also, I would like to thank Dr. Beatriz Pérez-Cadahía, who has worked very hard with me on a number of experiments that were included in this thesis. Her humor can cure any dull moment.

I am very grateful for the financial support from the CancerCare Manitoba Foundation and the National Cancer Institute of Canada.

Finally, I would like to thank my family and friends for providing endless sources of support over the years. Especially, my parents, Jasna and Vladimir, as well as my sister Vanja, who have been very supportive and encouraging over the course of my graduate studies.

TABLE OF CONTENTS

	Page
LIST OF FIGURES	iv
LIST OF COPYRIGHTED MATERIAL/OBTAINED PERMISSIONS.....	ix
ABBREVIATIONS	x
ABSTRACT.....	xvi
1.0 INTRODUCTION	1
1.1 Mitogen-activated protein kinase (MAPK) signal transduction pathways	1
1.1.1 Cellular signaling	1
1.1.2 MAPK signaling cascades	3
1.1.3 The RAS/RAF/ERK/MEK signaling cascade	3
1.1.4 RAS-MAPK signaling in human diseases/disorders	4
1.2 Chromatin: a dynamic substrate	7
1.2.1 Chromatin organization	7
1.2.2 The nucleosome	9
1.2.3 Chromatin modifications	12
1.3 Chromatin remodeling	13
1.3.1 ATP-dependent chromatin remodeling complexes	13
1.3.2 The mechanism of ATP-dependent chromatin remodeling	16
1.4 Histone post-translational modifications	20
1.4.1 Histone acetylation	24
1.4.2 Histone methylation	28
1.4.3 Histone phosphorylation	31
1.4.3.1 Histone H3 phosphorylation	32

1.4.3.2 Phosphorylation of histone H3 at Ser10/28 during mitosis/meiosis	33
1.4.3.3 Mitotic histone H3 Ser10/28 kinase and phosphatase	36
1.4.3.4 Phosphorylation of histone H3 at Ser10/28 during interphase	39
1.5 Mitogen- and stress-activated protein kinases 1 and 2 (MSK1/2).....	45
1.5.1 Activation of MSKs through signaling transduction pathways	46
1.5.2 MSK substrates	48
1.5.3 Function of MSKs	50
1.5.4 Physiological roles of MSKs	52
1.5.5 MSKs in immunity	53
1.5.6 MSKs and behaviour	54
1.5.7 MSKs in tumorigenesis	56
2.0 OBJECTIVES, RATIONALE AND HYPOTHESES	58
3.0 MATERIALS AND METHODS	60
3.1 Cell lines and cell culture conditions	60
3.2 Generation and maintenance of MSK1 stable knockdown mouse fibroblasts	61
3.3 Flow cytometric analysis of cells	62
3.4 Preparation of cellular extracts	62
3.5 Immunoprecipitations	62
3.6 Polyacrylamide gel electrophoresis (PAGE)	63
3.7 Detection of proteins by immunoblotting	64
3.8 Chromatin immunoprecipitation (ChIP/reChIP) assay	65
3.9 RNA isolation and real time RT-PCR analysis	67
3.10 H3 kinase assay	67
3.11 MSK1 kinase assay	68
3.12 Lysine acetyltransferase (KAT) assay	68

3.13 Cellular Fractionation	69
4.0 RESULTS	70
4.1 RAS-MAPK signaling is upregulated in <i>Hras</i> -transformed mouse fibroblasts	70
4.2 H3 kinase (MSK1) activity is elevated in <i>Hras</i> -transformed mouse fibroblasts	72
4.3 MSK1 cellular distribution in parental and <i>Hras</i> -transformed mouse fibroblasts	76
4.4 MSK1 associates with chromatin modifying/remodeling enzymes	77
4.5 MSK1 complex contains KAT activities	82
4.6 14-3-3-mediated MSK1 interactions with chromatin remodelers	86
4.7 RAS-MAPK-induced MSK1 recruitment and H3 modifications at the regulatory regions of IE genes in parental and <i>Hras</i> -transformed mouse fibroblasts.....	88
4.8 Recruitment of phospho-H3 binding proteins and chromatin remodeling/modifying enzymes to regulatory regions of IE genes in response to RAS-MAPK signaling	95
4.9 RAS-MAPK-induced formation of multi-protein complexes at the promoter regions of IE genes	97
4.10 The effect of MSK1 inhibition on IE gene transcriptional induction in response to RAS-MAPK signaling	99
4.11 The effect of H89 on the recruitment of MSK1, 14-3-3 isoforms, chromatin remodelers/modifiers, the resulting H3 modifications and transcription factors at the regulatory regions of IE genes	103
4.12 MSK1 regulates TPA-induced expression of <i>Jun</i> , <i>Cox-2</i> and <i>Fos11</i>	112
5.0 DISCUSSION	118
5.1 The activity of MSK1 is upregulated in <i>Hras</i> -transformed mouse fibroblasts	118
5.2 MSK1 associates with transcription factors, phospho-H3 binding proteins and chromatin modifying/remodeling enzymes	120

5.3 TPA-induced MSK1 recruitment is crucial for establishment of H3 modifications at regulatory regions of immediate-early genes	123
5.4 “Readers” of H3 phosphorylation marks are recruited to regulatory regions of IE genes in response to RAS-MAPK signaling	129
5.5 Chromatin modifying and remodeling enzymes are recruited to regulatory regions of IE genes in response to RAS-MAPK signaling	131
5.6 Recruitment of JUN transcription factor to regulatory regions of IE genes increases in response to RAS-MAPK signaling	133
5.7 MSK1 is important for the expression of IE genes in response to RAS-MAPK signaling	135
6.0 CONCLUSIONS	138
7.0 FUTURE DIRECTIONS	142
8.0 REFERENCES	144

LIST OF FIGURES

	Page
Figure 1: MAPK signaling cascades in mammalian cells	2
Figure 2: Schematic illustration of chromatin fiber condensation	8
Figure 3: Nucleosome core particle	10
Figure 4: Post-translational modifications of nucleosomal histones	21
Figure 5: Histone H3 phosphorylation sites and the known kinases/phosphatases	32
Figure 6: MSK1 activation	47
Figure 7: Increased levels of phosphorylated ERK1/2 in <i>Hras</i> -transformed mouse fibroblasts	71
Figure 8: Histone H3 kinase activity in parental and <i>Hras</i> -transformed mouse fibroblasts	72
Figure 9: MSK1 kinase activity in 10T1/2 and Ciras-3 mouse fibroblasts	74
Figure 10: MSK protein levels in parental and <i>Hras</i> -transformed mouse fibroblasts	75
Figure 11: Cellular distribution of MSK1 in 10T1/2 and Ciras-3 mouse fibroblasts	77
Figure 12: MSK1 association with chromatin modifying and remodeling enzymes	79
Figure 13: MSK1 association with chromatin remodelers, histone modifying enzymes, transcription factors and phospho-H3 binding proteins	80
Figure 14: Association of chromatin remodelers/modifiers, transcription factors and phospho-H3 binding proteins with MSK1	81
Figure 15: MSK1 protein complex contains lysine acetyltransferase (KAT) activity	83
Figure 16: Reverse-phase HPLC purification of individual histone proteins	84
Figure 17: MSK1-associated KAT activity has broad histone substrate specificity	85
Figure 18: MSK1-associated KAT activity is inhibited with curcumin	86

Figure 19: MSK1 associates with 14-3-3 proteins and BRG1 in parental mouse fibroblasts	87
Figure 20: Genomic structures of murine <i>Jun</i> , <i>Cox-2</i> and <i>Fos11</i> genes	89
Figure 21: The MNase-generated chromatin fragments are predominantly mononucleosomal	90
Figure 22: TPA-induced MSK1 recruitment at the <i>Jun</i> , <i>Cox-2</i> and <i>Fos11</i> regulatory regions in parental and <i>Hras</i> -transformed mouse fibroblasts	91
Figure 23: TPA-induced phosphorylation of H3 at Ser10 and Ser28 at the regulatory regions of <i>Jun</i> , <i>Cox-2</i> and <i>Fos11</i> in parental and <i>Hras</i> -transformed mouse fibroblasts.....	93
Figure 24: TPA-induced H3 acetylation and methylation along <i>Jun</i> , <i>Cox-2</i> and <i>Fos11</i> genes in parental and <i>Hras</i> -transformed mouse fibroblasts	94
Figure 25: TPA-induced recruitment of 14-3-3 proteins to regulatory regions of <i>Jun</i> , <i>Cox-2</i> and <i>Fos11</i> in parental and <i>Hras</i> -transformed mouse fibroblasts	96
Figure 26: TPA-induced recruitment of chromatin remodelers/modifiers to regulatory regions of <i>Jun</i> , <i>Cox-2</i> and <i>Fos11</i> in parental and <i>Hras</i> -transformed mouse fibroblasts	97
Figure 27: TPA-induced co-occupancy of MSK1, 14-3-3 proteins and chromatin remodelers/modifiers at the proximal regulatory regions of <i>Jun</i> , <i>Cox-2</i> and <i>Fos11</i>	99
Figure 28: H89 inhibits the TPA-induced expression of <i>Jun</i> , <i>Cox-2</i> and <i>Fos11</i> genes in parental and <i>Hras</i> -transformed mouse fibroblasts	101

Figure 29: H89 reduces the levels of TPA-induced RNAPII S5ph at proximal promoters of <i>Jun</i> , <i>Cox-2</i> and <i>FosII</i> in parental and <i>Hras</i> -transformed mouse fibroblasts.....	102
Figure 30: H89 has no effect on the levels of RNAPII S5ph in 10T1/2 and Ciras-3 cells	102
Figure 31: H89 inhibits TPA-induced nucleosomal response and chromatin remodeler/modifier recruitment to 5' proximal regulatory regions of <i>Jun</i> , <i>Cox-2</i> and <i>FosII</i> in parental mouse fibroblasts	105
Figure 32: H89 inhibits TPA-induced nucleosomal response and chromatin remodeler/modifier recruitment to 5' proximal regulatory regions of <i>Jun</i> , <i>Cox-2</i> and <i>FosII</i> in <i>Hras</i> -transformed mouse fibroblasts	106
Figure 33: H89 reduces TPA-induced H3 methylation at regulatory regions of <i>Jun</i> , <i>Cox-2</i> and <i>FosII</i> in parental and <i>Hras</i> -transformed mouse fibroblasts	107
Figure 34: H89 inhibits TPA-induced nucleosomal response and chromatin remodeler/modifier recruitment to 5' distal regulatory regions of <i>Jun</i> , <i>Cox-2</i> and <i>FosII</i> in parental mouse fibroblasts	108
Figure 35: H89 inhibits TPA-induced nucleosomal response and chromatin remodeler/modifier recruitment to 5' distal regulatory regions of <i>Jun</i> , <i>Cox-2</i> and <i>FosII</i> in <i>Hras</i> -transformed mouse fibroblasts	109
Figure 36: H89 abolishes TPA-induced recruitment of JUN to regulatory regions of <i>Jun</i> , <i>Cox-2</i> and <i>FosII</i> in parental and <i>Hras</i> -transformed mouse fibroblasts	110
Figure 37: H89 has no effect on MSK1 association with BRG1 and 14-3-3 ζ	111
Figure 38: MSK1 knockdown in parental and <i>Hras</i> -transformed mouse fibroblasts	112

Figure 39: MSK1 knockdown reduces TPA-induced expression of <i>Jun</i> , <i>Cox-2</i> and <i>FosII</i> in parental and <i>Hras</i> -transformed mouse fibroblasts	113
Figure 40: Protein levels of COX-2, FRA-1 and JUN are elevated in <i>Hras</i> -transformed mouse fibroblasts	115
Figure 41: MSK1 is required for the TPA-induced nucleosomal response	117
Figure 42: Schematic model representing the role of MSK1 and 14-3-3 in IE gene remodeling and induction in response to MAPK signaling	141

LIST OF COPYRIGHTED MATERIAL FOR WHICH PERMISSION WAS OBTAINED

	Page
MAPK signaling cascades in mammalian cells (Figure 1) reproduced with permission (Elsevier) from Gerits, N., <i>et al.</i> (2008). Relations between the mitogen-activated protein kinase and the cAMP-dependent protein kinase pathways: comradeship and hostility. <i>Cell Signal</i> 20, 1592-1607.	2
Schematic illustration of chromatin fiber condensation (Figure 2) reproduced with permission (Annual Reviews, Inc.) from Hansen, J.C. (2002). Conformational dynamics of the chromatin fiber in solution: determinants, mechanisms, and functions. <i>Annu Rev Biophys Biomol Struct</i> 31, 361-392.	8
Nucleosome core particle (Figure 3) reproduced with permission (Nature Publishing Group) from Luger, K., Mader, A.W., Richmond, R.K., Sargent, D.F., and Richmond, T.J. (1997). Crystal structure of the nucleosome core particle at 2.8 Å resolution. <i>Nature</i> 389, 251-260.	10
Post-translational modifications of nucleosomal histones (Figure 4) reproduced with permission (Nature Publishing Group) from Bhaumik, S.R., Smith, E., and Shilatifard, A. (2007). Covalent modifications of histones during development and disease pathogenesis. <i>Nat Struct Mol Biol</i> 14, 1008-1016.	21
MSK1 activation (Figure 6) reproduced with permission (Portland Press Ltd.) from McCoy, C.E., Macdonald, A., Morrice, N.A., Campbell, D.G., Deak, M., Toth, R., McIlrath, J., and Arthur, J.S. (2007). Identification of novel phosphorylation sites in MSK1 by precursor ion scanning MS. <i>Biochem J</i> 402, 491-501.	47

ABBREVIATIONS

A260	Absorbance at 260 nm
ACF	ATP-dependent chromatin assembly and remodeling factor
ADP	Adenosine diphosphate
α -MEM	Alpha-minimal essential medium
AP-1	Activator protein-1
ATP	Adenosine triphosphate
ATF1	Activating transcription factor-1
BAF155/170	BRG1/BRM-associated factor-155/170
BMK1	Big MAP kinase-1
bp	Base pair
BPTF	Bromodomain and PHD finger-containing transcription factor
BRM	Brahma
BRG1	Brahma-related gene-1
CARM1	Coactivator-associated arginine methyltransferase-1
CBP	CREB-binding protein
cDNA	Complementary deoxyribonucleic acid
C/EBP	CCAAT/Enhancer-binding protein
CHD1	Chromodomain helicase DNA binding protein-1
ChIP	Chromatin immunoprecipitation

CHRAC	Chromatin accessibility complex
COMPASS	Complex proteins associated with SET1
COX-2	Cyclooxygenase-2
CREB	cAMP response element-binding protein
DMEM	Dulbecco's modified eagle medium
DNA	Deoxyribonucleic acid
EDTA	(Ethylenedinitrilo) tetraacetic acid
EGTA	[Ethylenebis (oxyethylenitrilo)] tetraacetic acid
EGF	Epidermal growth factor
EHMT2	Euchromatic histone-lysine N-methyltransferase-2
eIF-4F	Eukaryotic translation initiation factor 4F
EKLF	Erythroid Kruppel-like factor
ELP3	Elongator protein-3
ERK	Extracellular signal-regulated kinase
ESET	ERG-associated protein with a SET domain
ETS	E-twenty six, transcription factor
EZH2	Enhancer of zeste homolog-2
FBS	Fetal bovine serum
FGF	Fibroblast growth factor
FRA-1	Fos-related antigen-1

GAP	GTPase activating protein
GCN5	General control nonderepressible-5
GDP	Guanine nucleotide diphosphate
GEF	Guanine nucleotide exchange factor
GLC7	GLyCogen-7
GRB2	Growth factor receptor binding protein-2
GTP	Guanine nucleotide triphosphate
H89	N-[2-[[3-(4-Bromophenyl)-2-propenyl]amino]ethyl]-5-isoquinolinesulfonamide dihydrochloride
HDAC1	Histone deacetylase-1
HMGN1	High mobility group nucleosomal binding domain-1
HP1	Heterochromatin protein-1
IE	Immediate-early
IFN- α	Interferon-alpha
IKK- α	IkappaB kinase-alpha
ING2	Inhibitor of growth family, member 2
IPL1	Increase in ploidy-1
ISWI	Imitation switch
JMJD2A	Jumonji domain containing 2A demethylase
JNK1/2/3	c-Jun N-terminal kinase-1/2/3
KAT	Lysine acetyltransferase

LSD1	Lysine-specific histone demethylase-1
MAP	Mitogen-activated protein
MAPK	Mitogen-activated protein kinase
MBT	Malignant brain tumor repeat/domain
MEF2	Myocyte enhancer factor-2
MEK1/2/5	MAP/ERK kinase-1/2/5
Min.	Minutes
MKK3/4/6/7	MAPK kinase-3/4/6/7
MLL	Mixed lineage leukemia-protein complex
MMLV	Moloney Murine Leukemia Virus
MNase	Micrococcal nuclease
MSK1/2	Mitogen- and stress-activated protein kinase-1/2
MST1	Mammalian Sterile20-like 1 kinase
MYST	MOZ, Ybf2/Sas3, Sas2 and TIP60
NGF	Nerve growth factor
NuRD	Nucleosome remodeling and deacetylase repressor
NURF	Nucleosome-remodeling factor
PAGE	Polyacrylamide gel electrophoresis
PBS	Phosphate buffered saline
PCAF	p300/CBP-associated factor

PCR	Polymerase chain reaction
PHD	Plant homeodomain
PKA	Protein kinase A
PKB	Protein kinase B
PKC	Protein kinase C
PP1	Protein phosphatase type 1
PP2	Protein phosphatase type 2
PRMT1	Protein arginine methyltransferase-1
PTM	Post-translational modification
RAR	Retinoic acid receptor
RB	Retinoblastoma protein
RNA	Ribonucleic acid
RNase	Ribonuclease
RT	Reverse transcriptase
SAPK2	Stress-activated protein kinase-2
SDC	Sodium deoxycholate
SDS	Sodium dodecyl sulfate
SET1	Suppressor of variegation, enhancer of zeste and trithorax-1
SET2	Suppressor of variegation, enhancer of zeste and trithorax-2
SOS	Son of sevenless

Sp1/Sp3	Specificity protein 1/3
SUC2	Sucrase-2 gene (yeast)
SUMO	Small ubiquitin-like modifier
SUV39H1/2	Suppressor of variegation 3-9 homolog-1/2
STAT3	Signal transducer and activator of transcription-3
SWI/SNF	Switch/sucrose non-fermentable
TBP	TATA-binding protein
TE	Tris-EDTA
TEMED	N,N,N',N-tetramethylethylenediamine
TIP60	Tat-interactive protein
TGF- β	Transforming growth factor-beta
TNF- α	Tumor necrosis factor-alpha
TNM	Tris-NaCl-MgCl ₂ buffer
TPA	12-tetradecanoate 13-acetate
Tris	Tris(hydroxymethyl)aminomethane
TBS	Tris buffered saline
TTBS	Tris buffered saline with Tween-20
VEGF-A	Vascular endothelial growth factor-A

ABSTRACT

Normal cellular behaviour in multicellular organisms is achieved by tight control of signaling pathway networks. The mitogen-activated protein kinase (MAPK) signaling cascade is one of these signaling networks, that when deregulated can lead to cellular transformation. Activation of the RAS-RAF-MEK-MAPK (ERK) signal transduction pathway or the SAPK2/p38 pathway results in the activation of mitogen- and stress-activated protein kinases 1 and 2 (MSK1/2). Subsequently, MSKs go on to phosphorylate histone H3 at Ser10 and Ser28. Here, we demonstrate that the activities of ERK and MSK1, but not p38, are elevated in *Hras*-transformed cells (Ciras-3) relative to these activities in the parental 10T1/2 cells. Analyses of the subcellular distribution of MSK1 showed that the H3 kinase was similarly distributed in Ciras-3 and 10T1/2 cells, with most MSK1 being present in the nucleus. In contrast to many other chromatin modifying enzymes, MSK1 was loosely bound in the nucleus and was not a component of the nuclear matrix. Our results provide evidence that oncogene-mediated activation of the RAS-MAPK signal transduction pathway elevates the activity of MSK1, resulting in the increased steady-state levels of phosphorylated H3, which may contribute to the chromatin decondensation and aberrant gene expression observed in oncogene-transformed cells.

Furthermore, upon activation of the ERK and p38 MAPK pathways, the MSK1/2-mediated nucleosomal response, including H3 phosphorylation at serine 28 or 10, is coupled with the induction of immediate-early gene transcription. The outcome of this response, varying with the stimuli and cellular contexts, ranges from neoplastic transformation to neuronal synaptic plasticity. Here, we used sequential co-immunoprecipitation assays and chromatin immunoprecipitation (ChIP) assays on mouse fibroblast 10T1/2, Ciras-3 and MSK1 knockdown 10T1/2 cells to show that H3 serine 28 and 10 phosphorylation leads to promoter remodeling.

MSK1, in complexes with phospho-serine adaptor 14-3-3 proteins and BRG1 (the ATPase subunit of the SWI/SNF remodeler) is recruited to the promoter of target genes by transcription factors such as ELK-1 or NFκB. Following MSK1-mediated H3 phosphorylation, BRG1 associates with the promoter of target genes via 14-3-3 proteins, which act as scaffolds. The recruited SWI/SNF remodels nucleosomes at the promoter of immediate-early genes enabling the binding of transcription factors like JUN and the onset of transcription. Since RAS-MAPK activated MSKs mediate H3 phosphorylation that is required for expression of various immediate-early gene products involved in cellular transformation, inhibition of MSK activity may be a therapeutic target that could be exploited in cancers with upregulated RAS-MAPK signaling.

1.0 INTRODUCTION

1.1 Mitogen-activated protein kinase (MAPK) signal transduction pathways

1.1.1 Cellular signaling

An essential way that guarantees harmonious functioning of cells in a multi-cellular organism lies in the ability of cells to properly communicate with each other. Communication at a cellular level occurs by exchanging signals that bind specifically to surface or intracellular receptors. Merging of a signal to its receptor results in a cascade of events that amplifies and transmits the incoming signal. This signal transduction requires the orchestrated action of protein kinases, which by sequential phosphorylation events enable conduction and ultimately translation of the signal into a cellular response. Since cells are constantly exposed to environmental signals, various signaling networks within the cells have evolved to allow for appropriate distribution of the incoming signals in order to control gene expression, cell growth, motility, differentiation, survival and apoptosis. Alterations in cellular signaling caused by mutations and/or abnormal activities of the signaling proteins are underlying causes of numerous human diseases, including cancer. Therefore, major experimental focus has been put forward on deciphering the molecular mechanisms of altered signaling cascades that lead to abnormal cellular phenotypes.

1.1.2 MAPK signaling cascades

Mitogen-activated protein kinase (MAPK) signaling pathways are among the most widely used mechanisms of eukaryotic cell regulation (Krishna and Narang, 2008). MAPKs are a conserved family of protein kinases that respond to a plethora of stimuli (Edmunds and Mahadevan, 2004). These enzymes are activated by MAPK kinases

(MAPKKs), which in turn are activated by MAPKK kinases (MAPKKKs), proteins that are linked to cell-surface receptor activation. MAPKs exert their effects via phosphorylation, thus these kinases can activate or inactivate a spectrum of either cytosolic or nuclear protein substrates, such as specific enzymes, transcription factors, cytoskeletal proteins and downstream signaling proteins. In mammals, four groups of MAPKs have been well characterized: extracellular regulated kinases (ERK1 and ERK2), Jun N-terminal kinases (JNK1, JNK2 and JNK3), p38 kinases (p38 $\alpha/\beta/\gamma/\delta$) and Big MAP kinase 1 (BMK1) or ERK5 (Figure 1).

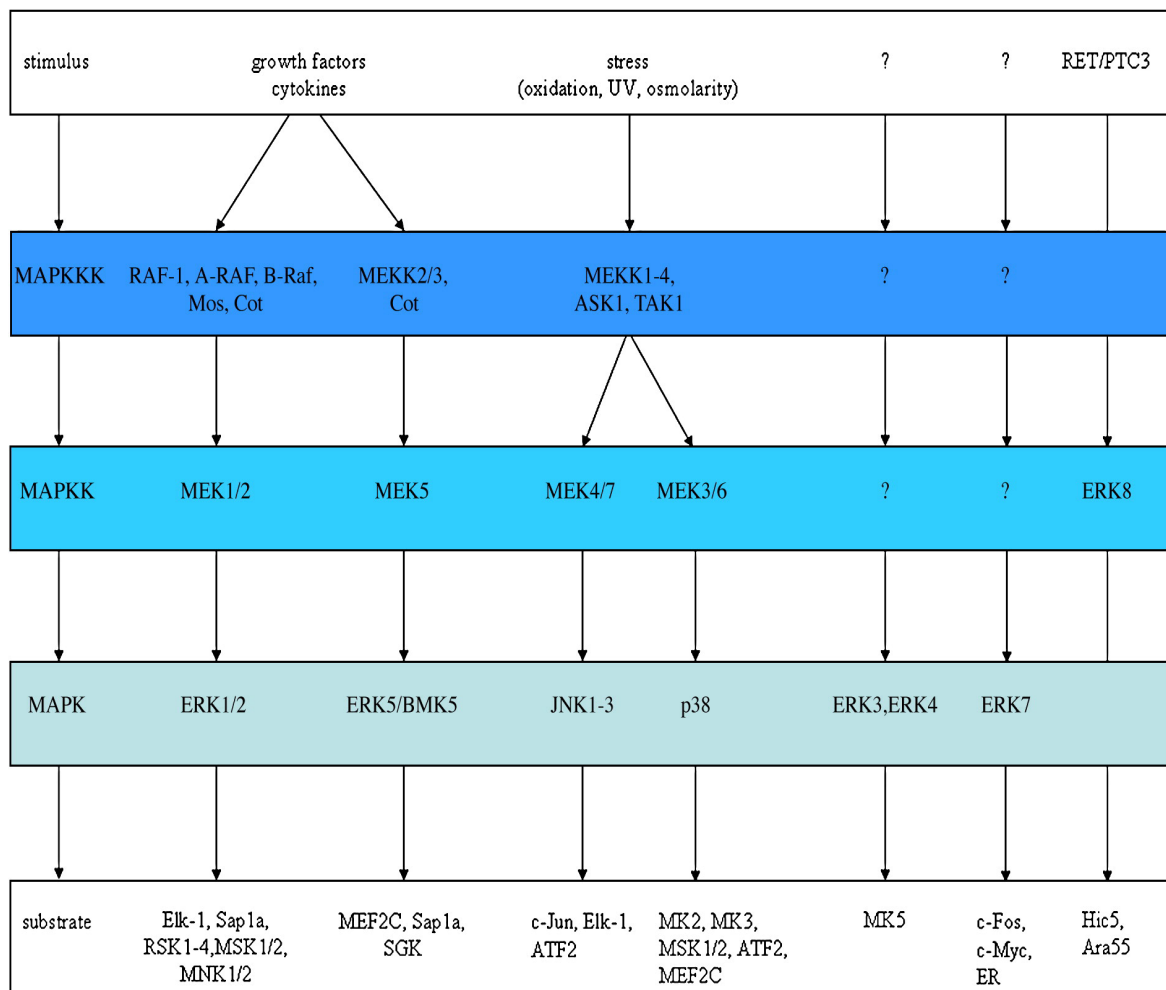


Figure 1: MAPK signaling cascades in mammalian cells.

The typical MAPK pathway consists of a tripartite module in which a MAPKKK phosphorylates a MAPKK, which in turn phosphorylates a MAPK. The nature of the signals that activates the different MAPK cascades is shown at the top of the figure, while some of the substrates are indicated at the bottom of the figure. *The text and the figure were reproduced with permission from (Gerits et al., 2008).*

These are activated by specific upstream MAPKKs: MEK1/2, MKK3/6, MKK4/7 and MEK5, respectively (Krishna and Narang, 2008). There are two additional MAPK groups, namely ERK3/4 and ERK7/8; however, these are atypical MAPKs that have not been extensively defined (Raman et al., 2007).

1.1.3 The RAS/RAF/ERK/MEK signaling cascade

One of the most studied signaling pathways is the ERK/MEK cascade. Numerous stimuli can activate this cascade, including growth factors, mitogens and tumor promoting phorbol esters. The RAS-MAPK pathway can be initiated by ligand-bound growth factor receptor tyrosine kinase activation via intrinsic tyrosine kinase activity and subsequent receptor dimerisation (Pearson et al., 2001). The SH2-domain containing proteins (e.g. GRB2) are then recruited to the receptor and bind to specific phosphotyrosine residues. GRB2 protein is constitutively bound to an effector kinase activator, termed SOS and is usually localized to the cytoplasm (Rajalingam et al., 2007). Re-localization of GRB2 activates SOS, which in turn activates a small guanine nucleotide binding protein, p21 RAS. The RAS proteins belong to a family of small guanine nucleotide binding proteins (G-proteins) that are activated when GTP-bound and inactivated when GDP-bound (Mitin et al., 2005). Two different classes of proteins control the activity of RAS proteins: GTPase activating proteins (GAPs) and guanine nucleotide exchange factors (GEFs). RAS GAP proteins reduce the pool of GTP-bound

RAS molecules by increasing the intrinsic GTPase activity of RAS. Therefore, GAPs act as “off” switches and reduce RAS activity. In contrast, GEFs facilitate the exchange of GDP for GTP, increasing the activity of RAS (Mitin et al., 2005). Three isoforms of RAS exist in mammals, namely H-RAS, K-RAS and N-RAS. At the C-terminal domains, RAS proteins contain a CAAX motif, in which cysteine is followed by two aliphatic amino acids (A) and any other amino acid (X). This motif is farnesylated by farnesyl transferase, causing RAS to be localized to both the plasma and internal membranes (Mor and Philips, 2006). Activated GTP-RAS recruits RAF kinase to the membrane where RAF catalyzes phosphorylation and activation of MEK1 and MEK2, which in turn are responsible for activation of ERK1 and ERK2 (Roux and Blenis, 2004). Once activated, ERKs dimerise and can translocate into the nucleus to phosphorylate various transcription factors, including ELK-1, c-FOS, c-MYC and STAT3 (Raman et al., 2007). ERKs can also be retained in the cytoplasm where they can phosphorylate numerous substrates in multiple compartments (Roux and Blenis, 2004).

1.1.4 RAS-MAPK signaling in human diseases/disorders

The MAPK signaling pathway is important for organismal development and has been elucidated through various genetic and biochemical approaches over the past several decades. RAS proteins are involved in mediating MAPK pathway signaling and have been shown to be critical for normal cell growth (Aoki et al., 2008). The three RAS isoforms share 85% amino acid sequence identity, with K-RAS being expressed in all cell types. Mouse knockout studies have shown that *Kras* is essential for development, whereas *Nras* and *Hras* are not required (Johnson et al., 1997). It has been shown that in *Hras*-transformed cells, the RAS-MAPK signaling is enhanced, contributing to aberrant

features of oncogene-transformed cells (Chadee et al., 1999; Drobic et al., 2004). Further, the importance of RAS-MAPK pathway in neoplasms was emphasized with the discovery of mutant alleles that hyperactivate the pathway in numerous human cancers. Mutations in receptor tyrosine kinases abnormally activate RAS and its downstream substrates (Gschwind et al., 2004). Also, activating point mutations in *RAS* genes have been observed in up to 30% of human tumors (Downward, 2003), the prevalence being the highest in adenocarcinoma of the pancreas (90%), colon (50%), thyroid (50%), lung (30%) and melanoma (25%) (Malumbres and Barbacid, 2003). These activating mutations occur in exons 12, 13 and 61 and significantly decrease intrinsic RAS GTPase activity, thereby rendering RAS in the GTP-bound active state. The most frequent mutations are found in *K-RAS* (~ 85%), less in *N-RAS* (~ 15%) and the least in *H-RAS* (~ 1%) (Aoki et al., 2008). Interestingly, each of the *RAS* family members is mutated in a specific subset of human malignancies: *K-RAS* is frequently mutated in epithelial cancers of the pancreas, lung and colon; *N-RAS* mutations are often present in melanoma, liver and myeloid malignancies and *H-RAS* mutations have been found in bladder cancers (Downward, 2003). Furthermore, deregulation of RAS-MAPK signaling observed in various cancers can be achieved through alterations in other components of the cascade. For example, activating mutations in *B-RAF*, a member of the *RAF* family of genes encoding effector kinases, have been observed with a high frequency in melanoma and to a lesser extent in thyroid, ovarian and colon cancers (Brose et al., 2002). Single amino acid substitutions are sufficient to promote the active B-RAF conformation, thereby constitutively activating the MAPK pathway. The loss of negative regulators of the RAS-MAPK signaling, such as GAPs, can indirectly hyperactivate the RAS-MAPK signaling

cascade (Downward, 2003). In addition, RAS-MAPK signaling is active in tumors that have overexpressed growth factor receptor tyrosine kinases, such as epidermal growth factor receptor (EGFR) and human epidermal growth factor receptor 2 (HER2) (Mendelsohn and Baselga, 2000). It is suggested that most human tumors display deregulation of RAS-MAPK signaling (Aoki et al., 2008), making this pathway an attractive target for therapeutic intervention.

It is important to note that carcinogenesis is a multi-step phenomenon, requiring not only mutations in oncogenes, but also mutations in the other components of cellular signaling. A mutation in an oncogene (e.g. *RAS*), along with an inactivating mutation of a tumor suppressor gene (e.g. *TP53*) and a DNA damage repair gene (e.g. *MLH1*) can lead to an enhancement of the pre-cancerous cell's ability to adapt to its microenvironment and eventually can lead towards uncontrolled malignant phenotype observed in human cancers (Rieger, 2004).

Germline mutations in the components of RAS-MAPK signaling cascade have been reported to cause several human disorders. It has been known for some time that inactivating mutations in *NF1* gene are responsible for neurofibromatosis type 1 (Legius et al., 1993). NF1 protein contains GAP related domain that regulates RAS through activation of RAS GTPase, Neurofibromin. *NF1* mutations disturb this GAP activity of Neurofibromin resulting in more active RAS and increased signaling through the RAS-MAPK pathway (Denayer et al., 2008). Furthermore, a study in 2005 described *de novo* heterozygous missense mutations of *HRAS* in patients with Costello syndrome, which illustrated for the first time that germline mutations of oncogenic *RAS* family member were responsible for a human disorder (Aoki et al., 2005). Mutations in *RAF1* (or *CRAF*),

a *RAF* isoform not usually mutated in human cancers, are found in patients with Noonan and LEOPARD syndromes (Pandit et al., 2007). All of the above mentioned disorders share a variable degree of mental retardation or learning disabilities, cardiac defects, facial dysmorphism, short stature and skin abnormalities. Moreover, an increased risk for malignancy has been described in these patients. The significant phenotypical overlap between these disorders is now attributed by the common deregulation of RAS-MAPK signaling pathway (Denayer et al., 2008).

1.2 Chromatin: a dynamic substrate

Signaling cascades control important biological outcomes through alterations of chromatin structure within the nucleus of the cell. Initiation of RAS-MAPK signaling activates various downstream kinases and enzymes that ultimately converge on specific nuclear substrates that affect the state of chromatin (Davie et al., 1999). Therefore, the chromatin architecture dynamically responds to cellular signaling and is involved in various cellular events, including replication, recombination, repair and gene expression. Eukaryotic chromatin is a physiological substrate that is necessary for proper interpretation of the DNA code; therefore it is an integral determinant of normal cellular functioning.

1.2.1 Chromatin organization

The enormous amount of genetic information that is contained in the nucleus of cells is integrated into a highly organized structure, termed chromatin. This nucleoprotein complex, consisting of DNA, histones and non-histone proteins functions as a physiological template of all eukaryotic genetic information (Figure 2).

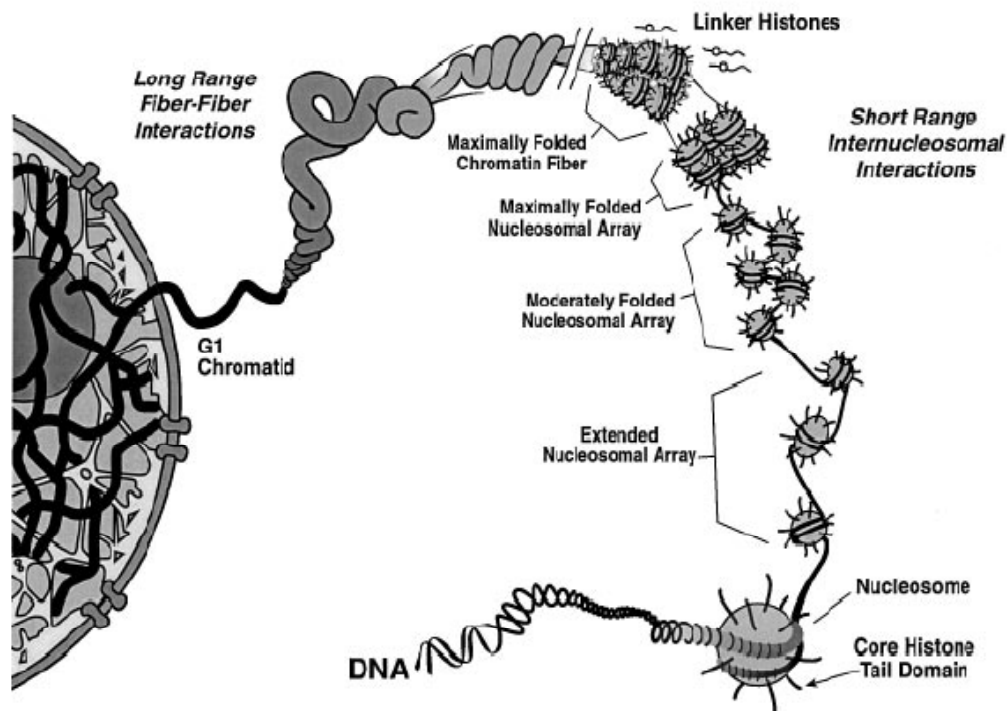


Figure 2: Schematic illustration of chromatin fiber condensation.

Shown are the steps involved in the folding of extended nucleosomal arrays into maximally folded chromatin fibers. The functional roles of the core histone tail domains and linker histones are discussed in the text. *The text and the figure were reproduced with permission from (Hansen, 2002).*

From mitosis to regulated gene expression, chromatin acts as a flexible structure necessary for proper functioning of the genome. Chromatin can be characterized into two main states: heterochromatin, which is densely compacted, inaccessible and for the most part, transcriptionally inert (Trojer and Reinberg, 2007) and euchromatin, which is decondensed, accessible and transcriptionally active (Jenuwein and Allis, 2001). Interplay between the different chromatin states dictates the biological outcomes at a cellular level; therefore, alterations of chromatin via chromatin remodeling and/or histone modifications play an important role in eukaryotic function.

1.2.2 The nucleosome

The basic repeating unit of chromatin is the nucleosome, consisting of 146 base pairs of DNA sharply bent and tightly wrapped approximately 1.65 times around a histone octamer (Luger et al., 1997). The histone octamer itself is composed of four core histone proteins, H2A, H2B, H3 and H4 (Figure 3). The octamer is organized as a (H3-H4)₂ tetramer with two H2A-H2B dimers located on both sides of the tetramer (Davie and Spencer, 2001). The core histone proteins contain a basic unstructured N-terminal domain, a globular histone fold domain, which mediates histone-histone and histone-DNA interactions, and a C-terminal unstructured tail (Luger et al., 1997). Sharp DNA bending has been found to occur at every helical turn (~ 10 base pairs) when the major groove of the DNA faces inwards towards the histone octamer and again ~ 5 base pairs away, with the opposite direction when the major groove faces outwards (Richmond and Davey, 2003). Neighbouring nucleosomes are separated by 10-50 base pairs of unwrapped linker DNA, that a fifth class of histone proteins (H1) can bind in order to connect the proximal nucleosomes (Davie et al., 1999). Histone H1 proteins differ in their structure when compared to core histones; H1 proteins have a tripartite structure composed of a central globular domain and lysine-rich N- and C-terminal domains (Davie and Spencer, 2001).



Figure 3: Nucleosome core particle.

Ribbon traces for the 146-bp DNA phosphodiester backbones (brown and turquoise) and eight histone protein main chains are shown (blue: H3; green: H4; yellow: H2A; red: H2B). The views are down the DNA superhelix axis for the left particle and perpendicular to it for the right particle. For both particles, the pseudo-twofold axis is aligned vertically with the DNA centre at the top. *The text and the figure were reproduced with permission from (Luger et al., 1997).*

The nucleosome core particles connected via histone H1 proteins and other chromatin-associated proteins can be further folded, resulting in a dense, relatively inaccessible, highly compact arrangement, referred to as higher order chromatin structure (Figure 2).

The N-terminal tails of histones emanate from the nucleosome (Rhodes, 1997) and it has been shown that H1 and the N-terminal tails of core histones stabilize higher order compacted chromatin fibers (Davie et al., 1999). It has been shown that the N-terminal histone tails undergo an induced folding when in contact with other proteins or DNA, therefore these inter- and intra-chromatin fiber interactions could mediate higher order folding of the chromatin (Richmond and Davey, 2003). The DNA within the nucleosome

core particle is relatively inaccessible to most regulatory protein complexes; yet specific proteins that either remodel or covalently modify the nucleosome can be recruited to the chromatin core particle via interactions with the core histone tails (Jenuwein and Allis, 2001). Modifications of core histone N-terminal tails may affect the tail folding and interactions with other proteins or DNA, destabilizing the nucleosome structure and ultimately the higher order chromatin architecture (Hayes et al., 1991); (Davie et al., 1999). Histone-DNA interactions within the nucleosome core particle are formed by hydrogen bonding of the histone main chain amide and the phosphate oxygen of the DNA. These bonds are reinforced by electrostatic interactions between the basic side chains and negatively charged phosphate groups and other nonpolar interactions (Davey et al., 2002). Theoretically, these interactions may allow formation of a nucleosome at any given DNA sequence; however, there might be an underlying sequence specificity in regard to nucleosomal positioning along DNA (Mellor, 2005). The nature of the DNA sequence wrapped around the histone octamer may be an important determinant of the nucleosome dynamics under the influence of ATP-dependent chromatin remodeling complexes, histone modifying enzymes and sequence-specific transcription factors (Vicent et al., 2004). Thus, the alterations of nucleosome structural features may have crucial inhibitory or permissive roles in regulating molecular events, such as gene expression.

1.2.3 Chromatin modifications

Experimental advances in the field of chromatin biology have unraveled many details regarding the organization of the core histone proteins within the nucleosome core particle, as well as the characterization of various enzymatic activities that influence chromatin structure. As previously mentioned, packaging of genomic DNA into chromatin represents a major obstacle for DNA binding proteins, this also being true for chromatin and histone modifying enzymes (Berger, 2007). There are three main categories of chromatin modifying enzymes: histone modifying enzymes, which covalently acetylate, phosphorylate, methylate or ubiquitinate histone proteins; DNA modifying enzymes that methylate CpG-rich sequences and ATP-dependent chromatin remodeling enzymes that physically disrupt histone-DNA contacts within the nucleosome to allow access of regulatory enzymes to DNA sequences and histones. Interestingly, a number of histone modifications exist on the nucleosome lateral surface, implying that the histone modifying enzymes are working in concert with ATP-dependent remodeling complexes in order to modify these residues (Cosgrove et al., 2004). The presence of histone modifications on the lateral surface of the nucleosome indicates that these modifications could play a direct role in modulating histone-DNA contacts within the nucleosome, thereby influencing the stability of nucleosome positioning and the ease with which the nucleosome could be translocated along DNA (Cosgrove et al., 2004), therefore significantly affecting various molecular processes.

1.3 Chromatin remodeling

Since chromatin presents a barrier to processes involving DNA, eukaryotic cells rely on multiple mechanisms to regulate the compaction state of chromatin. When specific regulatory proteins (e.g. transcription factors) are not able to bind to their specific sequences due to steric hindrance of histones or when torsional stress induced by RNA polymerase is not enough to displace nucleosomes, the action of chromatin remodeling complexes can contribute to the disruption of DNA-histone contacts within the nucleosome (Cosgrove et al., 2004). These disruptions can alter nucleosomal DNA accessibility, enhancing or restricting the ability of regulatory proteins to associate with necessary components that influence transformation of chromatin from a nonpermissive repressed state into a more open or transcriptionally active conformation, or vice versa (Racki and Narlikar, 2008). Furthermore, chromatin-remodeling factors are required to counteract the repressive nature of chromatin by displacing individual or multiple core histones (Whitehouse et al., 1999). The mode of action of the chromatin remodeling complexes is intricately associated with hydrolysis of ATP. The result of the remodeling is alteration in the structure and/or position of nucleosomes within the chromatin, through dissociation, sliding or relocation of individual nucleosomes (Langst et al., 1999); (Hamiche et al., 1999); (Lorch et al., 1999). Furthermore, the chromatin remodeling complexes have the ability to modulate single nucleosome stability in response to external stimuli; therefore, these remodeling factors can ultimately be considered as potent regulators of both nucleosome distribution and regulation of chromatin fluidity (Simone, 2006).

1.3.1 ATP-dependent chromatin remodeling complexes

The two best-characterized classes of chromatin remodeling complexes are the SWI/SNF- and ISWI-based families. The SWI/SNF complex is evolutionarily conserved and was first discovered in yeast (Racki and Narlikar, 2008). The individual subunits of yeast SWI/SNF were originally identified through two screens. The first screen was for mutants with faulty mating-type switching (SWI) because of the defective transcriptional activation of a gene that encodes for an endonuclease that initiates the switching process. The second screen was for mutants that were unable to grow on sucrose because of defective *SUC2* gene transcription (sucrose non-fermenting/SNF) (Winston and Carlson, 1992). Various genes were identified from both screens, designated as SWI or SNF, and ultimately it was determined that many of those genes were members of a multiprotein complex, later termed the SWI/SNF complex (Peterson et al., 1994). Further, the proteins within the SWI/SNF complex were shown to enhance transcriptional activation of numerous genes in response to various extracellular cues (Hirschhorn et al., 1992). Conserved complexes in *Drosophila* (Brahma) and human (hSWI/SNF) were also identified (Kwon et al., 1994). The critical subunit in the SWI/SNF complex is the SWI2/SNF2 motor subunit (e.g. BRG1, BRM), which has the ATPase/helicase motif and possesses chromatin-remodeling activity in the absence of other subunits (Phelan et al., 1999). This subunit also contains additional structural motifs that provide other functions. Firstly, SWI2/SNF2 and its homologues all harbor a bromo-domain, which can bind acetylated histone tails (Dhalluin et al, 1999). Such binding to histone tails could stabilize and retain the SWI/SNF complex on acetylated nucleosomes near promoters, an event important for transcriptional activation (Hassan et al., 2001b). Secondly,

SWI2/SNF2 homologues contain a DNA binding region homologous to AT-hooks present in high mobility-group I/Y binding domains. This motif can bind DNA in the minor groove, with a certain preference for AT-rich sequences (Hassan et al., 2001a). In mammalian systems, this region is important for tethering of BRM to chromatin (Bourachot et al, 1999). Thirdly, SWI2/SNF2 homologues contain regions that directly interact with transcription factors. BRG1 contains regions that interact with RB and HDAC (Dunaief et al, 1994; Zhang et al, 2000) and it has been shown that BRG1 interacts with EKLF and nuclear hormone receptors (Ichinose et al., 1997). With the use of biochemical assays, it has been demonstrated that the SWI/SNF complex, once recruited to regulatory regions, can disrupt nucleosome structure and increase accessibility to DNA in an ATP-dependent manner (Cote et al, 1994; Lusser & Kadonaga, 2003). Although, the 2 MDa SWI/SNF complex consists of 9-12 subunits, only four of these, BRG1 or BRM (mutually exclusive ATPase subunits that are human homologues of the yeast SWI2/SNF2 ATPase subunit), SNF5 (also known as INI1), BAF155 and BAF170, are able to remodel nucleosomes *in vitro* at a rate that is comparable to the entire remodeling complex (Phelan et al, 1999). The role of the other subunits is not as well defined as for the above-mentioned four proteins; however, there is emerging evidence to suggest that the other SWI/SNF subunits are likely to assist in directing the specificity of the complex through protein-protein interactions (Schnitzler et al., 1998). Also, SWI/SNF complex heterogeneity has been implicated into providing the specificity of the transcriptional regulation that is performed by the complex, by altering protein-protein interactions (Peterson and Logie, 2000). Furthermore, the ISWI (imitation switch) family of enzymes, first identified in *Drosophila*, includes ISWI-based

remodeling complexes NURF (nucleosome-remodeling factor), ACF (ATP-dependent chromatin assembly and remodeling factor) and CHRAC (chromatin accessibility complex) (Becker and Horz, 2002). These complexes contain the ISWI ATPase subunit, which, like the SWI/SNF shares a homology with the yeast SWI2/SNF2 subfamily of ATPases. In contrast to the SWI/SNF-based remodeling complexes, the similarities are restricted to the ATPase subunit. Members of the ISWI-based family of chromatin remodeling factors are smaller when compared to the SWI/SNF counterparts and these complexes contain fewer subunits (up to 4) (Peterson and Logie, 2000). The SWI/SNF- and ISWI-based remodeling complexes are functionally diverse in that each type of the complex remodels chromatin using a different mechanism. The ATPase core of the SWI/SNF complex can use either naked DNA or nucleosomes as a substrate, whereas ISWI ATPase is optimally induced by intact nucleosomes with undisturbed histone N-terminal tails (Cote et al., 1998). Although fairly similar in structure, ISWI remodelers may have different functions. CHRAC and ACF complexes tend to cluster and assemble nucleosomes *in vitro* and consequently promote transcriptional deactivation (Dirscherl and Krebs, 2004). In contrast, the ISWI-based NURF complex has been shown to act in a similar manner as the SWI/SNF complex, in that it acts to perturb and destabilize the chromatin structure (Lusser and Kadonaga, 2003).

1.3.2 The mechanism of ATP-dependent chromatin remodeling

The process of chromatin remodeling can be divided into a 3-step mechanism. The initial binding of the complex to the nucleosome may involve either diffusion or scanning along a chromatin substrate or a more target-mediated model. After the nucleosome to be modified is identified, physical alteration of nucleosomal structure

takes place. The exact mechanism used to couple ATP hydrolysis to structural changes in chromatin remains unclear. Finally, after ATP hydrolysis and/or the histone displacement, the chromatin-remodeling complex needs to be released in order to reach its next target (Langst and Becker, 2004).

SWI/SNF complexes must recognize and bind to their chromatin substrate before stimulating ATPase activity. Binding of chromatin remodelers to both DNA and nucleosomes through associations with the minor groove of DNA and the core histones has been shown in numerous *in vitro* studies (Cote et al., 1998). Further, it has been shown that SWI/SNF has a higher affinity for core histones than DNA, suggesting that the interactions with the histone core induce dissociation of histones *in trans* (i.e. transferring the histones to alternative DNA regions or to histone chaperone proteins) (Georgel et al., 1997). The yeast SWI/SNF remodeling activity has been linked to changes in rotational phasing of DNA (i.e. relative position of histone contacts in relation to the major or minor groove of DNA), which results in perturbation of histone-DNA contacts and variations in nucleosome stability, as evident from generation of new DNase I hypersensitive sites from SWI/SNF-remodeled chromatin (Lorch et al., 1999). As a consequence of SWI/SNF binding and ATP-dependent chromatin remodeling, the histone-DNA contacts are modified, increasing the accessibility of DNA-binding proteins to nucleosomal DNA (Utlely et al., 1997). In order for SWI/SNF to remodel specific nucleosomes (e.g. on promoter regions), additional factors may be required for the recruitment. The SWI/SNF complex has been found to be associated with the RNA polymerase II complex, suggesting that this holoenzyme might recruit SWI/SNF to promoter regions (Alen et al., 2002). Moreover, SWI/SNF subunits, such as SWI3, SWI5

and SWI2/SNF2 ATPase are stably associated with the Mediator complex, which acts as an interface between specific regulatory proteins and the general transcription machinery of eukaryotes (Kim et al, 1994; Wilson et al, 1996; Myers & Kornberg, 2000) and is securely associated with the C-terminal domain of RNA polymerase II (RNAP II) holoenzyme complex (Wilson et al, 1996). Furthermore, specific post-translational modifications of core histones at specific loci may act as nucleosomal tags for remodeling, providing further specificity required for transcriptional regulation by SWI/SNF and ISWI complexes (Simone, 2006). The bromo-domain of the SWI/SNF ATPase subunit can recognize acetylated histone H4 tails (Winston and Allis, 1999), and the ability of SWI/SNF to bind chromatin is enhanced in the presence of hyperacetylated nucleosomes (Hassan et al., 2001b), support the idea that SWI/SNF recruitment might be modulated by the contact of SWI2/SNF2 ATPase bromo-domain and acetylated histones. In contrast, the ISWI members lack a bromo-domain, but can still bind chromatin, since they contain SANT and SLIDE domains, which are putative DNA- and nucleosome-binding motifs (Grune et al, 2003). The ability of ISWI to regulate specific genes has been linked to methyltransferase SET1-dependent methylation of histone H3 *in vivo* (Santos-Rosa et al, 2003), providing a link between ISWI-based chromatin remodeling and histone modifications. The targeted recruitment of chromatin remodeling complexes to specific nucleosomes may be also accomplished through interactions with various transactivation domains of transcription factors (Simone, 2006). Collectively, all of the above-mentioned modes of recruitment to chromatin may play a role in ensuring appropriate specificity of the recruited remodeling complex. Once the remodeling complexes are on the chromatin, ATP-dependent alterations in DNA-histone contacts

occur in order to initiate specific cellular events. The intrinsic ATPase activity of SWI/SNF complexes is critical for activation and function of chromatin remodeling complexes. The indispensable role of the ATPase subunit has been established both *in vivo* and *in vitro*, where mutations in the catalytic core of ATPase subunit abolish the SWI/SNF chromatin remodeling activity (Cote et al, 1994; Peterson & Logie, 2000), suggesting that ATP hydrolysis is key to rearranging and reducing DNA-histone contacts. The observation that the nucleosomes become accessible only when ATP is present indicates that the physical presence of SWI/SNF ATPase subunit near its target region may be required to maintain chromatin in permissive remodeled state (Gavin et al., 2001). One of the proposed models for SWI/SNF chromatin remodeling is the 2-step model, where the initial binding of SWI/SNF to its substrate is ATP hydrolysis-independent and may or may not cause alterations in chromatin structure (Vignali et al., 2000). The second step involves ATP-dependent disruption of DNA-histone contacts, resulting in alterations of DNA topology and nucleosome sliding (Lusser and Kadonaga, 2003). The torsional stress, introduced by SWI/SNF complex may induce formation of a small bulge or loop in the DNA, which could propagate throughout the nucleosome structure, destabilizing histone octamer-DNA contacts (Fry and Peterson, 2001). It has been suggested that the initial disruption of the histone octamer, followed by transfer in both *cis* and *trans* to different DNA locations uses the thermal release of energy from ATP hydrolysis (Panigrahi et al., 2003). Such remodeling of chromatin may involve the formation of altered nucleosomes, where the two adjacent nucleosomes would cluster together, changing the spacing and enhancing the accessibility of DNA (Lorch et al., 2001). Similar mechanistic models have been proposed for ISWI-based disruption of

chromatin structure (Fyodorov and Kadonaga, 2002). The final step of chromatin remodeling is the release of remodeling complexes from the chromatin template. It has been suggested that after ATP hydrolysis and the release of reaction product, SWI/SNF- and ISWI-based complexes may undergo conformational changes (e.g. due to post-translational modifications) that are sufficiently significant to lower the affinity for nucleosomes (Racki and Narlikar, 2008). Also, the dynamic turnover of transcription factors or other chromatin-associated proteins may dictate the release of remodeling complex from the altered nucleosome (Nagaich et al, 2004). It is important to note that higher-order folding of chromatin plays a crucial role in the accessibility of chromatin-remodeling complexes to DNA and histones, adding another layer of complexity. Higher-order unfolding of chromatin may be required for proper binding of SWI/SNF- and ISWI-based complexes, as studies have shown that the presence of linker histones and polynucleosomal templates affect the remodeling process (Schnitzler et al, 2001; Boeger et al, 2004). Studies in yeast strains with Sin mutations (specific mutations in histone residues that alleviate the requirement of the yeast SWI/SNF chromatin remodeling complex) have linked disruption of higher-order chromatin structure with transcriptional regulation, where remodeling complexes may act as modulators of dynamic alterations in chromatin folding (Wechsler et al, 1997; Cosgrove et al, 2004) and in turn regulate important molecular outcomes.

1.4 Histone post-translational modifications

Histones are evolutionarily conserved proteins with a flexible amino-terminal tail and a histone fold, a globular domain that mediates substantial interactions between histones to form the nucleosomal scaffold (Luger et al., 1997). Structural studies have

Globally, histone modifications may mediate the establishment of distinct chromatin environments, partitioning the genome into heterochromatin and euchromatin domains. Heterochromatin is an important component of eukaryotic genomes, since it can provide protection of chromosome ends and influence separation of chromosomes in mitosis (Dimitri et al., 2009). Silent heterochromatin in mammals is generally associated with low levels of histone acetylation and high levels of histone methylation (H3K9, H3K27 and H420), whereas actively transcribed euchromatin regions contain high levels of histone acetylation and trimethylation of H3K4, H3K36 and H3K79 (Rando and Chang, 2009). Furthermore, histone modifications may account for the disruption between nucleosome contacts, which would have effects on the higher-order chromatin structure. Histone acetylation has the most potential to alter chromatin structure since it neutralizes the basic charge of lysine residues (Choi and Howe, 2009). Biophysical studies have shown that inter-nucleosomal contacts are important for higher-order chromatin structure; therefore, any alterations in histone charges will undoubtedly have structural consequences on chromatin folding (Rando and Chang, 2009). Recent development of strategies to make recombinant nucleosomes modified at specific residues has allowed investigators to address the notion that histone modifications affect higher-order chromatin folding. Studies utilizing chemical ligation of modified tail peptides onto recombinant histone core preparations have shown that acetylation of histone H4 at K16 had a negative effect on the formation of 30-nanometer chromatin fiber and the generation of higher-order structures (Shogren-Knaak et al, 2006). Another mechanism by which histone modifications could alter chromatin structure would be through recruitment of non-histone proteins containing enzymatic activities, which would further

modify chromatin. It has been shown that certain histone modifications are recognized and bound by domains present within specific proteins. Histone methylation is recognized by chromo-like domains of the Royal family (chromo, tudor, MBT) and nonrelated PHD domains, acetylation is recognized by bromo-domains, while phosphorylation is recognized by a domain present within 14-3-3 proteins (Rando and Chang, 2009). Furthermore, specific proteins are recruited to these modified histone residues to provide further functions. For example, BPTF, a component of the NURF chromatin-remodeling complex, recognizes trimethylated K4 of H3 via a PHD domain, tethering the SNF2H ATPase and activating the expression of the HOXC8 gene (Wysocka et al, 2006; Li et al, 2006). Equally important function of histone modifications may be prevention of protein binding to chromatin. Methylation of histone H3 at K4 deterred binding of NuRD complex (Nishioka et al, 2002), whereas phosphorylation of H3 at T3 and acetylation at K9/K14 prevented binding of INHAT complex (Schneider et al, 2004). Both of these complexes have repressive functions; therefore, their chromatin occlusion via histone modifications may promote transcriptional activation (Margueron et al., 2005). The presence of various modifications on histone N-terminal tails creates an environment in which cross-talk between different modifications can occur. Binding of a protein could be inhibited by an adjacent modification, as it is the case of H3 phosphorylation at S10 affecting the binding of HP1 to methylated K9 of H3 (Fischle et al, 2005). Enzyme catalytic activity could be altered by modification of its substrate recognition site. For example, isomerization of H3P38 compromised methylation of H3K36 by SET2 methyltransferase (Nelson et al, 2006). In contrast, an enzyme could recognize its substrate more efficiently if an adjacent

modification is present, as the studies have shown that yeast GCN5 acetyltransferase recognized H3K14 acetylation more efficiently if H3S10 phosphorylation was present, in order to promote transcriptional activation (Lo et al, 2000; Clements et al, 2003). Cross-talk among histone modifications can also occur if the modifications are present on different histone tails, as in the case of H2B ubiquitination being required for trimethylation of H3K4 (Shilatifard, 2006). Therefore, communication between different histone modifications may modulate important molecular outcomes.

1.4.1 Histone acetylation

Histone acetylation can occur on all of the four core histone proteins (Figure 4). This histone modification is catalyzed by lysine acetyltransferases (KATs), which transfer an acetyl moiety from acetyl-coenzyme A to the ϵ -amine of lysine residues. These enzymes are regarded as transcriptional coactivators and include GCN5/PCAF and CBP/p300 (Nagy & Tora, 2007). The action of KATs is counter-balanced by histone deacetylases (HDACs); therefore, histone acetylation levels are controlled by the interplay of KATs and HDACs. Since histone acetylation can neutralize the positive charge of lysine residues and possibly weaken the interactions with DNA, many studies have focused on the effects of histone acetylation on chromatin structure. Most studies suggest that histone acetylation generates subtle changes in the structure of mononucleosomes. It has been shown that nucleosome preparations with hyperacetylated histone tails induced a modest increase in transient unwrapping of DNA from the edge of the nucleosome (Anderson et al, 2001). Furthermore, chemical acetylation of histone H3 generated a more open mononucleosome structure, as shown by measuring the distances between linker DNA (Toth et al., 2006). Acetylation of histones *in vitro* by CBP

destabilized individual nucleosomes, as determined by measuring the tensional force of the nucleosomal arrays undergoing continual stretching (Morales and Richard-Foy, 2000). Chemical ligation of synthetic tetra-acetylated H3 tails onto histone globular domains and further incorporation into mononucleosome structures resulted in a 2-fold increase of the intrinsic mononucleosome sliding (Ferreira et al., 2007). Furthermore, histone acetylation has been implicated in altering the structure of nucleosomal arrays. Using linear nucleosomal arrays, it was shown that histone acetylation induced an extended chromatin conformation, albeit in the absence of the linker histone H1 (Garcia-Ramirez et al., 1995). With crystallization of the nucleosome core particle came the observation that amino acids 16-19 of histone H4 made extensive contacts with the H2A-H2B dimer on an adjacent particle (Luger et al., 1997). Since K16 of H4 is subject to acetylation, it has been suggested that this modification might disrupt internucleosomal contacts and unravel higher-order chromatin structures. Indeed, with the use of chemical peptide-ligation to generate nucleosomal arrays that are singly acetylated at H4K16, it has been demonstrated that this H4 modification inhibited the formation of compact 30-nanometer chromatin fibers (Shogren-Knaak et al, 2006). The role of acetylation of H4K16 in regard to chromatin structure and transcription has been confirmed by multiple genetic studies in yeast (Vaquero et al., 2007). Thus, experimental evidence suggests that H4K16 acetylation has a role in regulation of chromatin fiber compaction; however, whether acetylation of other histone residues has similar effects has not been elucidated. In addition, histone acetylation has been linked to transcriptional activation of genes (Nagy & Tora, 2007). The hallmark of transcriptionally active genes is the acetylation of histone N-terminal tails, which occurs predominantly at promoters and 5' ends of

transcribed units, where the level of acetylation corresponds with the rate of transcription (Liu et al., 2005). Upon initiation of MAPK signaling, a large population of nucleosomes at gene promoters becomes highly acetylated on histones H3 and H4 (Thomson et al, 2001), providing evidence that histone acetylation is a dynamic event during transcriptional activation. Targeted histone acetylation is achieved by interactions of KATs with transcription factors, components of the transcription machinery and the RNA polymerase holoenzyme (Utley et al, 1998; Sterner & Berger, 2000). In yeast, it has been shown that histone acetylation facilitates binding of TBP and RNA polymerase II to various promoter regions, suggesting that histone acetylation is a necessary step in transcriptional initiation (Bhaumik & Green, 2002; Qiu et al, 2004). Moreover, loss of histone deacetylase activity in yeast resulted in transcription initiation from cryptic intragenic promoters, implying that histone acetylation promotes enhanced nucleosomal DNA accessibility (Carrozza et al, 2005). It is important to note that histone acetylation has been observed not only at promoter regions of genes, but also throughout the transcribed unit (H3K14ac, H3K23ac, H4K12ac and H3K16ac), suggesting that histone acetylation is involved in transcription elongation (Wang et al, 2008). The loss of two H3-specific KATs (GCN5 and ELP3) in yeast resulted in a transcriptional decrease of numerous genes, which showed normal TBP binding (Kristjuhan et al, 2002), indicating that the loss of acetylation disrupted a step downstream of transcription initiation. Furthermore, yeast GCN5 has been found throughout gene regions, modulating nucleosome eviction and RNA polymerase II processivity during transcription of long genes (Govind et al, 2007). Interactions between KATs and components of the transcription elongation machinery have also been observed (Cho et al, 1998; Wery et al,

2004), further supporting the role of histone acetylation in transcription elongation. However, there is accumulating evidence to suggest that histone acetylation on its own is not able to support transcription, but that the process of transcriptional activation requires additional mechanisms, such as the action of chromatin remodelers (Suganuma and Workman, 2008). Histone acetylation has been linked with facilitating alterations in nucleosome structure via recruitment of chromatin remodeling complexes that contain bromodomains (Barbaric et al, 2001). It has been shown that tetra-acetylated H3 enhanced binding of yeast chromatin-remodeling complex to nucleosomes, and that tetra-acetylated H4 promoted histone octamer transfer by destabilizing the nucleosome structure (Ferreira et al., 2007). Also, there are numerous demonstrations of co-recruitment of KATs and chromatin remodeling complexes by the same DNA-bound transcriptional activator (Amati et al., 2001). These studies suggest that histone acetylation promotes the binding of chromatin remodeling complexes and renders nucleosomes more sensitive to the action of chromatin remodelers. In this context histone acetylation may act as a molecular “tag” to be specifically recognized by proteins that contain bromodomains, thereby recruiting transcription machinery and chromatin-modifying enzymes to specific regions of the genome. Furthermore, histone acetylation has been implicated in the histone code, in which multiple histone modifications, acting in a combinatorial fashion, specify unique downstream outcomes (Strahl and Allis, 2000). However, genome-wide studies have shown that cells display a small subset of all possible histone acetylation patterns (Liu et al., 2005). There are over 60 possible acetylation patterns on the H3 tail, but a low number of distinct patterns are observed *in vivo*. With the use of ChIP and subsequent massively parallel DNA sequencing (ChIP-

Seq) it has been revealed that acetylation of K9, K18, K27 and K36 of H3 is predominantly observed at promoters of human CD4+ T-cells, while acetylation of K14 and K23 of H3, which also localized at promoters, extended significantly downstream (Wang et al, 2008). Similar patterns were observed with acetylation of H4, with acetylated K5 and K8 being localized at promoters, while acetylation of K12 was detected throughout the transcribed unit (Wang et al, 2008). Although an extremely powerful tool, the ChIP technique possesses possible disadvantages that might confuse the interpretation of data. This is especially relevant to acetylation levels and its turn over, when modification-specific antibodies are used during the ChIP procedure (Clayton et al., 2006). The issues of the precise specificity of antibodies used, the random occlusion of antibodies that may occur and the drift of antibody specificity may contribute to variability in the recovery of particular chromatin fragments during the ChIP procedure (Edmondson et al, 2002). These issues may make ChIP data misleading, especially where clear quantitative and statistically tested information is crucial to interpretation. Nevertheless, whether the above mentioned histone acetylation signatures have unique functional readouts or whether they are simply due to substrate specificities of various KATs recruited during transcription initiation or elongation is still unclear. Although the use of the histone code would be helpful to define the outcome of a specific subset of histone modifications, it is unlikely to reflect the true presence of a predictable code.

1.4.2 Histone methylation

Histones can be methylated on arginine and lysine residues. Histone methylation can occur in mono-, di- and trimethylated forms on K4, K9, K27, K36 and K79 of H3

and K20 of H4 (Shilatifard, 2006). The lysine residues on histones are methylated on the ϵ -nitrogen by SET domain or non-SET domain containing lysine methyltransferases (KMTase). The mammalian KMTases, SUV39H1, SUV39H2, EHMT2 and ESET are known to methylate H3K9. EZH2 catalyzes the methylation of H3K27 and PR-SET7 can methylate H4K20 (Trojer P, 2006). SET1 and SET2 enzymes have been shown to catalyze methylation of H3 K4 and K9, respectively (Hublitz et al., 2009). Methylation of H3K4 is another hallmark of transcriptional gene activation (Ruthenburg et al., 2007); therefore, extensive research has been focused on identifying complexes that mediate this histone modification. The yeast Set1 associates with seven other polypeptides to form a complex termed COMPASS (Miller et al, 2001). COMPASS can catalyze the mono-, di- and trimethylation of H3K4 (Wu et al, 2008). Human MLL is homologous to Set1 and has been found in a complex containing H3K4 methyltransferase activity (Steward et al., 2006). Furthermore, histone arginine methylation can be either mono- or dimethylated. The dimethylation of histone arginine residues is found in either symmetrical or asymmetrical configurations (Shilatifard, 2006). The transfer of methyl groups on specific arginine residues of H3 and H4 proteins is catalyzed by CARM1 and PRMT1 enzymes (Shilatifard, 2006). Histone methylation is a reversible process, performed by two classes of enzymes, amine oxidases such as LSD1 and hydroxylases of the JmjC family (Klose and Zhang, 2007). Histone methylation has been implicated in various biological processes, depending on the site and type of histone modification. Arginine methylation of H3 and H4 has been shown to regulate transcriptional activation of steroid-responsive genes (Lee et al., 2005). Also, various studies have shown that H4R3 methylation is responsible for the establishment and maintenance of a wide range of other

histone modifications (Huang et al., 2005). As previously mentioned, COMPASS catalyzes methylation of H3K4, and this complex has been found associated with RNA polymerase II at transcriptionally active genes (Gerber and Shilatifard, 2003). Numerous studies have shown that H3K4 methylation is an integral mark of transcriptionally active gene regions in mammalian cells (Shilatifard, 2006). Histone methylation of H3 at K4 and K36 may cooperate with the dynamic H2B ubiquitination at promoters of genes during the onset of transcription (Henry et al., 2003). Furthermore, histone methylation does not directly affect transcription; rather, it recruits other additional components required for downstream effects (Lee et al., 2005). Several factors required for active transcription, such as chromatin remodelers NURF and CHD1, have been shown to interact with di- and trimethylated H3K4 (Sims and Reinberg, 2006). In contrast, proteins associated with gene silencing, such as histone demethylase JMJD2A and HDAC-associated protein ING2, can also bind di- and trimethylated H3K4 (Shi et al, 2006). Furthermore, H3K9 methylation has been associated with heterochromatin formation (Shankaranarayana et al., 2003); (Grewal and Moazed, 2003), which differs from the functions that have been associated with H3K4 and H3K36 methylation. H3K9 methylation is catalyzed by SUV39H, which has been found at transcriptionally silent heterochromatin, leading to recruitment of the transcriptional repressor HP1 (Ayyanathan et al, 2003). HP1 and SUV39H have been also implicated in transcriptional repression at euchromatic loci, since the co-repressor protein RB recruited HP1 and SUV39H to cell cycle control genes, including *CyclinE* (Nielsen et al, 2001; Vandel et al, 2001). Similarly, H3K27 and H4K20 methylation events are involved in heterochromatin formation and heterochromatic gene silencing (Sims and Reinberg, 2006). Therefore,

depending on which histone residues are methylated, different cellular outcomes can occur via recruitment of specific factors.

1.4.3 Histone phosphorylation

Histone phosphorylation occurs on all core histone proteins (Nowak and Corces, 2004) and the biological ramifications are very context dependent. For example, histone H4 S1 phosphorylation is an evolutionary conserved event with a role in chromatin condensation in the later stages of gametogenesis (Krishnamoorthy et al, 2006). Phosphorylation of H2B (on Ser14 in human; on Ser10 in yeast) by MST1/ySTE20 kinase correlated with chromosome condensation and disappeared during meiotic divisions (Ahn et al., 2005). This H2B phosphorylation event is also linked to chromatin compaction during apoptosis in human and yeast cells (Ahn et al., 2005). Phosphorylation of H2A has been associated with mitotic chromosome condensation (Barber et al, 2004). However, when mammalian cells are exposed to DNA damaging agents, S139 of H2A.X is phosphorylated and required for the proper process of non-homologous end-joining DNA repair (Rogakou et al., 1998). Thus, H2A phosphorylation may mediate localized structural changes in chromatin that initiate DNA repair. Furthermore, histone phosphorylation is implicated in the process of transcription. Phosphorylation of H310 has been linked to RAS-MAPK mediated gene activation in mammalian cells (Nowak and Corces, 2004). Also, it has been demonstrated that a small fraction of H3 is both acetylated (K14) and phosphorylated (S10) on the same H3 tail of immediate-early genes; thus, these two H3 modifications may mediate cross-talk required to stimulate gene activation (Clayton et al., 2006).

1.4.3.1 Histone H3 phosphorylation

Histone H3 is decorated with the most PTMs out of the four core histone proteins (Espino et al., 2005). Phosphorylation of histone H3 was observed more than thirty years ago (Shoemaker and Chalkley, 1978) and today there are several fairly well characterized and conserved phospho-H3 residues: Thr3, Ser10, Thr11 and Ser28 (Figure 5).

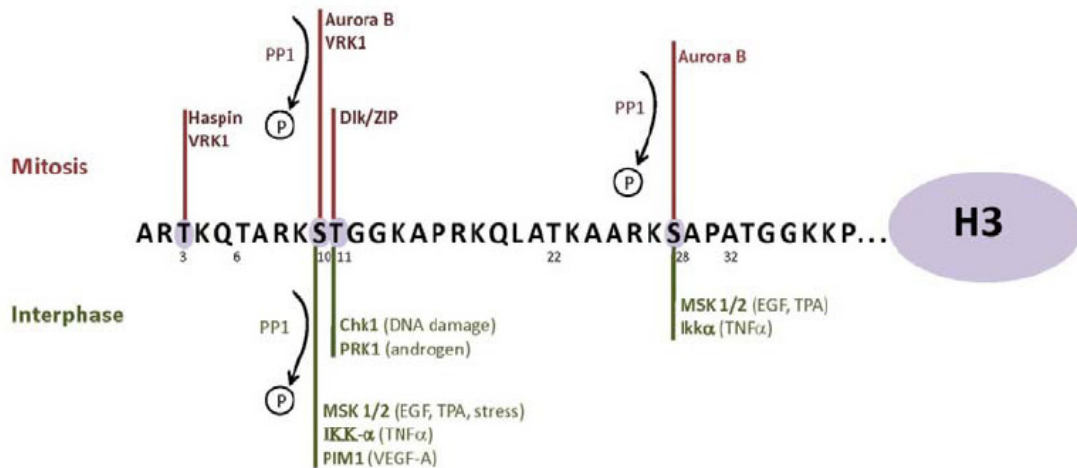


Figure 5: Histone H3 phosphorylation sites and the known kinases/phosphatases.

Kinases and phosphatases responsible for H3 N-terminal tail phosphorylation and dephosphorylation during mitosis and interphase reported to date. Indicated between brackets are stimuli reported to activate the specific kinases.

All of these phospho-H3 marks are present during mitosis, suggesting a possible role in chromatin condensation. Furthermore, phospho-H3 Ser10, Thr11 and Ser28 are known to be involved in transcriptional activation of specific genes (Cerutti and Casas-Mollano, 2009). Therefore, histone H3 phosphorylation is associated with two opposed chromatin states: the highly condensed mitotic chromosomes and the more accessible chromatin structure observed at active genes during interphase (Prigent and Dimitrov, 2003). This apparent paradox implies that the effect of H3 phosphorylation on chromatin structure might be context-dependent and influenced by other histone PTMs. The two most studied

H3 phosphorylation events are the S10 and S28 phospho-modifications, which globally occur during mitosis and are minimally present in interphase cells.

1.4.3.2 Phosphorylation of histone H3 at Ser10/28 during mitosis/meiosis

Phosphorylation of histone H3 throughout different stages of mitosis is conserved in eukaryotes and numerous studies have characterized H3 Ser10 phosphorylation during this phase of the cell cycle (Gurley et al., 1978). In mammalian cells, phosphorylation of H3 at Ser10 is first evident in pericentromeric heterochromatin in late G2-interphase cells. Subsequently, the phosphorylation of H3 Ser10 spreads along the chromosomes and is completed at prophase, and is still evident at the metaphase plate (Hendzel et al., 1997). The temporal and spatial relationship between chromosome condensation and phosphorylation of H3 at Ser10 is clearly evident from immunofluorescence studies (Goto et al., 2002). On the other hand, dephosphorylation of H3 at Ser10 begins in late anaphase and is completed in early telophase before detectable post-mitotic decondensation of chromosomes (Hendzel et al., 1997). This finding suggested that phosphorylation of H3 at Ser10 coincides with the condensation of chromosomes. Nevertheless, a subsequent study showed that H3 Ser10 phosphorylation is necessary for the initiation of chromosome condensation rather than its maintenance during mitosis (Van Hooser et al., 1998) since mammalian cells could be arrested in late G2 phase by saturating the mitotic H3 kinase with H3-Ser10-sequence containing peptides. In *Drosophila*, attenuation of H3 Ser10 phosphorylation led to partially condensed chromosomes during mitosis (Giet & Glover, 2001). Furthermore, in the ciliated protozoan, *Tetrahymena thermophila*, the H3 S10A mutant strain showed abnormal chromosome segregation and extensive chromosome loss during mitosis and meiosis

(Wei et al., 1999). These findings implicate H3 Ser10 phosphorylation as an important event in chromosome condensation and segregation. However, H3 Ser10 phosphorylation is not required for chromosome condensation and mitosis in all organisms. In *S. cerevisiae*, the S10A mutation does not alter mitotic and/or meiotic chromosome transmission (Hsu et al, 2000). Hsu JY and colleagues propose that the functional redundancy of H2B phosphorylation might be able to compensate for the missing H3 Ser10 phosphorylation during mitosis in budding yeast (Hsu et al, 2000). This observation, along with other features related to chromosome structure and chromosome segregation that *S. cerevisiae* presents, suggest that this organism might not be a suitable model for the study of H3 Ser10 phosphorylation during mitosis. In *Drosophila*, attenuation of H3 phosphorylation was correlated with abnormal mitotic chromosome morphology although there was a weak correlation with chromosome condensation (Adams et al, 2001; Prigent & Dimitrov, 2003). Furthermore, in maize meiocytes the distribution of H3 phosphorylated at Ser10 correlated mainly with sister chromatid cohesion at different meiotic stages, suggesting that H3 Ser10 phosphorylation might not have a direct role in chromosome condensation (Kaszas and Cande, 2000). Therefore, the correlation between H3 Ser10 phosphorylation and chromosome condensation is evident in some cases, but the absolute connection between the two events is not universal; thus, the exact cellular consequence of H3 Ser10 phosphorylation during mitosis is not completely resolved.

In addition to phosphorylation of H3 at Ser10, the H3 N-terminal tail can also be phosphorylated at serine 28 during mitosis and meiosis (Prigent and Dimitrov, 2003). The distribution of H3 Ser28 phosphorylation is very similar to that observed of H3

Ser10 (Goto et al., 1999). H3 Ser28 phosphorylation appears at the onset of mitosis in prophase and is maintained until early anaphase. However, the H3 Ser28 signal starts disappearing during late anaphase and early telophase (Goto et al., 1999). Interestingly, H3 Ser28 phosphorylation was shown to coincide with chromosome condensation in mammalian cells (Goto et al., 1999). The relative abundance of phospho-H3 Ser10 and Ser28 appears to be different during mitosis. The level of phospho-H3 Ser28 was not as prevalent as that of phospho-H3 Ser10, implicating differential spatiotemporal regulatory mechanisms for the two phospho-sites on the H3 tails (Goto et al., 2002). Overall, H3 Ser28 phosphorylation during mitosis/meiosis coincides with the phosphorylation of H3 Ser10 in most of the organisms examined. However, the onset and the abundance of phosphorylation of Ser10 and Ser28 residues might differ depending on the organism. Furthermore, immunofluorescence results provided evidence of both Ser10 and Ser28 phosphorylation occurring along the same chromosomes during mitosis (Goto et al., 1999), although it is not known if both the H3 Ser10 and Ser28 phosphorylation events simultaneously occur on the same H3 tail within the same nucleosome on the mitotic/meiotic chromosomes.

It is interesting to note that several other *in vivo* modifications co-exist with phospho-H3 Ser10 or Ser28 on the same H3 tail during mitosis (Garcia et al., 2005). A tandem mass spectrometry (MS) study in mitotic HeLa cells revealed that acetylation of H3 at Lys9 or Lys14 was present on the same H3 tails as H3 Ser10 phosphorylation (Garcia et al., 2005). Co-existence of phospho-H3 Ser10 with Ser28 could not be detected in this study due to specific tryptic digestion of peptides used for tandem MS. Moreover, the co-existence of mono, di- or tri-methylated H3 at Lys27 and/or Lys36 along with

phosphorylated H3 at Ser28 during mitosis was also observed (Garcia et al., 2005). Further, this study demonstrated that the H3 phosphopeptides containing methyl marks on Lys residues were in greater abundance than the H3 phosphopeptides containing Lys acetyl marks. These observations imply that H3 phosphorylated at Ser10 and/or Ser28 could regulate binding of effector molecules to methylated Lys9 or Lys27. Indeed, it has been shown that mitotic H3 Ser10 phosphorylation compromised association of HP1 to H3 methylated at Lys9, ejecting HP1 from chromatin (Fischle et al, 2005). This could have an effect on rearrangement of higher-order mitotic chromatin structure that may require the release of tightly associated proteins, such as HP1, during mitosis.

1.4.3.3 Mitotic histone H3 Ser10/28 kinase and phosphatase

The relative abundance of H3 Ser10 and Ser28 phosphorylation during mitosis is tightly regulated by the corresponding kinase and phosphatase activities specific for the two residues within the N-terminal domain of H3. Numerous studies have identified members of the Aurora kinase family as the enzymes responsible for phosphorylation of H3 Ser10 and Ser28 during the M phase of the cell cycle (Crosio et al, 2002; Goto et al, 1999; Hsu et al, 2000). The unicellular *S. cerevisiae* contains only one protein belonging to this kinase family, called Ipl1 (Glover et al., 1995), known to phosphorylate H3 at Ser10 during mitosis. *Caenorhabditis elegans* and *Drosophila* have two aurora kinases, Aurora A and Aurora B (Reich et al, 1999); (Schumacher et al, 1998a; Schumacher et al, 1998b), while mammals possess an additional kinase, Aurora C (Adams et al, 2001). Mammalian aurora kinases contain 67-76% homology within their catalytic domains, respectively, and are regulated in a cell-cycle dependant manner with peak expression profiles at the G2/M transition phase (Bischoff et al, 1998; Kimura et al, 1999; Terada et

al, 1998). The intracellular localization of the three Auroras has revealed association of these kinases with chromatin structures (Crosio et al, 2002). Aurora A has been localized to centrosomes of interphase cells and at the spindle poles of metaphase cells, whereas Aurora B has been localized at the midbody of anaphase cells and at the post-mitotic bridge evident in telophase cells (Crosio et al, 2002). In addition, Aurora C, a spermatogenesis-dedicated kinase (Prigent and Dimitrov, 2003), has been observed at centrosomes of anaphase cells (Crosio et al, 2002). Even though *in vitro* experiments showed that Aurora A was able to phosphorylate H3 Ser10 (Crosio et al, 2002), the knock down of Aurora A kinase showed no reduction of H3 Ser10 phosphorylation during mitosis in *C. elegans* and *Drosophila*. This suggested that Aurora A is not directly involved in mediating this phosphorylation event in the two organisms (Giet & Glover, 2001; Hsu et al, 2000). In *Xenopus*, the *in vitro* results suggest that both Aurora A and Aurora B might have a role in mitotic H3 Ser10/28 phosphorylation (Murnion et al., 2001). On the other hand, experimental results in mammalian cells provide evidence implicating Aurora B as the mitotic H3 Ser10/28 kinase (Prigent and Dimitrov, 2003). Co-localization of Aurora B and H3 phosphorylation was observed from late G2 phase until metaphase in mammalian cell lines (Crosio et al, 2002). Inhibition of Aurora B by hesperadin, ZM447439 or siRNA knock down caused a dramatic reduction in H3 Ser10 phosphorylation during mitosis (Loomis et al, 2009; Kang et al, 2007). Further, the over-expression of a kinase dead Aurora B in HeLa cells caused abolishment of mitotic H3 Ser10/28 phosphorylation and abnormal mitosis characterized by incomplete chromosome condensation and misalignment of chromosomes at the metaphase plate (Goto et al., 2002). This effect on chromosome condensation could be due to the role of

mitotic kinase or the corresponding PTM on recruitment of condensin proteins (Giet & Glover, 2001). Interestingly, over-expression of Aurora kinases has been observed in many human cancer cell lines suggesting an important role of Aurora enzymes in the regulation of cell proliferation. For example, Aurora A over-expression led to cell transformation (Bischoff et al, 1998), whereas over-expression of Aurora B caused an increase in H3 Ser10 phosphorylation that was associated with chromosome instability often seen in malignant cells (Katayama et al, 2003). A potent and selective Aurora kinase inhibitor, VX-680, has been shown to decrease H3 phosphorylation at Ser10 in MCF-7 cells and inhibit tumor growth *in vivo* leading to regression of leukemia, colon, and pancreatic tumors. Since VX-680 exerts its effects in various types of cancers, it could offer a new approach for the treatment of multiple malignancies (Harrington et al, 2004).

The mitotic H3 kinase activity is counterbalanced by specific phosphatases. Identification of Ipl1 as the mitotic H3 Ser10 kinase in budding yeast paved the way for deciphering the counteracting phosphatase, GLC7, a type 1 protein phosphatase (PP1) (Hsu JY, 2000). PP1 was reported to dephosphorylate H3 Ser10 *in vivo* in yeast, *C.elegans* and vertebrates (de Carvalho et al, 2008; Hsu et al, 2000). It has been demonstrated that Aurora B is activated by the PP1/PP2A inhibitor, okadaic acid, and that human Aurora B kinase forms a complex with PP1 in order to regulate spatiotemporal features of H3 phosphorylation during mitosis (Sugiyama et al, 2002). In mammalian cells, PP1 dephosphorylates H3 at Ser10 and Ser28 residues; however, H3 Ser28 residue seems to be more sensitive to PP1 activity (Goto et al., 2002). In late G2 cells, H3 Ser28 phosphorylation is absent, but when mammalian cells are pretreated with

the PP1/PP2A inhibitor calyculin A, the H3 Ser28 phosphorylation becomes detectable at late G2 heterochromatin (Goto et al., 2002).

Therefore, Aurora B likely phosphorylates both H3 Ser10 and Ser28 residues during late G2 phase to aid in the initiation of chromosome condensation. Upon entry into mitosis (from prophase to metaphase) the levels of H3 Ser10 and Ser28 increase via the activity of Aurora B. It has been proposed that phosphatase activity of PP1 is abolished once PP1 is phosphorylated by Cdc2 prior to entry into mitosis (Goto et al., 2002). After chromosome segregation, Aurora B dissociates from chromosomes (Terada et al, 1998) and H3 phosphorylation at both Ser10/28 starts to gradually decrease. The level of H3 Ser28 phosphorylation during mitosis decreases faster when compared to H3 Ser10 phosphorylation, presumably due to a differential preference of PP1 for Ser10 and Ser28 residues of H3 (Goto et al., 2002).

1.4.3.4 Phosphorylation of histone H3 at Ser10/28 during interphase

Phosphorylation of histone H3 occurs in interphase cells; however, it is restricted to a significantly smaller fraction of nucleosomes (Goto et al., 2002). Inducible phosphorylation of H3 at Ser10 and Ser28 at interphase has been linked to transcriptional activation of a specific set of genes (Cerutti and Casas-Mollano, 2009). Stimulation of mammalian cells with growth factors and phorbol esters has been shown to cause a rapid immediate-early (IE) gene induction with accompanying phosphorylation of H3 on serine residues within its highly charged, basic N-terminal domain (Mahadevan et al., 1991). IE genes (e.g. *JUN*, *FOS*, *FOSL1*, *COX-2*) are transiently activated in response to intracellular signaling cascades and encode for inducible transcription factors, such as JUN, FOS and FRA-1 that have been implicated in cellular transformation (Herdegen and

Leah, 1998; Sng et al., 2004). Concomitant timing of IE gene induction and H3 phosphorylation was termed the “nucleosomal response” and was the first link between gene induction and H3 phosphorylation. Further studies confirmed this correlation with the use of the chromatin immunoprecipitation (ChIP) assay to directly assess the presence of phosphorylated H3 at IE genomic regions (Chadee et al, 1999; Thomson et al, 2001). It is noteworthy to mention that H3 phosphorylation is tightly linked with acetylation of H3 Lys9 and Lys 14 on the same H3 tails within nucleosomes of IE genes via independent mechanisms (Thomson et al, 2001). Pathway-specific activated downstream kinases lead to rapid increase in the levels of H3 Ser10/28 phosphorylation that have been correlated with transcriptional activation of a number of genes (Dunn et al., 2005). A phorbol ester, 12-O-tetradecanoylphorbol-13-acetate (TPA), is known to bind the catalytic domain of PKC and induce membrane translocation and activation of the PKC enzyme (Hurley and Meyer, 2001), thus initiating RAS/ERK/MAPK signaling and the activation of downstream targets, such as mitogen-and-stress-activated protein kinases 1 and 2 (MSK1/2), which are known to phosphorylate H3 at Ser10 and Ser28 (Drobic et al., 2006). H3 phosphorylation was shown to be required for proper *Fos* gene induction in response to TPA (Soloaga et al, 2003). It has been shown that H3 Ser10 phosphorylation at the *Fos* promoter can be regulated by more than one kinase depending on the activating stimulus: EGF-induced MSK1/2 or TNF- α -induced IKK- α (Anest et al, 2004; Duncan et al, 2006). To make matters more complex, the interplay of different kinases responding to the same stimulus and acting on the same gene regions was recently reported. In human umbilical-vein endothelial cells (HUVECs) exposed to VEGF-A, PIM1 kinase was recruited to the *FOSL1* enhancer region along with an increase of H3

Ser10 phosphorylation (Zippo et al, 2007). Interestingly, H3 phosphorylation was observed at a more upstream region of the *FOSL1* enhancer where PIM1 kinase did not associate, suggesting that another kinase might be responsible for this upstream H3 phosphorylation. Pre-treatment of HUVECs with a MSK preferential inhibitor, H89, had no effect on VEGF-A induced H3 Ser10 phosphorylation at the *FOSL1* enhancer region, but dramatically reduced H3 Ser10 phosphorylation at the upstream region (Zippo et al, 2007) suggesting that MSK1/2 could regulate H3 phosphorylation at this region of *FOSL1*. Thus, it seems that more than one kinase could regulate H3 Ser10 phosphorylation at different regions of the same gene in response to the same stimulus in order to achieve proper transcriptional gene activation. The impact of H3 kinase activity and subsequent H3 Ser10 phosphorylation on gene expression could be explained by recruitment of factors necessary for transcription. MSK1 was shown to modulate phosphorylation of H3 at Ser10 as well as recruitment of transcription factors, chromatin remodeling enzymes and RNA polymerase II to target genes (Vicent et al., 2006).

Inducible phosphorylation of H3 at Ser28 on the nucleosomes of specific genes with regard to transcriptional activation has not been as well studied as H3 Ser10 phosphorylation. Recently, in G0 phase chicken erythrocytes, the ChIP assay was utilized to provide direct evidence of H3 Ser28 phosphorylation at the promoter regions of transcriptionally active genes where this H3 phosphorylation event may act as an active mark of gene activation (Sun et al., 2007). Furthermore, in *Hras*-transformed mouse fibroblasts, TPA-induced phosphorylation of H3 Ser10 and Ser28 co-localized with a transcriptionally initiated form of RNA polymerase II in interphase (Dunn et al, 2009). In the same cells, it was shown that TPA-induced H3 Ser28 phosphorylation was present at

the immediate early *Jun* promoter, providing further evidence that this H3 modification is associated with transcriptional gene activation (Dunn et al, 2009).

Genome wide transcriptome analysis in yeast revealed that H3 Ser10 phosphorylation may not be universal for transcription at all promoters; rather, it is required at a specific set of gene promoters (Lo et al, 2005). During heat shock in *Drosophila*, global phosphorylation of H3 decreased at interphase (Johansen & Johansen, 2006). Upon closer inspection, it was observed that at transcriptionally active heat shock loci, H3 phosphorylation significantly increased along with the increased recruitment of heat shock transcription factors to these regions (Nowak and Corces, 2000). JIL-1 has been described as the kinase responsible for regulating the level of H3 phosphorylation at interphase cells in *Drosophila* (Johansen & Johansen, 2006). Moreover, it was shown that JIL-1 mediated H3 Ser 10 phosphorylation plays a role in early transcriptional elongation of a broad range of genes in *Drosophila* (Ivaldi et al, 2007). However, this study was recently challenged by another group that reported involvement of JIL-1 mediated H3 Ser10 phosphorylation in structural features of chromatin necessary to counteract heterochromatinization and gene silencing at active loci (Cai et al, 2008). However, the *in vitro* evidence suggests that H3 S10 phosphorylation on its own has no significant effect on the structural features of nucleosomes (Fry et al., 2004).

The functional relevance of H3 phosphorylation at Ser10 and Ser28 in interphase cells has been linked with gene expression as previously mentioned. However, experimental evidence suggests that these two phosphorylation events occur independently at distinct chromatin regions (Dunn et al., 2005). In TPA-induced mouse fibroblasts, immunofluorescence clearly demonstrated that most foci of phosphorylated

H3 Ser10 did not co-localize with foci of H3 phosphorylated at Ser28 in interphase, suggesting that these two phosphorylated H3 residues are not targeted to the same chromatin regions (Dunn et al., 2005). In addition, sequential immunoprecipitation studies using formaldehyde cross-linked chromatin fragments (200-300 bp in size) from anisomycin-treated mouse fibroblasts demonstrated that anti-phosphoH3Ser10 antibody was able to recover all of the phosphoH3Ser10 epitope without depletion of phosphoH3Ser28, implying that the two H3 phosphorylation modifications are not located on the same H3 tail *in vivo* (Dyson et al, 2005). These observations imply that H3 phosphorylated at Ser28 has a distinct spatial distribution compared to that of H3 phosphorylated at Ser10, which is quite interesting, since both serine residues are phosphorylated by the same kinases, MSK1 and MSK2 in response to TPA and anisomycin. Other proteins already bound on the nucleosomes, such as HMGN1 may regulate this differential phospho-H3 localization (Lim et al, 2004). Also, recruitment of the kinase by a specific protein or multiprotein complex might dictate which of the two serine residues will be phosphorylated on the H3 tail, which most likely contains pre-existing modifications, such as acetylation and/or methylation.

The correlation of H3 Ser10 and Ser28 phosphorylation and gene activation is based on the presence of these H3 phospho-marks at the promoters of transcriptionally active genes (Cerutti and Casas-Mollano, 2009). What functional roles could these phospho-marks be involved in at these promoters? Experimental data suggest that phosphoH3Ser10 might have a role as part of the binary switch process, as proposed during mitosis. It has been shown that in response to cellular stimulation the recruitment of MSK1 and the levels of H3S10ph and H3K14ac increased at a transcriptionally active

gene promoter (Vicent et al., 2006). Interestingly, this increase was paralleled by a reduction in HP1 γ binding at the promoter, without changes in the levels of H3K9me3. Together these series of events might suggest that the establishment of phospho-H3Ser10 could influence gene induction by ejecting HP1 γ and previously placed repressive complexes at the gene promoter (Vicent et al., 2006). Another possible role of the phospho-H3 Ser10 in transcriptional activation could involve the 14-3-3 family of proteins, recently proposed as chromatin binding proteins. There are seven 14-3-3 protein isoforms and in mammalian cells, specific 14-3-3 isoforms have been characterized as phospho-H3Ser10 or Ser28 binding proteins (Macdonald et al, 2005). The binding affinity for phospho-H3Ser10 is more stable if the Lys14 residue is acetylated (Walter et al., 2008). Furthermore, 14-3-3 ζ proteins are recruited to promoters of *Jun* and *Fos* along with an increase of H3S10phK14ac levels (Macdonald et al, 2005). Recruitment of 14-3-3 at the *HDAC1* promoter region was correlated with dissociation of HP1 γ and siRNA knock down of 14-3-3 proteins abolished *HDAC1* gene expression (Winter et al., 2008). These observations indicate that 14-3-3 proteins recognize phospho-acetyl H3 modifications, and in turn may mediate transcriptional activation of genes. However, the precise mechanism is unknown. It may be possible that 14-3-3 proteins are recruited within a multiprotein complex to genomic regions where 14-3-3 could stabilize the complex at the nucleosomal level by directly binding to pre-existing H3 modifications. Also, binding of 14-3-3 proteins to phospho-acetylated H3 tails could recruit other histone modifying and/or chromatin remodeling activities to aid in the initiation of gene activation. Therefore, stimulus-specific activation of H3 kinase would lead to the establishment of a phospho-H3 Ser10 mark at specific gene promoters, where H3K9me3-

bound HP1 could be ejected and 14-3-3 isoforms may then bind the phospho-H3 Ser10 mark and recruit other critical components required for transcriptional activation of specific genes.

While globally, the rest of the chromatin marks such as acetylation and methylation are “read” by proteins that bear a known binding domain, as is the case of chromo and bromodomains recognizing acetyl and methyl marks, respectively, the domain recognizing phospho-marks remains unknown. Recently, 14-3-3 proteins have emerged as a family of phospho-serine/threonine binding proteins that could have this function. In this regard, preliminary evidence identified the 14-3-3 family of proteins as the “readers” of both phospho-Ser10 and Ser28 under the frame of RAS-MAPK signaling pathway activation (Macdonald et al, 2005). The exact mode of action and outcome of 14-3-3 binding remains to be determined; however, the recruitment of chromatin remodeling complexes and the integrants of the transcriptional machinery downstream of the signaling pathway may be the consequence of 14-3-3 phospho-H3 recognition. Therefore, upon activation of RAS-MAPK signaling, MSK-directed phosphorylation of H3 at Ser10 and Ser28 may act as a molecular tag to be “read” by 14-3-3 proteins, in turn initiating transcriptional activation of specific genes by stabilizing and increasing the residency time of transcriptional protein complexes at the regulatory gene regions (Perez-Cadahia et al., 2009).

1.5 Mitogen- and stress-activated protein kinases 1 and 2 (MSK1/2)

The two kinase isoforms MSK1 and MSK2 are widely expressed proteins in tissues, including heart, brain, placenta, lung, liver, kidney and pancreas (Deak et al, 1998). They belong to a group of structurally related kinases called the AGC kinase

family. This group includes other kinases, such as p70 ribosomal S6 kinase (S6K), protein kinase B (PKB), protein kinase C-related kinase (PRK), p90 ribosomal S6 kinase (RSK) and serum- and glucocorticoid-inducible kinase (SGK) (Frodin M, 2002). MSKs were identified as belonging to this kinase family by homology searching using the MAPK-activated protein kinase-1 (MAPKAP-K1) N-terminal domain sequence (Deak et al, 1998). The isoforms of MAPKAP-K1 are unique in that they possess 2 distinct kinase domains within the single polypeptide, the N-terminal and C-terminal kinase domains. The role of the C-terminal kinase domain is to initiate the activation of the N-terminal kinase domain (Dalby et al, 1998; Vik & Ryder, 1997). The importance of the C-terminal kinase domain for MSK activation is evident by the finding that an inactivating mutation in the C-terminal kinase domain of MSK1 abolishes its activation (Deak et al, 1998). Human MSK1 encodes an 802 amino acid protein, while mouse MSK1 encodes an 863 amino acid protein. On the other hand, human MSK2 protein is 705 amino acids long, while mouse MSK2 encodes a 773 amino acid protein. Nevertheless, MSKs are fairly conserved. Human MSK1 and MSK2 share 75% amino acid sequence identity, while human and mouse MSK2 share 90% amino acid sequence identity (Deak et al, 1998).

1.5.1 Activation of MSKs through signal transduction pathways

MSKs are activated *in vivo* by 2 major signaling cascades; the RAS-MAPK and p38 stress kinase signal transduction pathways. Activation of the RAS-RAF-MEK-ERK signaling pathway with stimuli such as growth factors (EGF) and phorbol esters (TPA) leads to activation of MSK1 and MSK2. Using the inhibitors of TPA-induced RAS-MAPK pathway such as PD-184352, PD-98059 and UO126, it has been elucidated that MSKs are directly phosphorylated by activated ERKs (Wiggin et al, 2002; Davie, 2003).

On the other hand, MSK activation can be achieved through stimuli such as UV-irradiation and anisomycin (Zhong et al, 2001; Soloaga et al, 2003). This MSK activation is mediated by stress-activated protein kinase-2 (SAPK2)/p38 kinase as evident from studies utilizing the inhibitor SB-203580, which blocks the activation of SAPK2 (Deak et al, 1998; Davie, 2003). Once either the RAS-MAPK or p38 stress kinase signaling pathways are triggered, MSK1 is phosphorylated by activated ERKs or p38 kinase at threonine residues (Thr 581 and Thr 700 for hMSK1) in the activation loop of the C-terminal kinase domain and a serine residue in the linker region (Ser 360). This phosphorylation event leads to an autophosphorylation of a serine residue in the hydrophobic motif of MSK1 (Ser 376) by the C-terminal kinase domain (Figure 6).

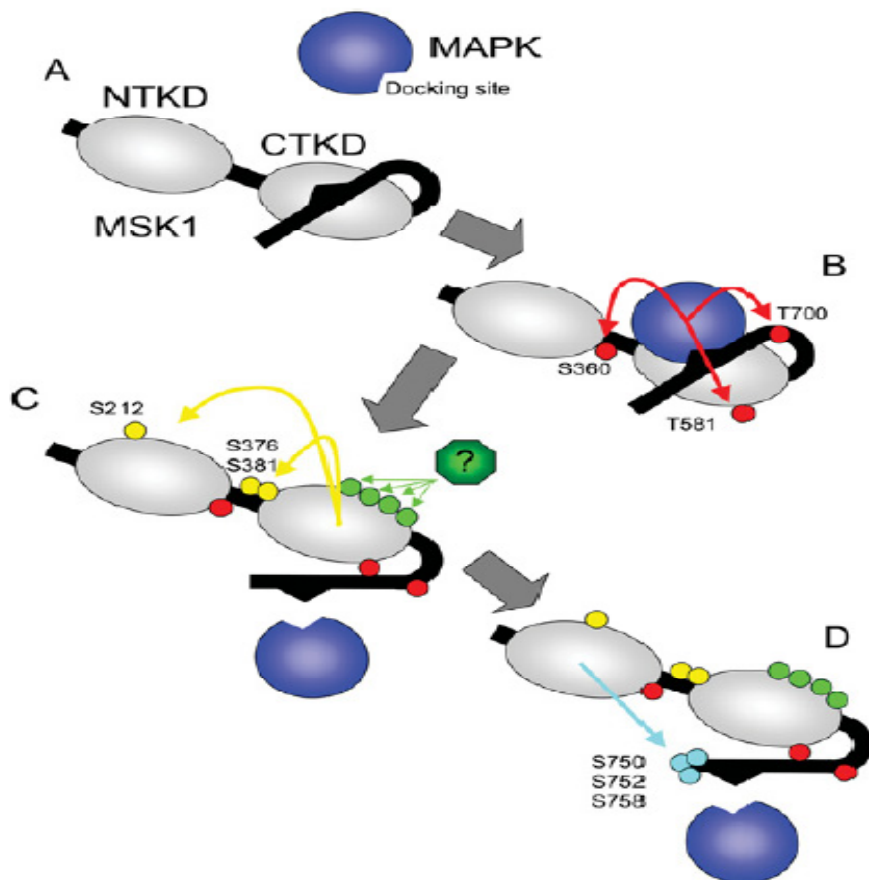


Figure 6: MSK1 activation.

Inactive MSK1 (A) is not phosphorylated. Active ERK1/2 or p38 MAPK bind to the docking motif, phosphorylating Ser360, Thr581 and Thr700 (red circles; B) Thr581 is in the activation loop of the C-term. kinase domain and its phosphorylation may be required for active confirmation of the activation loop. Thr700 is proposed to lie in a hinge region between the C-term. kinase domain. MSK1 is also phosphorylated on four sites by an unidentified kinase (green circles). The activated C-term. kinase domain then activates the N-term. kinase domain via the phosphorylation of Ser212, Ser376 and Ser381 (yellow circles; C) Once activated, the N-term. kinase domain is able to phosphorylate substrates, and additionally phosphorylates three sites, Ser750, Ser752 and Ser758 (blue circles; D) at C-terminus of MSK1. *The text and the figure were reproduced with permission from (McCoy et al., 2007).*

This intramolecular phosphorylation of the serine residue in the hydrophobic motif promotes phosphorylation of the serine residue in the activation loop of the N-terminal kinase domain of MSK1 (Ser 212) leading to full activation of the enzyme (Wiggin et al, 2002). It can be assumed that MSK2 undergoes similar activation steps as MSK1. Furthermore, stimuli such as FGF, NGF, TNF, TGF- β , neurotrophins, lysophosphatidic acid, lipopolysaccharides, IFN- α and erythropoietin have all been reported to activate MSK1 (Deak et al, 1998; Abecassis et al, 2004; Arthur et al, 2004; Schuck et al, 2003; Li et al, 2004; Caivano & Cohen, 2000; Wierenga et al, 2003), and possibly MSK2; most of these stimuli are believed to activate either the RAS-MAPK signal transduction pathway and/or the p38 kinase signaling cascade or other signaling events. Activation of MSKs by numerous stimuli indicates that these kinases have roles in modulation of multiple cellular functions.

1.5.2 MSK substrates

MSKs are predominantly nuclear proteins; however, a portion of MSKs is localized to the cytosol of mouse fibroblasts and HEK 293 cells (Deak et al, 1998). Cytosolic MSK1 phosphorylates eIF4E-binding protein 1 (4E-BP1) at Ser 64 after UV-irradiation. Normally, 4E-BP1 binds strongly to eIF-4F on the mRNA cap impeding the formation of a functional eIF-4F complex necessary for initiation of translation. Once 4E-

BP1 is phosphorylated, it dissociates from eIF-4F relieving the translational block. Further experiments involving 4E-BP1 and MSKs need to be carried out to elucidate a possible mechanism for UV-promoted tumorigenesis and the role MSKs could be contributing to this process (Liu et al, 2002). Nuclear MSKs phosphorylate a range of targets including histone H3 at Ser 10 and Ser 28 and HMGN1 (formerly named HMG-14) at Ser 6, 20 and 24 in response to mitogens and stress-stimuli. Studies with single MSK1 or MSK2 knockout cells and double MSK knockout cells showed complete abolishment of HMGN1 phosphorylation at Ser 6 in response to TPA and anisomycin, while H3 phosphorylation at Ser 10 and Ser 28 was severely reduced. The remaining H3 phosphorylation detected in the MSK knockout was presumably due to mitotic phosphorylation of H3 in late G2 phase of the cell cycle (Soloaga et al, 2003). Nuclear MSKs have been shown to phosphorylate various transcription factors including cyclic AMP-responsive element binding protein (CREB) and ATF1. Mitogen-mediated activation of the RAS-MAPK signaling pathway or stress-induced p38 kinase pathway leads to phosphorylation of CREB at Ser 133 and ATF1 at Ser 63. MSK1/2 double knockout cells show complete abolishment of phosphorylation of CREB at Ser 133 and ATF1 at Ser 63 after stress induction. In addition, MSK double knockout cells show great reduction of CREB and ATF1 phosphorylation after mitogen induction; however, the phosphorylation is not completely abolished. It has been shown that this residual phosphorylation can be blocked by PD-184352 suggesting that this phosphorylation event could be catalyzed by another ERK-activated kinase in the absence of MSKs (Wiggin et al, 2002; Arthur & Cohen, 2000). As previously mentioned, MSKs, more specifically MSK1, can be potently activated by the p38 stress kinase pathway. UV-irradiation of

mouse epidermal JB6 cells stimulates activation of MSK1 and subsequent phosphorylation of targets, including AKT (PKB) at threonine 308 and Ser 473, BAD at Ser 112 (*in vitro*) and STAT3 at Ser 727 (Nomura et al, 2001; She et al, 2002; Zhang et al, 2001). Cells expressing N-terminal or C-terminal kinase dead mutants of MSK1 showed reduced phosphorylation of AKT, BAD and STAT3 after UV-irradiation. Moreover, a preferential MSK1 inhibitor, H89, suppressed the phosphorylation of STAT3 at Ser 727 (Zhang et al., 2001). Further, erythropoietin-activated-MSK1 has been reported to phosphorylate STAT3 at Ser 727 in erythroid cells. Erythropoietin activates MSK1 via an ERK-dependent pathway as judged by inhibitor studies that elucidated the p38 kinase pathway was not involved (Wierenga et al., 2003). Altogether, MSK1 mediates phosphorylation of STAT3 at Ser 727 via the RAS-MAPK and p38 stress kinase pathways, implicating its role in mitogen- and stress-induced transduction of signals that possibly will affect the DNA binding ability of STAT3, thereby contributing to its transcriptional activity. Furthermore, nuclear MSK1 phosphorylates the p65 subunit of NF- κ B at Ser 276 in response to TNF (Vermeulen et al., 2003), as well as the transcription factor ER81 at Ser 191 and Ser 216 (Janknecht, 2003).

1.5.3 Function of MSKs

As previously mentioned, MSK1 has been implicated in regulation of translational control by phosphorylation of 4E-BP1, a crucial protein involved in the release of translational block after UV-irradiation (Liu et al., 2002). Additionally, MSKs are involved in the transcriptional activation of genes, including the inflammatory gene interleukin-6 (*IL-6*) and IE genes such as *Fos* and *Jun* (Soloaga et al., 2003; Vermeulen et al., 2003). H89, a member of the H-series of protein kinases and a potent inhibitor of

MSK1, inhibits TPA- and EGF-stimulated H3 phosphorylation and expression of immediate-early genes, including *Fos*, *Jun*, *Myc* and urokinase plasminogen activator (*uPA*) in mouse fibroblasts and *Hras*-transformed mouse fibroblasts (Thomson et al., 1999). Interestingly, H89 inhibition of TPA-induced immediate early gene expression and H3 phosphorylation at Ser 10 was particularly acute in oncogene-transformed cells (Strelkov and Davie, 2002). H89 also inhibited MSK1-directed phosphorylation of H3 at Ser 10 and Ser 28 in mouse epidermal JB6 cells treated with ultraviolet B (Zhong et al., 2001). Although H89 inhibits MSK1's ability to phosphorylate H3, it does not inhibit MSK1 phosphorylation activity towards CREB (Thomson et al., 1999). However, knocking out the expression or inhibiting the activation of MSK1/2 compromises the expression of IE genes, suggesting that MSK-mediated phosphorylation of H3 is an important step for proper IE gene expression (Strelkov and Davie, 2002). Mitogen-induced recruitment of MSK1 to the promoter region of *FOS* is mediated by the transcription factor ELK-1, suggesting that MSK is recruited to specific genomic regions via transcriptional activators (Zhang et al., 2008). However, MSK recruitment might be cell-type and context dependent and not dependent exclusively on transcription factors, but rather by multiprotein complexes (Drobic et al., 2006). As transcription factors, non-histone chromosomal proteins and histones are MSK substrates; activation of these kinases may influence transcription at multiple levels. At the level of transcription initiation MSKs may phosphorylate H3, which in collaboration with other histone modifications, may promote remodeling of nucleosomes at regulatory DNA elements, such as promoters and enhancers, allowing transcription factor access and formation of the pre-initiation transcription machinery. Further, MSK phosphorylation of transcription

factors (CREB, ATF1 and the p65 subunit of NF- κ B) may alter their ability to bind to their target DNA and to recruit specific coactivators. Also, MSK-mediated phosphorylation of the H3 tail may promote interactions with coactivators, other chromatin modifying enzymes and SWI/SNF chromatin remodeling complexes (Arthur, 2008). It is still unclear how MSKs integrate various types of signals and account for target gene and cell type-dependent specificity. As mentioned previously, it was reported that MSKs mediate EGF-induced, but not TNF α -induced phosphorylation of H3S10 at the *Fos* promoter (Anest et al., 2004) and VEGF-A-induced H3S10 phosphorylation of an upstream, but not the enhancer region of *FOSL1* (Zippo et al., 2007). Also, some stimuli preferentially activate one MSK isoform over the other. For example, in mouse dorsal striatum, cocaine strongly activated MSK1, but not MSK2, and the MSK1 knockout was sufficient to abolish CREB and H3 phosphorylation (Brami-Cherrier et al., 2005).

1.5.4 Physiological roles of MSKs

Activation of RAS-MAPK and p38 kinase signaling pathways results in transcriptional induction of various immediate-early genes. Regulation of IE gene induction by ERK and p38 cascades is partly achieved through direct phosphorylation of transcription factors, such as ETS, MEF2 and AP1 complexes (Turjanski et al., 2007). However, a proportion of these IE genes, such as *Fos*, *Dusp1* and *Nur77* are also regulated by CREB (Mayr and Montminy, 2001). MSKs are known to regulate CREB-dependent IE gene induction downstream of ERK and p38 signaling pathways (Arthur, 2008). Nevertheless, MSK knockout mice show no severe phenotype; in fact these mice are fertile and have no obvious developmental problems (Wiggin et al., 2002). Despite these observations, specific cell types from MSK knockout mice are deficient in mitogen

or stress induced phosphorylation of CREB, ATF1 and histone H3, which in turn caused reduction in transcription of specific IE genes (Wiggin et al., 2002). Misregulation of MSK activity has been linked to only two disease states up to now. Increased activity of MSK1 and MSK2 has been observed in lesional psoriatic epidermis, along with corresponding increases in CREB and ATF1 phosphorylation levels when compared to non-lesional skin (Funding et al., 2007; Funding et al., 2006); (Funding et al., 2007). Inhibition of IL1 β -induced MSK1/2 activation was achieved in human keratinocytes with the use of dimethylfumarate (DMF), a reagent that is commonly used to treat psoriasis. DMF also abolished phosphorylation of CREB, ATF1 and NF κ B p65 (Gesser et al., 2007). On the other hand, MSK1 expression was reduced in the striatum of post-mortem Huntington's disease (HD) patients and R6/2 mice, an animal model used for studying HD (Roze et al., 2008). Under these conditions, H3S10 phosphorylation was impaired, but not CREB phosphorylation (Roze et al., 2008), suggesting an additional level of control that might determine signal specificity. Furthermore, MSK activation has been implicated in various other physiological events, including immunity and neuronal function.

1.5.5 MSKs in immunity

The role of MSKs in the regulation of inflammatory genes, such as *IL-1*, *IL-6*, *IL-8* and *Cox-2* is characterized by transcriptional activation of NF κ B and CREB, as well as phosphorylation of H3 at the nucleosomes of regulatory regions of inflammatory genes (Vermeulen et al., 2003). It has been reported that anti-inflammatory agents, such as glucocorticoids can alter the subcellular distribution of nuclear MSK1 to the cytoplasm. This MSK1 redistribution prevents MSK1 recruitment to promoter regions of

inflammatory genes causing impaired phosphorylation of NFκB p65 and abolishment of H3 phosphorylation (Beck et al., 2008). Furthermore, it has been shown that MSKs are involved in negative feedback pathways required for prevention of uncontrolled inflammation in macrophages (Ananieva et al., 2008). In response to LPS, the expression of *DUSP1* (dual specificity phosphatases 1) and anti-inflammatory cytokine interleukin 10 (*IL-10*) is upregulated in macrophages derived from bone marrow of wild type mice and not from the double MSK knockout mice (Ananieva et al., 2008). DUSP1, also known as MAPK phosphatase 1, regulates the activity of p38 MAPK, and is therefore indirectly capable of mediating the activity of MSKs. Since MSKs target both pro- and anti-inflammatory genes, these kinases might be important for regulation of equilibrium in the immune system (Ananieva et al., 2008).

1.5.6 MSKs and behaviour

It has been well documented that both ERK signaling and CREB play crucial roles in IE gene induction in neurons, affecting differentiation and survival of neurons, as well as certain neuronal processes, such as long term potentiation (LTP) and memory (Sweatt, 2004). These observations implicate that MSKs might mediate specific functions in neurons, since ERKs directly activate MSKs in order to phosphorylate CREB. Indeed, it has been shown that MSK1 can be activated in response to neurotrophins via ERK1/2 cascade in cortical neurons (Arthur et al., 2004). Interestingly, MSK2 does not appear to be activated by neurotrophins in cortical neurons. The single MSK1 knockout was able to abolish neurotrophin-induced phosphorylation of CREB to the same extent as the double MSK1/2 knockout, while the single MSK2 knockout had no effect (Arthur et al., 2004). These observations are in contrast to other cell types, such as macrophages and

fibroblasts, where single knockout of either MSK1 or MSK2 could partially impair CREB phosphorylation, and where the double MSK1/2 knockout was required to completely abolish phosphorylation of CREB (Wiggin et al., 2002). Furthermore, lack of CREB phosphorylation in MSK1 or MSK2 knockouts reduced the BDNF-induced transcription of CREB-dependent IE genes *Fos*, *Nurr1* and *Dusp1* in cortical neurons (Arthur et al., 2004). Furthermore, elevated cAMP levels and PKA activation can lead to activation of ERK1/2 in neurons, where cAMP signaling and CREB phosphorylation have been implicated in hippocampal-dependent memory (Mantamadiotis et al., 2002). It has been reported that hippocampal-dependent tasks and long term potentiation (LTP) inducing stimuli resulted in the induction of CREB-dependent IE genes (Pittenger et al., 2002). Consistent with this, MSK1 can be activated via ERK1/2 in the hippocampus in response to fear conditioning stimulus in mice (Sindreu et al., 2007). Furthermore, histone H3 phosphorylation has been detected in neurons and has been suggested to act as an epigenetic mark during LTP and memory formation (Chwang et al., 2006); (Levenson and Sweatt, 2005). It has been shown that fear conditioning stimuli lead to increases of CREB and H3S10 phosphorylation in the hippocampus and that these phosphorylation events are abolished by the knockout of MSK1 (Chwang et al., 2007). Also, MSK1 knockout mice have been found to have impaired responses in fear conditioning, passive avoidance and water maze tests, all of which require hippocampal long term memory (Chwang et al., 2007). Moreover, MSKs have been shown to be involved in the response to cocaine in mice. Phosphorylation of CREB and H3S10 in the striatum of MSK1 knockout mice was prevented following cocaine administration (Brami-Cherrier et al., 2005). Further, the locomotor sensitization, which measures increased activity of mice

following repeated cocaine injections, was reduced in MSK1 knockout mice (Brami-Cherrier et al., 2005). These observations imply that MSK1 might have a role in addiction; however, more research is required to determine whether MSK1 inhibition can promote or block addiction.

1.5.7 MSKs in tumorigenesis

Steady-state levels of phosphorylated H3S10/S28 are elevated in *Hras*-transformed mouse fibroblasts, and this correlated with increased activity of MSK1 in the transformed cells (Drobic et al., 2004). Also, *Hras*-transformed mouse fibroblasts exhibit a higher metastatic potential when compared to parental mouse fibroblasts (Egan et al., 1987). Furthermore, it has been established that EGF-mediated phosphorylation of H3S10 is indispensable for neoplastic cell transformation (Choi et al., 2005). In mouse epidermal-JB6 cells that over-express wild type H3, EGF-induced cell transformation was promoted, whereas in cells over-expressing S10A or S28A H3 mutants, cell transformation was suppressed (Choi et al., 2005). Consistent with these observations, it has been shown that MSK1 has a role in cell proliferation and transformation. The two tumor promoting agents, TPA and EGF, which are widely used to study cell potential for malignant transformation, were able to induce transformation of JB6 mouse cells via MSK1 activation (Kim et al., 2008). Inhibition of MSK1 activity by H89 or knockdown with siRNA resulted in impaired TPA- and EGF-mediated JB6 cell colony formation. Cell proliferation was inhibited in MSK1 knockdown cells when compared to MSK1 wild type cells. Further, TPA- and EGF-induced phosphorylation of H3S10, as well as AP-1 activation was increased in cells over-expressing wild type MSK1; however, these phosphorylation/activation events were abolished in MSK1 knockdown cells (Kim et al.,

2008). Therefore, MSK1 was shown to play an important role in cell transformation through phosphorylation of H3S10 and AP-1 activation (Kim et al., 2008).

2.0 OBJECTIVES, RATIONALE AND HYPHOTHESES

The main objective of the studies presented in this thesis was to determine the role of the MAPK-activated H3 kinase, MSK1 in the expression of inducible immediate-early genes. Since MSK1 is activated by the RAS-MAPK signaling pathway (Davie, 2003), the project focused on two major areas: deciphering the effects of upregulated RAS-MAPK signaling on the activation status of MSK1 and examining the role of MSK1 in chromatin remodeling that leads to expression of RAS-MAPK responsive genes.

Previous studies from our lab have shown that upregulated RAS-MAPK signaling in oncogene-transformed cells causes altered chromatin structure with elevated phosphorylation levels of MSK1 substrates, histone H3 and HMGN1 (Chadee et al., 1999). To understand the effects of upregulated RAS-MAPK signaling on the chromatin structure in oncogene-transformed cells, MSK1 activity was examined in parental and *Hras*-transformed cells. Also, we investigated the protein expression and sub-cellular localization of MSK1. We hypothesized that oncogene-mediated activation of the RAS-MAPK pathway elevates the activity of MSK1, resulting in the increased steady-state levels of phosphorylated H3, which may contribute to the chromatin de-condensation and aberrant gene expression observed in these cells.

We chose the parental (10T1/2) and *Hras*-transformed (Ciras-3) mouse fibroblasts as the cell systems to test the above stated hypothesis. The parental 10T1/2 cells were stably transformed with T-24 Ha-*ras* in order to generate the Ciras-3 cell line (Egan et al., 1987). The parental 10T1/2 cells are not tumorigenic or metastatic, whereas *Hras*-transformed Ciras-3 cells are highly tumorigenic and metastatic (Egan et al., 1987).

Therefore, these two cell lines are useful for studying the effects of RAS-MAPK signaling in a “normal” versus “cancer-like” scenario.

The other major area of interest was the role of MSK1 in the expression of IE genes. Previous studies have implicated MSK1 in regulation of IE genes, such as *Jun*, *Fos* and *Myc* (Strelkov and Davie, 2002). However, the mechanism of IE gene regulation by MSK1 is not clearly defined. Therefore, the objectives for this part of the project were: 1) to examine the associations of MSK1 with other chromatin modifying and remodeling enzymes that have been implicated in transcriptional activation of genes; 2) to determine if MSK1 is recruited to genomic regions of IE genes under the frame of RAS-MAPK signaling; 3) to assess the importance of MSK1 on the recruitment of other factors required for transcriptional activation and 4) to directly assess the role of MSK1 in the expression of IE genes in parental and *Hras*-transformed cells. We hypothesized that MSK1 establishes H3 phosphorylation at the regulatory regions of IE genes, which is crucial for subsequent recruitment of factors necessary for proper transcriptional gene activation.

The genes chosen for the study were *Jun*, *Cox-2* and *FosII*. Cell type- and stimulus-dependent expression of *Jun* and *Cox-2* has been reported to be under MSK1 regulation (Soloaga et al., 2003), whereas *FosII* strongly responds to RAS-MAPK signaling (Verde et al., 2007) and was chosen as a candidate gene for our study. The gene products of *Jun*, *Cox-2* and *FosII* have all been implicated in tumorigenesis (Verde et al., 2007); thus, deciphering the extent of MSK involvement in their expression is beneficial to understanding cancer.

3.0 MATERIALS AND METHODS

3.1 Cell lines and cell culture conditions

The parental mouse fibroblast 10T1/2 cell line was obtained from the American Type Culture Collection (ATCC) (Rockville, MD). The Ciras-3 cell line was derived from 10T1/2 by transfection with the T24 H-*ras* oncogene (Egan et al., 1987). The Ciras-3 cell line contains a constitutively overexpressed T24 H-*ras* oncogene.

Mouse fibroblast 10T1/2 and Ciras-3 cells were grown at 37°C in a humidified atmosphere containing 5% CO₂ in α -MEM medium supplemented with 10% (v/v) fetal bovine serum (FBS), penicillin G (100 units/mL), streptomycin sulfate (100 μ g/mL) and amphotericin B (250 ng/mL). Human embryonic kidney (HEK) 293 cells were grown in DMEM medium supplemented with 10% (v/v) fetal bovine serum. When cells reached 80-90% confluence they were trypsinized and an aliquot containing one tenth the number of cells was added to a new plate containing fresh medium. For 150 mm cell culture plates, cells were seeded at approximately 4×10^5 cells per plate.

To induce RAS-MAPK signaling, 90-95% confluent 10T1/2 and Ciras-3 cells were serum starved for 24 and 48 hours, respectively, in α -MEM medium supplemented with 0.5% FBS and treated with 100 nM 12- O-tetradecanoyl-phorbol-13-acetate (TPA) [Sigma] for 15 or 30 min. When required, 10T1/2 and Ciras-3 cells were pre-treated with 10 μ M H89 (Calbiochem) for 30 min or with 100 nM RpcAMP (Sigma) for 1 h prior to TPA treatment.

When required, 75% confluent HEK293 cells were transfected with 0.5 μ g of pCMV5-FLAG-MSK1 construct (gift from Dr. J.S. Arthur, University of Dundee, UK) using DreamFect transfection reagent as per manufacturer's instructions (OZ

Biosciences, France). Non-transfected and transfected cells were harvested 48 hours post-transfection and the resulting cellular extracts were used for subsequent immunoprecipitation experiments.

3.2 Generation and maintenance of MSK1 stable knockdown mouse fibroblasts

(collaboration with Dr. S KP Kung and Jenny Yu)

Empty GIPZ lentiviral vector and the GIPZ Lentiviral shRNA mir clones for the mouse MSK1 (clone V2LMM_54318-SENSE 2240, Thermo Scientific Open Biosystems, USA) were obtained from the Biomedical Functionality Resource at the University of Manitoba. To produce replication incompetent lentiviral vector particles for mouse fibroblasts transduction, we transfected the GIPZ vector, the packaging vector and the VSV-G env-expressing plasmid into HEK293T cells using the BD CalPhos™ Mammalian Transfection kit, as described previously (Kung et al., 2000; Laemmli, 1970). To generate stable MSK1 knockdown 10T1/2 and Ciras-3 mouse fibroblasts, we seeded 5×10^4 cells in a 24-well plate 24 hours before transduction. Medium was aspirated and replaced with 250 μ l of the lentiviral supernatant (at 1×10^6 TU) and 8 μ g/ml of Polybrene. After incubation for 2 hours at 37°C in 5% CO₂, the culture medium that contained the lentiviral vectors was removed. The transduced cells were cultured in 1 ml of fresh media for 3 days before they were selected for puromycin resistance (at a final concentration of 8 μ g/ml). Freshly prepared selective media was added every 2-3 days and the cells were monitored for cell survival by light microscopy, and/or for TurboGFP expression by flow cytometry using BD FACSCalibur. After 10 days, puromycin resistant cells were expanded in puromycin-containing media until the desired confluence was reached.

3.3 Flow cytometric analysis of cells

The percentage of cells in the different stages of the cell cycle was determined by fluorescent-activated cell sorting (FACS). 3×10^6 cells were harvested by trypsinization and washed twice with 5 ml of 1XPBS, pH 7.3. The cells were centrifuged at 1000 x g and the cell pellet was resuspended in 2 ml of 1XPBS, pH 7.3. The cell suspension was added drop-wise while vortexing to 4 ml of pre-chilled 70% ethanol. The ethanol-fixed cells were pelleted at 1000 x g for 5 min and the supernatant was discarded. The cells were resuspended in 2 ml of 1XPBS, pH 7.3 containing 5 $\mu\text{g/ml}$ RNase A (Sigma) and incubated at 37°C for 30 min. After the incubation, 1 μl of the 10 mg/ml ethidium bromide solution was added to the tube and the cells were vortexed. The tubes were wrapped in aluminum foil and sent for FACS analysis (Dr. E. Rector).

3.4 Preparation of cellular extracts

Cells were harvested and lysed in 400 μl of ice-cold Nonidet P40 (NP-40) buffer [150 mmol/L NaCl, 50 mmol/L Tris-HCl (pH 8.0), 0.5% Nonidet P40, 1 mmol/L phenylmethylsulfonyl fluoride, 1 mmol/L sodium orthovanadate, 1.0 mmol/L NaF, 1.0 $\mu\text{g/mL}$ leupeptin, 1.0 $\mu\text{g/mL}$ aprotinin, and 25 $\mu\text{mol/L}$ β -glycerophosphate]. The lysed suspension was sonicated twice for 5 seconds. The resulting cell extracts were subjected to centrifugation at 10,000 x g for 10 minutes at 4°C, and the supernatant was saved. The protein concentration of the supernatant was determined using the Bio-Rad Protein Assay as per manufacturer's instructions (Bio-Rad Laboratories, Hercules, CA).

3.5 Immunoprecipitations

For immunoprecipitations in HEK293 cells, 500 μg or 1 mg of total cell extract were incubated with 20 μg of anti-MSK1 antibodies overnight at 4°C. 20 μl of protein G-

Sepharose beads were added the following day and incubated for 2 h at 4°C. The beads were washed with ice-cold NP-40 buffer two times. Input (20 µg), bound, un-bound and nonspecific (no antibody IP, beads only) fractions were resolved on SDS-10%-PAGE and immunoblotted with indicated antibodies. In some instances, non-specific antibodies (anti-FLAG) were used in control immunoprecipitations. For immunoprecipitations in cycling 10T1/2 and Ciras-3 cells or in untreated and 30' TPA treated 10T1/2 cells, 20 µg of anti-MSK1, 15 µg of anti-BRG1 and 10 µg of anti-14-3-3ζ antibodies were incubated with 1 mg of total cell extract overnight at 4°C. Further processing of the samples was as described above. For sequential immunoprecipitations, 30 min TPA-treated 10T1/2 cells were treated with the membrane-permeable protein cross-linking reagent dimethyl 3,3'-dithiobispropionimidate-2-HCl (DTBP, 2mM, Pierce) for 30 min at 37°C. The reaction was stopped with ice-cold 0.1 M Tris-HCl (pH 7.5) and the cells were lysed and incubated with anti-MSK1 antibodies as described above. The immunoprecipitated proteins were eluted with 0.2 M glycine (pH 2.6) for 10 min at room temperature and re-immunoprecipitated with antibodies against BRG1.

3.6 Polyacrylamide gel electrophoresis (PAGE)

Proteins were separated in SDS polyacrylamide slab gels (Laemmli, 1970). The running gel was comprised of 10% or 15% acrylamide, which was added from a 30% (w/v) stock, 0.1% (w/v) SDS and 375 mM Tris, pH 8.8. To this solution 0.15% (w/v) ammonium persulfate and 0.03% (v/v) TEMED was added and the gel was poured in the glass plates and allowed to polymerize for approximately 1 hour. The stacking gel was comprised of 4% (w/v) acrylamide, 0.1% (w/v) SDS and 125 mM Tris, pH 6.8, 0.15% (w/v) ammonium persulfate and 0.08% (v/v) of TEMED. The stacking gel was poured on

top of the running gel and allowed to polymerize for approximately 30 min. The gels were run on a Mini-Protean® 3 Cell apparatus (BioRad) towards the anode at 125 V for approximately 1 hour. The running buffer was comprised of 193 mM glycine, 1% (w/v) SDS, 25 mM Tris, pH 8.3. The sample loading buffer for SDS-PAGE (6 x stock: 277 mM SDS, 396 mM Tris, 402 mM dithiothreitol, 40% (v/v) glycerol, 0.4% bromophenol blue, pH 6.8) was added to the samples prior to electrophoresis. Samples were boiled for 5 min, quickly spun down in a centrifuge and loaded on the gel. A protein standard (Rainbow Marker, Amersham) was also run to track the migration of different molecular weight proteins. Coomassie Blue staining was used to visualize the proteins analyzed by SDS-15%-PAGE, while the transfer of proteins to nitrocellulose membrane and immunochemical staining with various antibodies allowed analysis of the proteins separated by SDS-10%-PAGE.

3.7 Detection of proteins by immunoblotting

Once the proteins were separated by SDS-PAGE and transferred to a nitrocellulose membrane, immunoblotting with specific antibodies was used to detect particular proteins of interest. Nitrocellulose membranes were blocked with 5% (w/v) non-fat dry milk in 0.05% TTBS (0.05% Tween-20, 0.1M Tris-HCl, pH 8.0, 0.3 M NaCl) for 1 hour at room temperature. The membranes were then incubated with antibodies against MSK1 (1:2000; Sigma), MSK2 (1:700; Zymed), BRG1 (1:2000-1:5000; Milipore), PCAF (1:800; AbCam), HDAC1 (1:1000; ABR), Sp3 (1:1000; Milipore), NFκB p65 (1:1000; Milipore), 14-3-3ζ (1:2000; SantaCruz), ERK1/2 (1:1000, Cell Signaling) or phospho-p42/p44 MAPK (1:1000; Cell Signaling) overnight at 4°C. The following day, the membranes were washed in 0.05% TTBS for 15 min. The membranes

were then incubated with a goat anti-rabbit antibody (1:3000) linked to horseradish peroxidase in 0.05% TTBS for 45 min. The membranes were washed again with 0.05% TTBS for 20 min. The Western Lightning™ Plus-ECL reagent (Perkin Elmer Lifesciences) was used as per manufacturer's instructions to detect the desired proteins.

3.8 Chromatin immunoprecipitation (ChIP/reChIP) assay

10T1/2 and Ciras-3 cells were treated with 1% formaldehyde for 10 min at room temperature. After harvesting, the cells were pelleted and resuspended in cell lysis buffer (5 mM PIPES pH 8.0, 85 mM KCl, 0.5% NP-40, 1 mM phenylmethylsulfonyl fluoride, 1 mM sodium orthovanadate, 1 mM NaF, 1 µg/mL leupeptin, 1 µg/mL aprotinin, and 25 mM β-glycerophosphate). After 10 min rotation at 4°C, the cellular material was spun at 2000 x g for 10 min to obtain the nuclei. The nuclear pellet was resuspended in MNase digestion buffer (10 nM Tris-HCl pH 7.5, 0.25 M sucrose, 75 mM NaCl, plus above indicated phosphatase/protease inhibitors) and the A260 was measured. In order to obtain □150bp DNA fragments, 2.5 units of MNase per A260 of nuclear suspension were added in the presence of 3 mM CaCl₂ and incubated at 37°C for 20 min. The MNase reaction was stopped by the addition of EDTA pH 8.0 (5 mM final concentration). In order to release nuclear material, the samples were adjusted to 0.5% SDS and rotated for 1 hour at room temperature. Insoluble material was pelleted at 2000 x g for 10 min and the soluble material was diluted to 0.1% SDS with radio-immunoprecipitation assay (RIPA) buffer along with the above mentioned phosphatase/protease inhibitors. 12 A260 of protein G-Sepharose (Pierce) pre-cleared 10T1/2 lysate was incubated with 12 µl of anti-MSK1 (Sigma, M5437) or anti-H3S10ph (Santa Cruz, sc-8656-R), anti-H3S28ph (Milipore, 07-145), anti-H3K9acK14ac (Milipore, 06-599), anti-14-3-3ε (Santa Cruz, sc-1020), anti-14-

3-3ζ (Santa Cruz, sc-1019), anti-BRG1 (Milipore, 07-478), anti-PCAF (AbCam, ab12188-50), anti-JUN (Santa Cruz, sc-1694), or anti-RNAPII S5ph (AbCam, ab5131-50) overnight at 4°C. Magnetic protein G Dynabeads (Invitrogen) were added for 2 h at 4°C. The specificity of the antibodies against H3S10ph and H3S28ph was determined in several ways. In immunoblot experiments, both antibodies only detected H3. Using commercial (Abcam) H3 peptides with S10ph or S28ph, these antibodies only recognized one or the other peptide. With regards to acetylation interfering with the detection of phospho-H3 modifications, our lab has previously reported that these antibodies detected S10ph or S28ph when H3 was hyperacetylated (Dunn et al., 2005). With regards to the MSK1 antibody, in immunoblot experiments we found that the antibody only detected one band. We have also shown that in MSK1 knockdown experiments, the MSK1 signals detected in immunoblot experiments were greatly diminished. For reChIP assays, after the elution of the first ChIP assay, the samples were diluted 10 times with reChIP dilution buffer (15 mM Tris-HCl pH 8.1, 1% Triton X-100, 1 mM EDTA, 150 mM NaCl) and subjected to the ChIP procedure again. Negative controls included performing ChIP/reChIP assays without adding antibody. DNA-protein fragments were processed as previously described (He S, 2005). Input and ChIP/reChIP DNAs were quantified using the PicoGreen assay. Equal amounts of input, ChIP (0.1 ng) or reChIP (0.05 ng) DNA were used to perform SYBR Green real time PCR on the iCycler IQ5 apparatus (BioRad). The enrichment was calculated as follows: Fold enrichment = $R^{(Ct_{input} - Ct_{ChIP})}$, where R is the rate of amplification. Values for each time point were normalized to time 0 values. Primer sequences were designed using the Oligo5 software and are shown in Table 1.

3.9 RNA isolation and real time RT-PCR analysis

Total RNA from untreated and treated 10T1/2 and Ciras-3 cells was isolated using the RNeasy Mini Kit (QIAGEN). 10 ng/μl of RNA in 80 μl volume was used for cDNA conversion (Invitrogen). Real time PCR reactions were performed on the iCycler IQ5 (BioRad) using SYBR Green for labeling. The fold change was normalized to GAPDH levels in untreated and treated samples.

Table 1: Primer sequences used to amplify ChIP DNA and cDNA

Jun (-711)	Primer Sequence 5' to 3'	Cox-2 (-493)	Primer Sequence 5' to 3'	Fosl1 (-1113)	Primer Sequence 5' to 3'
Forward	CGCAGCGGAGCATTACCTCA	Forward	AAATTAACCGGTAGCTGTGTG	Forward	TCACCAGACTCAGCCACTTAC
Reverse	CCATTGGCTTGCCTCGTTCTC	Reverse	CCGGGATCTAAGGTCCTAA	Reverse	GCCATCATAACCCCACT
Jun (-146)		Cox-2 (-111)		Fosl1 (-187)	
Forward	TTACCTCATCCCCTGAGCCTT	Forward	AAGCCTAAGCGGAAAGACAGA	Forward	CCCCCGTGGTCAAGTGGTT
Reverse	CCATTGGCTTGCCTCGTT	Reverse	GGCTGCTAATGGGAGAAC	Reverse	TGGCGGCTGCGGTTCTGACT
Jun (129)		Cox-2 (903)		Fosl1 (989)	
Forward	GGACTGTTTCCGTTTGTCT	Forward	AAACCGTGGGGAATGTATGAG	Forward	ACAATCGCGCTCCACATTCTC
Reverse	CAAATGCTCCCAAATACC	Reverse	CCAGTCCGGGTACAGTCACA	Reverse	CGCAGCTCCTCCCTCCC
Jun (1115)		Cox-2 (1982)		Fosl1 (2249)	
Forward	CCAAGAAGCTCGGACCTTCTCA	Forward	GCCTTCTCCAACCTCTCTAC	Forward	CCTATCCCCAGTACAGTCCC
Reverse	GGTGATGTGCCATTGCT	Reverse	ACTCACCTTCACACCCA	Reverse	ATCGCTGTTTCTTACCTGCTC
Jun (2953)		Cox-2 (4255)		Fosl1 (7676)	
Forward	TGGTTGAAAGCTGTATGAAGT	Forward	GACCCAGAGCTCCTTTCAAC	Forward	CAAGGGTAAGGGTGTGTC
Reverse	GGGTCCCTGCTTTGAGA	Reverse	GGGGGTGCCAGTGATAGAGT	Reverse	TCTAGAGCTGGCCTATCATAA
GAPDH	Primer Sequence 5' to 3'				
Forward	TTCCGTGTTCTACCCCAATGTGT				
Reverse	GGAGTTGCTGTTGAAGTCGCAGGAG				

3.10 H3 kinase assay

10T1/2 and Ciras-3 cells were lysed with NP-40 buffer, and the insoluble material was removed by centrifugation for 10 min at 10,000 x g. Cell cycle-matched total cell extracts (10 μg) were incubated with 2 μg of H3-H4 tetramer fraction isolated from mature chicken erythrocytes as described previously (Strelkov and Davie, 2002), 10 mmol/L MgCl₂, 1 μmol/L microcystin-LR and ± 10 μmol/L H89 for 10 minutes at 4°C. Reactions were started with the addition of 50 μmol/L ATP and 5 μCi of [γ-³²P]-ATP (3,000 Ci/mmol/L) and incubation at 30°C for 30 minutes. Reactions were stopped with

the addition of SDS-PAGE loading buffer and incubation on ice for 20 minutes. Furthermore, cell cycle-matched total cell extracts (500 µg) were incubated with 3.5 µg of anti-MSK1 antibody coupled to 10 µl of protein G-Sepharose at 4°C for 24 hours. The protein G beads were washed three times with 500 µl of buffer B and twice with buffer C (Thomson et al., 1999). The beads were then resuspended in buffer C containing already mentioned protease and phosphatase inhibitors, 5 µg H3-H4 tetramer and ± 10 µmol/L H89. Reactions were carried out as described above. The H3-H4 tetramer and MSK1 immunoprecipitates were analyzed by SDS-15%-PAGE, and visualization and quantification of signals were analyzed by autoradiograph and phosphorimager analysis.

3.11 MSK1 kinase assay

50 ng of purified active MSK1 (Milipore) was incubated with 1 µg of histone H3 (Roche Diagnostics) or H3-H4 fraction along with Mg²⁺/ATP solution and 5 µCi [γ -³²P]-ATP at 30°C for 15 minutes. The reaction was stopped by the addition of SDS-PAGE loading buffer and incubation on ice for 10 minutes. The samples were resolved by SDS-15%-PAGE. The gel was stained with Coomassie Blue stain. Visualization of the phosphorylation signal was detected by phosphorimager analysis and autoradiography.

3.12 Lysine acetyltransferase (KAT) assay

MSK1 immunoprecipitations from HEK293 cellular extracts were performed as previously described. The beads were resuspended in 10 µl of NP-40 buffer and 1 x KAT activity buffer (50 mM Tris-HCl pH 7.5, 50 mM sodium butyrate) in the presence of 0.5 µCi acetyl ³H CoA (Perkin Elmer Lifesciences) and 10 µg of mature avian erythrocyte histone preparation (Strelkov and Davie, 2002). The samples were incubated at 37°C for 30 min. 500 µg of HEK293 cellular extract and no antibody (beads only) IP were also

incubated with 0.5 μCi acetyl ^3H CoA and 10 μg of mature chicken erythrocyte histone preparation, as positive and negative controls, respectively. Incubating the samples on ice for 10 min stopped the KAT reaction. Each sample was spotted onto the P81 phosphocellulose paper and washed with 50 ml of the 50 mM Na_2CO_3 solution. After air-drying the samples for 20 minutes, each sample was placed in a vial containing 5 ml of scintillation fluid. Incorporation of ^3H within the histones (KAT activity) was measured by counting the amount of radioactivity as compared to blank and negative controls. When required, MSK1 IP samples and HEK293 cellular extracts were treated with 60 μM curcumin (Sigma) for 30 min at 37°C prior to the addition of ^3H -labeled acetyl-CoA. Furthermore, individual histone proteins, obtained by separating a total mature avian erythrocyte histone preparation via C18 reverse-phase HPLC as previously described (Shechter et al., 2007), were used as the substrates for KAT reactions.

3.13 Cellular Fractionation

Cellular fractionations were carried out with a slight modification as described previously (Sun et al., 2001). In brief, 10T1/2 and Ciras-3 cells were resuspended in Tris- NaCl-Mg^{2+} (TNM) buffer [100 mmol/L NaCl, 300 mmol/L sucrose, 10 mmol/L Tris-HCl pH 7.4, 2 mmol/L MgCl_2 and 1% thiodiglycol] containing the already mentioned protease and phosphatase inhibitors in the NP-40 buffer. Lysis of cells was performed by passage through a syringe with a 22-gauge needle. The cytosol and nuclei were isolated from lysed cells by centrifugation at 6000 x g. Isolated nuclei were inspected by microscopic analyses. The nuclei were resuspended in TNM buffer and nuclear extraction was performed by the addition of Triton X-100 to a final concentration of 0.5% and incubation on ice for 5 minutes. After centrifugation at 6000 x g for 10 minutes, the

supernatant, termed the Triton X-100-soluble fraction, was saved. The nuclear pellet was resuspended in TNM buffer with 0.5% Triton X-100, and this fraction was termed the Triton X-100-insoluble fraction. The resulting fractions were run (equal volume) on SDS-10%-PAGE gels, transferred to nitrocellulose membranes and immunochemically stained with antibodies of interest.

4.0 RESULTS

4.1 RAS-MAPK signaling is upregulated in *Hras*-transformed mouse fibroblasts

In order to evaluate the extent of RAS-MAPK signaling in parental and *Hras*-transformed mouse fibroblasts, cell cycle-matched 10T1/2 and Ciras-3 cells were used. Figure 7A shows that the majority of the 10T1/2 and Ciras-3 cells were in G1 phase of the cell cycle. Expression of the constitutively active c-Ha-*ras* oncogenes in Ciras-3 mouse fibroblasts is thought to result in the persistent stimulation of the RAS-MAPK pathway (Chadee et al., 1999). The relative activities of the RAS-MAPK pathway in these cells were evaluated by immunoblot analyses of ERK1 and ERK2 and their phosphorylated isoforms. Figure 7B shows that the steady state of activated phosphorylated ERKs was greater (approximately 6-fold) in Ciras-3 cells.

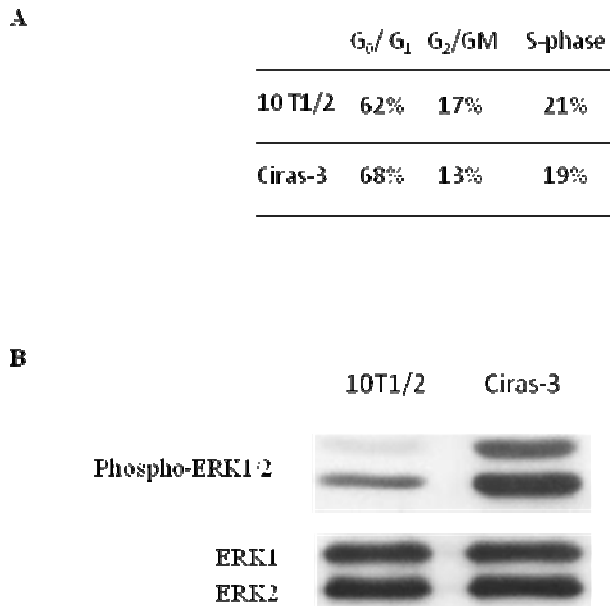


Figure 7: Increased levels of phosphorylated ERK1/2 in the *Hras*-transformed mouse fibroblasts.

A) Cell cycle distribution of 10T1/2 and Ciras-3 cells as determined by FACS analysis.

B) Total cellular extracts (20 μ g) from 10T1/2 and Ciras-3 mouse fibroblasts were resolved by SDS-10%-PAGE, transferred to a nitrocellulose membrane and immunochemically stained with anti-phospho-p44/42 MAPK (*top panel*) and anti-ERK (*bottom panel*) antibodies.

Over-expression of c-Ha-*ras* has also been reported to activate the p38 pathway (Deng et al., 2004). However, phosphorylated (activated) p38 was not observed in immunoblot analyses of cell extracts from cell cycle-matched parental and oncogene-transformed cells (Drobic et al., 2004). These data show that the steady-state activities of ERK1 and ERK2 are greater in the Ciras-3 than in the parental 10T1/2 cell line.

4.2 H3 kinase (MSK1) activity is elevated in *Hras*-transformed mouse fibroblasts

Because the relative activity of the H3 phosphatase, protein phosphatase 1, was similar in Ciras-3 and 10T1/2 (Chadee et al., 1999), it could be surmised that increased H3 kinase activity in the Ciras-3 cells would account for the increased levels of phosphorylated H3 at Ser10/28 (Chadee et al., 1999; Dunn et al., 2009). *In vitro* H3 kinase assays, with equal amounts of cell extracted protein from cell cycle-matched cells and H3-H4 tetramer as the substrate in the presence of ^{32}P , were performed. Figure 8 shows that H3 kinase activity in Ciras-3 cell extract was greater than that of the 10T1/2 cells.

10 μM H89	-	-	-	-	+	+	-
Ciras-3 extract	-	+	-	+	-	+	-
10T1/2 extract	+	-	+	-	+	-	-
H3-H4	-	-	+	+	+	+	+
Mg $^{2+}$ / ^{32}P -ATP	+	+	+	+	+	+	+

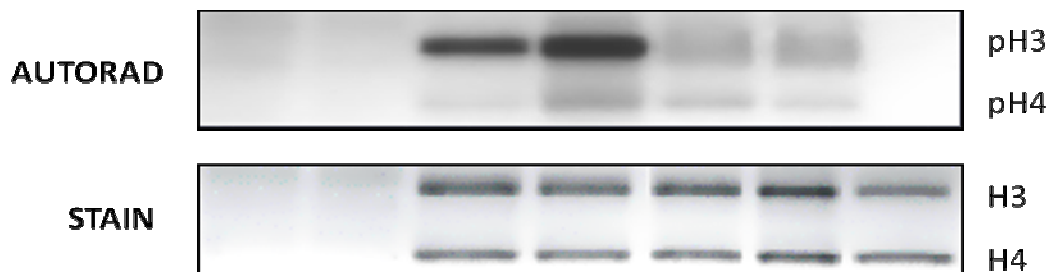


Figure 8: Histone H3 kinase activity in parental and *Hras*-transformed mouse fibroblasts.

Cell extracts (10 μg) isolated from 10T1/2 and Ciras-3 cells were incubated with the H3-H4 fraction (2 μg), $\text{Mg}^{2+}/\text{ATP}/[\gamma\text{-}^{32}\text{P}]\text{ATP}$, and the presence or absence of H89. Samples were resolved by SDS-15%-PAGE. The gels were analyzed by Coomassie Blue staining (*stain; bottom panel*) and autoradiography (*autorad; top panel*).

A 3-fold increase in H3 kinase activity in the Ciras-3 cell extracts (average of three separate preparations) was observed when compared to H3 kinase activity from 10T1/2 cell extracts. Histone H4 was also weakly labeled in this assay. As a control, no H3 kinase activity was detected when either the histone substrate or cell extract was absent. H89 is a potent inhibitor of MSK1 (Thomson et al., 1999). To determine whether the H3 kinase activity was due to MSK1, the Ciras-3 and 10T1/2 cell extracts were pre-incubated with H89. Presence of the kinase inhibitor significantly reduced the H3 kinase activity in both cell extracts (Figure 8). The remaining H3 kinase activity may be due to Aurora B, the mitotic H3 kinase. It was observed that in contrast to MSK1, Aurora B was relatively insensitive to H89 inhibition in the *in vitro* kinase assays (Drobic et al., 2004). However, H89 is also a potent inhibitor of protein kinase A, which may also phosphorylate H3 (Davies et al., 2000; Salvador et al., 2001). To directly test whether the MSK1 H3 kinase activity was greater in Ciras-3 cells, MSK1 was immunoprecipitated under high stringency conditions from the cell extracts and assayed for H3 kinase activity. Figure 9 shows that MSK1 activity was greater in the immunoprecipitated Ciras-3 fraction than from the 10T1/2 cell extract.

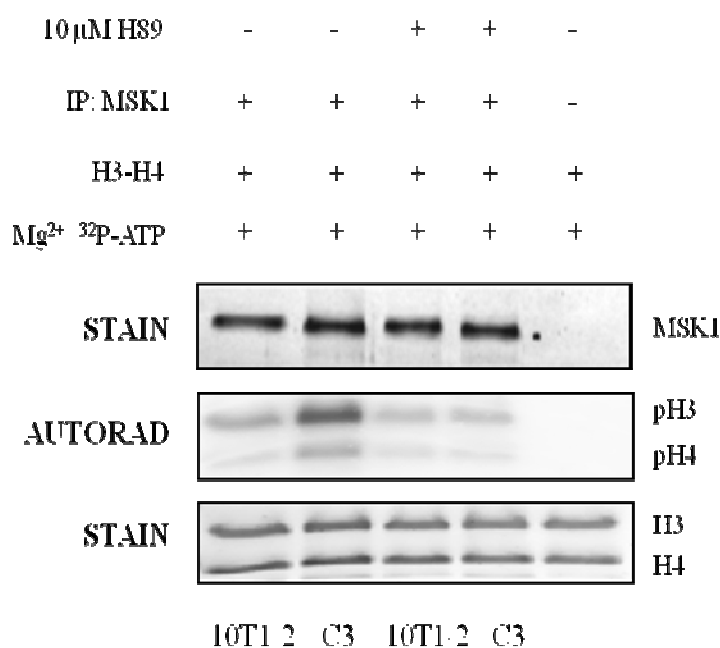
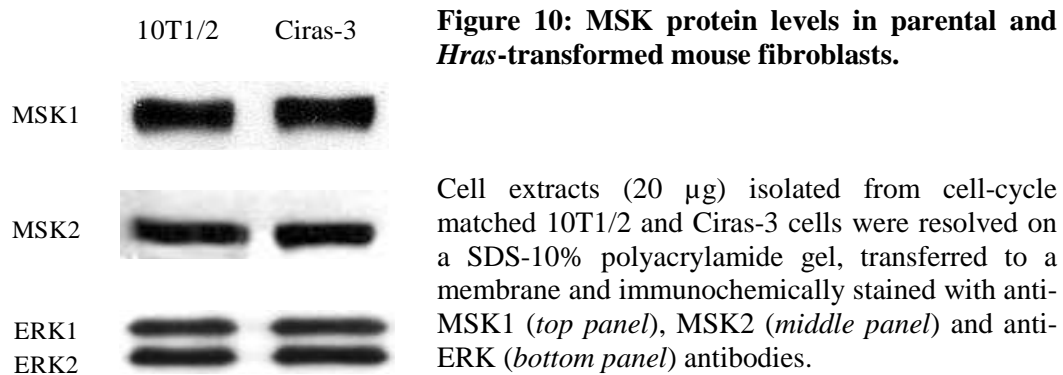


Figure 9: MSK1 kinase activity in 10T1/2 and Ciras-3 mouse fibroblasts. Immunoprecipitation of MSK1 from 10T1/2 and Ciras-3 cell extracts (500 μ g) was performed and the resulting fractions were incubated with the H3-H4 tetramer fraction (5 μ g) in Mg²⁺/ATP/[γ -³²P]ATP and the presence or absence of H89. The samples were resolved by SDS-15%-PAGE. The gels were analyzed by the Coomassie Blue staining and autoradiography. The *top panel* is a stained gel showing the amount of MSK1 IP.

The H3 kinase activity of MSK1 in both preparations was inhibited by H89. In addition to radiolabeling of H3, weak labeling of H4 was observed and H89 suppressed the labeling of this histone protein. In control experiments when the primary antibody was not included or the immunoprecipitate was not added, H3 kinase activity was not detected. The increased MSK1 activity observed in the Ciras-3 sample was not due to an increase in the amount of MSK1 protein immunoprecipitated from the Ciras-3 cell

extract, as the stained gel shown in Figure 9 (*top panel*) revealed that the MSK1 immunoprecipitates from the cell extracts had similar amounts of MSK1. In repeats of these analyses ($n = 4$), an average 3-fold increase in the MSK1 activity was observed in the Ciras-3 immunoprecipitates relative to that in the 10T1/2 preparations. Constitutive activation of the RAS-MAPK pathway results in the altered expression at the protein level of signaling and cell cycle proteins (Calipel et al., 2003). The previous immunoprecipitation analyses shown in Figure 9 provided evidence that MSK1 protein levels were similar in Ciras-3 and 10T1/2 cell extracts. To explore this further, the protein levels of MSK1 and MSK2 were compared with total protein levels of ERKs by immunoblot analyses of cell cycle-matched cellular extracts from 10T1/2 and Ciras-3 cells. Figure 10 shows that the protein levels of MSK1 in the two cell lines were equivalent in accordance with the immunoprecipitation results.



Similar results were observed for MSK2 (Figure 10, *middle panel*). These observations suggest that the increased phosphorylation of H3 observed in *Hras*-transformed mouse fibroblasts is due to an increase in the activity, but not protein levels of MSK1 and MSK2.

4.3 MSK1 cellular distribution in parental and *Hras*-transformed mouse fibroblasts

MSK1 is located in both the nucleus and the cytoplasm (Thomson et al., 1999). Nuclear MSK1 would be responsible for phosphorylating transcription factors and H3 associated with immediate-early genes, whereas MSK1 located in the cytoplasm has an interesting role in translation by phosphorylating 4E-BP1 (Liu et al., 2002). To determine whether MSK1 subcellular distribution was altered in the *Hras*-transformed mouse fibroblasts, cellular fractionation was performed with 10T1/2 and Ciras-3 cells. Cells were lysed in TNM buffer without any detergents to minimize loosely bound nuclear proteins from leaking out of the nuclei. The nuclei were then resuspended in TNM buffer with 0.5% Triton X-100 and incubated on ice to release loosely bound nuclear proteins (Triton S fraction). The resulting pellet contained the tightly bound nuclear proteins, which includes proteins associated with the nuclear matrix (Triton P). Equal amounts of cell fractions were analyzed by immunoblotting. As a reference, the distribution of MSK1 was compared with the nuclear transcription factor Sp3 and chromatin-modifying enzyme, histone deacetylase 1 (HDAC1). Sp3 has three isoforms, the expressions of which are regulated at the level of translation by selection of different translation initiation sites on the Sp3 mRNA (Davie et al., 2008). A consistent observation in analyses of these cell fractions was that the relative level of the short Sp3 isoforms compared with the long isoform was greater in the Ciras-3 cells (Figure 11). This observation suggests that the translational machinery is altered in the *Hras*-transformed cells. Figure 11 shows that the distribution of MSK1 among the various cellular fractions was similar for Ciras-3 and 10T1/2 cells.

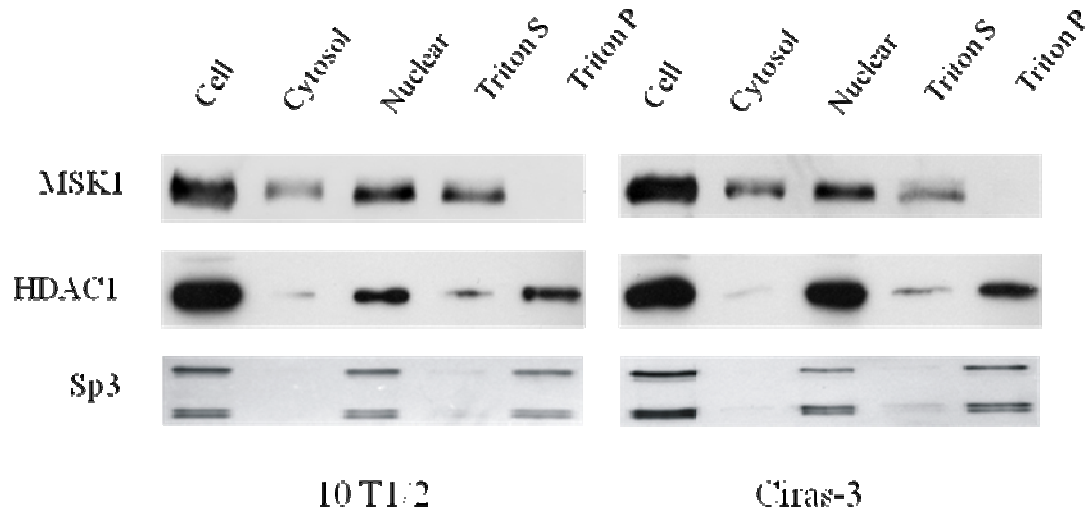


Figure 11: Cellular distribution of MSK1 in 10T1/2 and Ciras-3 mouse fibroblasts.

Cellular fractionation of parental and oncogene-transformed mouse fibroblasts was performed. Equal volumes for all fractions isolated from 10T1/2 and Ciras-3 cells were loaded and analyzed by SDS-10%-PAGE, transferred to a membrane, and immunochemically stained with anti-MSK1 (*top panel*), anti-HDAC1 (*middle panel*), and anti-Sp3 (*bottom panel*) antibodies. The three Sp3 bands correspond to the long and two short Sp3 isoforms.

In contrast to Sp3 and HDAC1, MSK1 was present in the cytosolic fraction. However, most MSK1 was located in the nuclear fractions in Ciras-3 and 10T1/2 cells. Also dissimilar from Sp3 and HDAC1, most, if not all, MSK1 was extracted from the nucleus with 0.5% Triton X-100.

4.4 MSK1 associates with chromatin modifying/remodeling enzymes

The kinase assays revealed that MSK1 was able to phosphorylate H3 as well as H4. Recently, mass spectrometry studies have demonstrated additional *in vivo* phospho-modifications of H3 at T118 and H4 at S47 (Cosgrove et al., 2004). These two H3 and H4 residues are located on the lateral nucleosomal surface and have been implicated in nucleosome sliding in yeast (Flaus et al., 2004; Fleming and Pennings, 2001). Therefore, phosphorylation of H3T118 and H4S47, along with other histone modifications, might mediate nucleosome destabilization and promotion of transcription (Cosgrove et al.,

2004). The H3T118 and H4S47 residues contain the MSK consensus sequence, RXS; therefore, both of the sites could be targeted by MSKs. In order for MSK to access these residues within the nucleosomal fold, concerted recruitment of the kinase with chromatin modifying and remodeling enzymes to the nucleosome would have to take place (Cosgrove et al., 2004). To test if MSK1 associates with other histone modifying enzymes and chromatin remodeling proteins, HEK293 cells were transfected with FLAG-MSK1 construct and low stringency FLAG immunoprecipitation (IP) was performed, followed by immunoblotting with antibodies to candidate proteins, such as H3 specific lysine acetyltransferase, PCAF and the ATPase subunit of SWI2/SNF2 chromatin remodeling complex, BRG1. Figure 12 shows that the FLAG immunoprecipitate contained PCAF and BRG1.

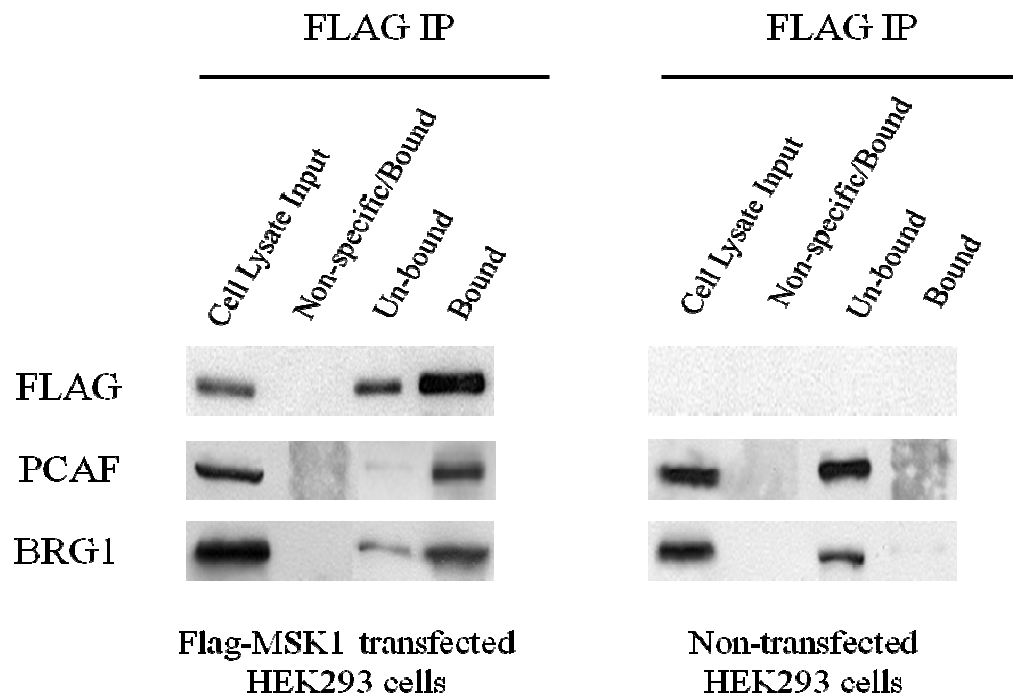


Figure 12: MSK1 association with chromatin modifying and remodeling enzymes. HEK293 cells were transfected with or without Flag-MSK1 plasmid construct and the resulting cell lysates (500 µg) were incubated with anti-FLAG, BRG1 and PCAF antibodies. The whole “Bound” and “Non-specific” fractions were resolved on SDS-10%-PAGE and immunoblotted with the indicated antibodies.

In control experiments, FLAG IP was performed with untransfected HEK293 cell extracts to show that PCAF and BRG1 were specifically associated with FLAG-MSK1. To examine these associations in more detail, endogenous MSK1 IP was performed from HEK293 cell extracts, followed by immunoblotting with specific antibodies. Figure 13 shows that the endogenous MSK1 IP fraction contained PCAF and BRG1.

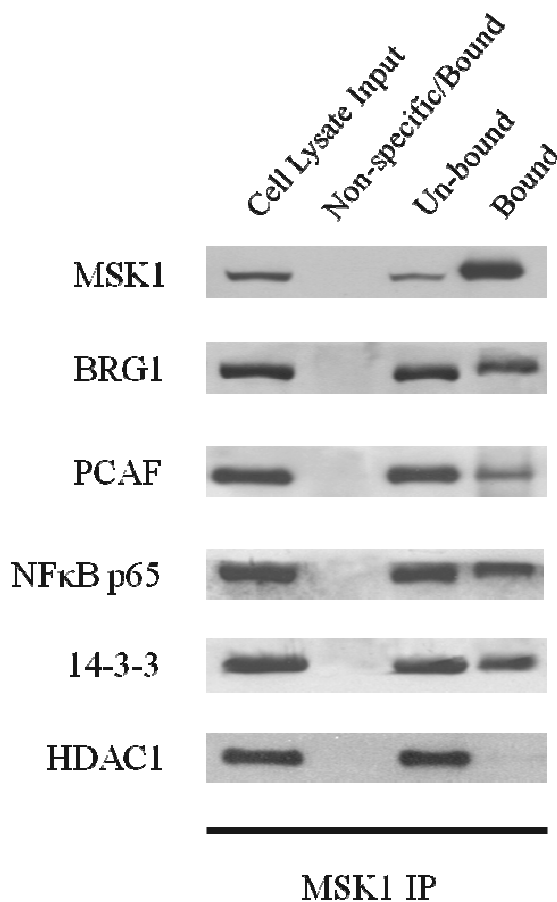


Figure 13: MSK1 association with chromatin remodelers, histone modifying enzymes, transcription factors and phospho-H3 binding proteins.

Aliquots of 500 µg HEK293 cell lysate were incubated with anti-MSK1 antibodies. The whole “Bound” and “Non-specific” (beads only) fractions and equivalent volumes of “Cell Lysate Input” and “Un-bound” fractions, corresponding to 25 µg of cell lysate, were resolved on the SDS-10%-PAGE and membranes were immunoblotted with indicated antibodies.

In order to validate the integrity of the IP assay, immunoblotting with antibody to NFκB p65 was performed as previous studies have shown that MSK1 phosphorylates and associates with NFκB p65 (Vermeulen et al., 2003). Figure 13 shows that NFκB p65 was

present in the MSK1 immunoprecipitate, whereas the transcriptional repressor HDAC1 was not. Further, immunoblotting with a full-length 14-3-3 antibody revealed the presence of 14-3-3 proteins in the MSK1 immunoprecipitate. Specific 14-3-3 isoforms have been shown to bind phospho-H3 tails (Macdonald et al., 2005; Walter et al., 2008), implying that these isoforms may associate with MSK1 and be recruited to nucleosomal H3 tails. To further verify these protein-protein associations, PCAF, BRG1, NFκB p65 and 14-3-3 immunoprecipitations from HEK293 cell extracts were performed and immunoblotting with MSK1 antibody was carried out. Figure 14 shows that PCAF, BRG1, NFκB p65 and 14-3-3 associate with MSK1.

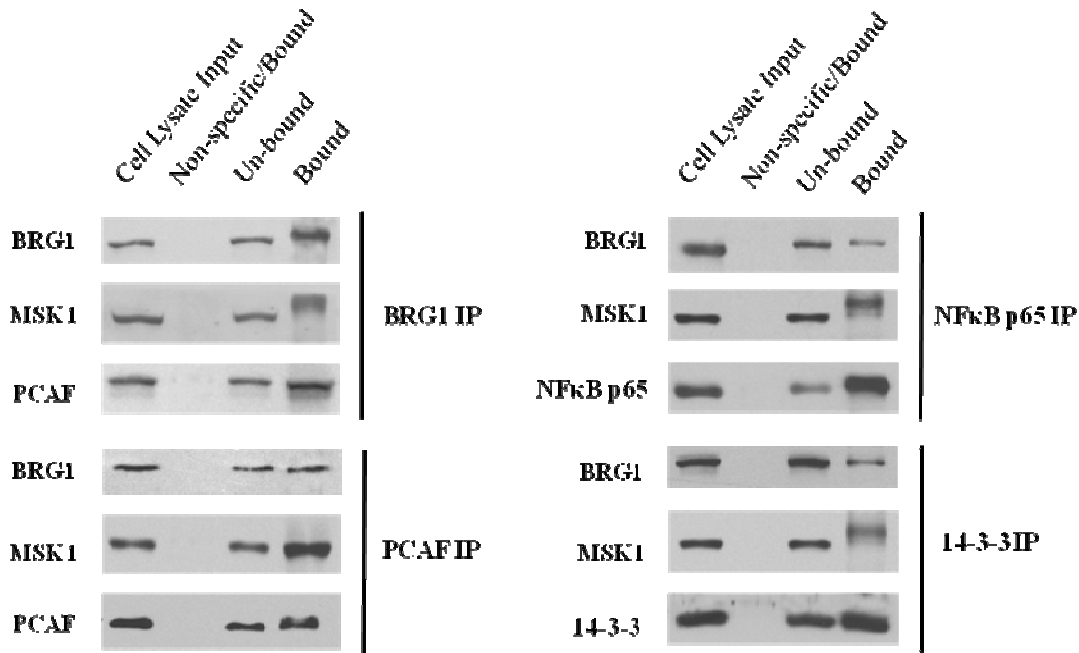


Figure 14: Association of chromatin remodelers/modifiers, transcription factors and phospho-H3 binding proteins with MSK1.

Aliquots of 500 μg HEK293 cell lysate were incubated with anti-BRG1, PCAF, NFκB p65 and 14-3-3-FL antibodies. The whole “Bound” and “Non-specific” fractions and equivalent volumes of “Cell Lysate Input” and “Un-bound” fractions, corresponding to 25 μg of cell lysate, were resolved on SDS-10%-PAGE and immunoblotted with indicated antibodies.

Immunoblotting of BRG1, NFκB p65 and 14-3-3 IP fractions with a MSK1 antibody revealed a MSK1 band shift, implying possible post-translational modifications of MSK1, such as phosphorylation, glycosylation or ubiquitination (Dyson et al., 2005). Additionally, PCAF and BRG1 associate together, as seen in Figure 14. Furthermore, Figure 14 demonstrates that NFκB p65 and 14-3-3 IP fractions also contained BRG1. As controls, immunoprecipitations were performed with no antibody (non-specific/bound fractions), demonstrating the fidelity of specific immunoprecipitations. Collectively, these experiments in HEK293 cells demonstrated that MSK1 is associated with transcription factors, chromatin modifying/remodeling proteins and phospho-H3 binding proteins.

4.5 MSK1 complex contains KAT activities

Co-immunoprecipitation experiments demonstrated that MSK1 associates with the H3 KAT, PCAF (Figure 14). In order to further demonstrate the existence of KATs within MSK1 complex from HEK293 cells, KAT assays were performed. MSK1 complex was immunoprecipitated under low stringency conditions from HEK293 cell lysates and assayed for KAT activity in the presence of ³H-acetyl-CoA co-enzyme and the total core histone preparation as the substrate. Figure 15 shows that the immunoprecipitated MSK1 complex contained KAT activity towards free histones.

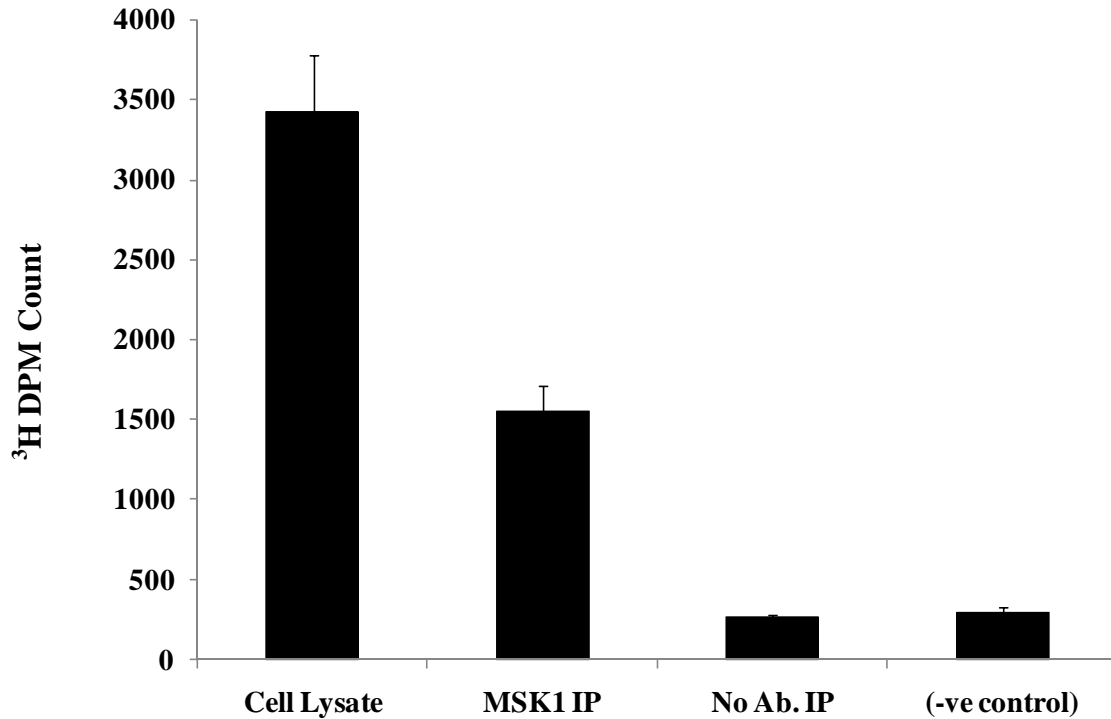


Figure 15: MSK1 protein complex contains lysine acetyltransferase (KAT) activity. Low stringency MSK1 IP was performed from HEK293 cell lysate. Each of the IP samples (with and without MSK1 antibody) and the +ve control (1.0 mg of cell lysate) were incubated with 0.25 iCi ³H-labeled acetyl-CoA and 10 µg of total histone preparation from mature avian erythrocytes. Negative control included the MSK1 IP sample that was incubated at 100°C for 10 minutes prior to the KAT assay. Radioactivity (KAT activity) was measured with scintillation counting. n = 3.

To investigate if the KAT activity present within the MSK1 complex exhibits any substrate specificity, the total histone preparation was resolved via the HPLC C18 column to purify individual histone proteins (Figure 16). The KAT assay was performed with immunoprecipitated MSK1 complex from HEK293 cell lysates and individual histones, H2A, H2B, H3 and H4 as substrates in the presence of ³H-acetyl-CoA. Figure 17 shows that MSK1-associated KAT activity does not exhibit histone specificity, suggesting the presence of more than just PCAF within the MSK1 complex.

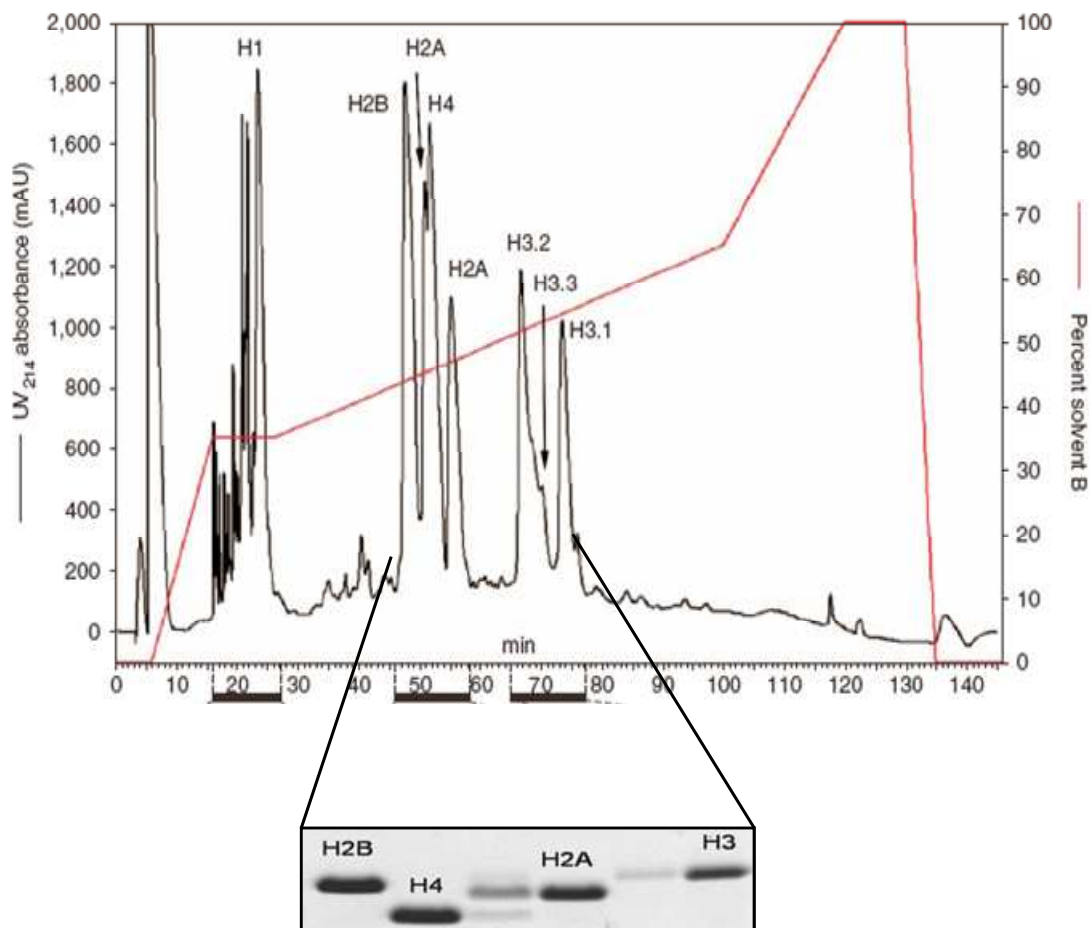


Figure 16: Reverse-phase HPLC purification of individual histone proteins.

Chromatogram and Coomassie-stained gel from reversed-phase HPLC (RP-HPLC) separation of histones. Histones from a mature avian erythrocyte total histone preparation were separated on a C8 reversed-phase column in a ddH₂O/acetonitrile gradient. The chromatogram shows the retention of proteins on the column over the course of the acetonitrile gradient program. Peak fractions were lyophilized and a small sample of each re-dissolved fraction was run on an SDS-polyacrylamide gel electrophoresis (SDS-15%-PAGE) gel and Coomassie stained.

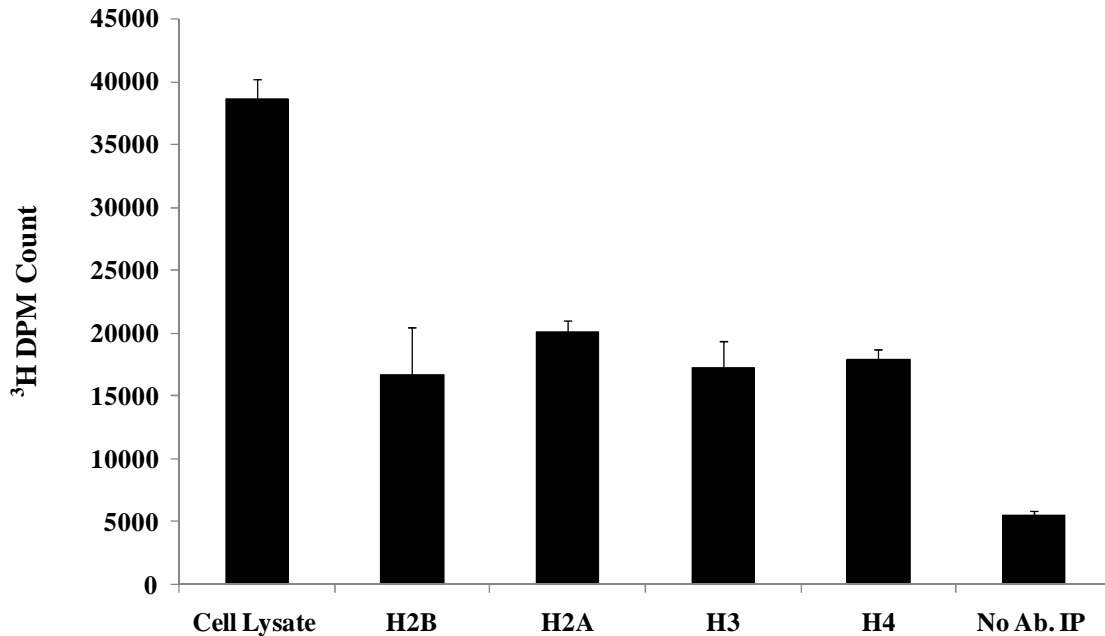


Figure 17: MSK1-associated KAT activity has broad histone substrate specificity.

Low stringency MSK1 IP was performed from cycling HEK293 cell lysate (TCE). Each of the IP samples (with and without MSK1 antibody) and the +ve control (1.0 mg of HEK293 cell lysate) were incubated with 0.25 μ Ci ³H-labeled acetyl-CoA and 1.0 μ g of individual histones (H2B, H2A, H3 and H4). Individual histones were obtained via C18 reverse-phase HPLC separation from mature avian erythrocyte total histone preparations. Radioactivity (KAT activity) was measured with scintillation counting. n = 3.

To test for the presence of other KATs, such as CBP/p300, a specific inhibitor of CBP/p300, curcumin (Marcu et al., 2006) was used to pre-treat the immunoprecipitated MSK1 complex prior to performing the KAT assay. Figure 18 shows that in the presence of curcumin, KAT activity within the immunoprecipitated MSK1 complex was markedly decreased, suggesting the presence of CBP/p300 within the MSK1 complex. As negative controls for all of the KAT assays, immunoprecipitations without antibody were carried out and the resulting ³H incorporation was monitored.

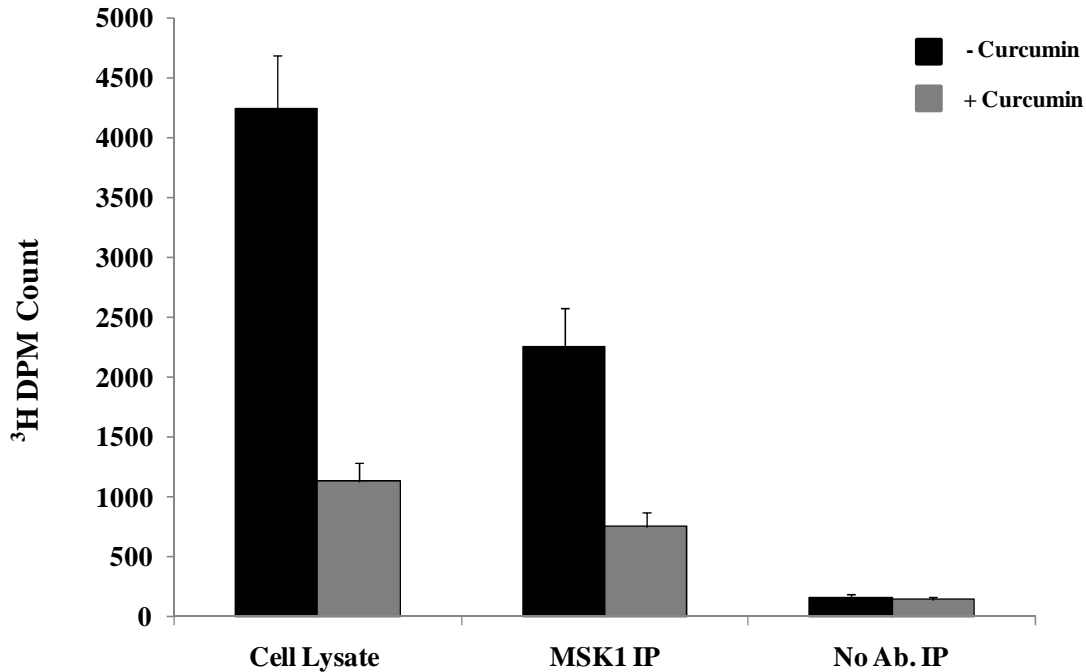


Figure 18: MSK1-associated KAT activity is inhibited with curcumin. Low stringency MSK1 IP was performed from cycling HEK293 cell lysates. Each of the IP samples (with and without MSK1 antibody) and the +ve control (1.0 mg of HEK293 cell lysate) were incubated with 0.25 μ Ci ³H-labeled acetyl-CoA and 10 μ g of total histone preparation from mature avian erythrocytes at 37°C for 1 hour. Curcumin (60 μ M) was added to the samples (grey columns) for 30 minutes at 37°C prior to the addition of ³H-labeled acetyl-CoA. Radioactivity (KAT activity) was measured with scintillation counting. n = 3.

4.6 14-3-3-mediated MSK1 interactions with chromatin remodelers

Results from HEK293 co-immunoprecipitations indicate that MSK1 associates with 14-3-3 proteins (Figures 13 and 14). Previously, it has been shown that RAS-MAPK-induced H3 phosphorylation and 14-3-3 ζ were targeted to promoter regions of IE genes in 10T1/2 cells (Macdonald et al., 2005), where 14-3-3 isoforms, such as 14-3-3 ϵ and 14-3-3 ζ may bind this phospho-H3 mark (Walter et al., 2008). Since 14-3-3 proteins exist as homo- or heterodimers, it is possible that 14-3-3 dimers act as scaffolds to anchor proteins at the promoter of IE genes once the phospho-H3 modifications is bound by 14-3-

3 (Bridges and Moorhead, 2004). One of the 14-3-3 sites would bind to H3S10ph or H3S28ph, while the other site could bind to a component within the nucleosome-remodeling complex. To test this scenario in 10T1/2 cells, co-immunoprecipitations with MSK1, 14-3-3 ζ and BRG1 were performed. Figure 19 shows that both BRG1 and 14-3-3 ζ were present in the MSK1 immunoprecipitate from a 10T1/2 cell lysate.

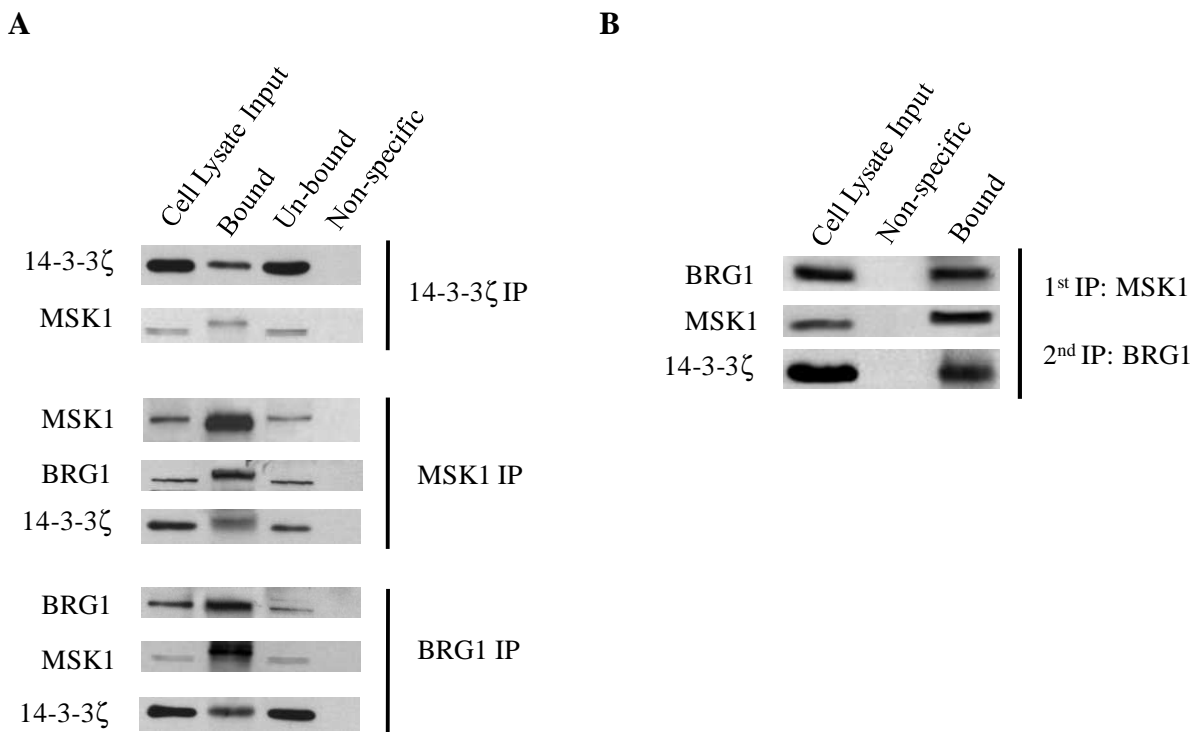


Figure 19: MSK1 associates with 14-3-3 proteins and BRG1 in parental mouse fibroblasts.

A) Aliquots of 500 μ g 10T1/2 cell lysate were incubated with anti-14-3-3 ζ , MSK1 and BRG1 antibodies. The whole “Bound” and “Non-specific” fractions and equivalent volumes of “Cell Lysate Input” and “Un-bound” fractions, corresponding to 25 μ g of cell lysate, were resolved on SDS-10%-PAGE and immunoblotted with indicated antibodies. **B)** 1 mg of cell lysate prepared from TPA-stimulated (30 minutes) 10T1/2 cells that were crosslinked with DTBP, was sequentially incubated with anti-MSK1 and anti-BRG1 antibodies. The corresponding fractions were resolved on SDS-10%-PAGE and immunoblotted with indicated antibodies.

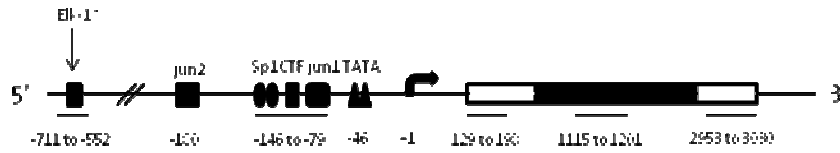
Reciprocally, BRG1 antibodies were able to co-immunoprecipitate MSK1 and 14-3-3 ζ . Further, 14-3-3 ζ IP fractions contained MSK1 and BRG1. Thus, 14-3-3 ζ is associated with MSK1 and BRG1 in 10T1/2 cells. To investigate if a ternary complex is formed

between MSK1, 14-3-3 ζ and BRG1, DSP-cross-linked TPA-stimulated (30 min) 10T1/2 cell lysate was subjected to sequential immunoprecipitations, first with antibodies against MSK1, and second with antibodies against BRG1. Figure 19B shows that BRG1 was sequentially co-immunoprecipitated with MSK1 and 14-3-3 ζ , suggesting that these three proteins are within the same multi-protein complex. Therefore, in response to RAS-MAPK signaling, MSK1 may be recruited to regulatory regions of IE genes, along with transcription factors and chromatin modifying/remodeling enzymes to initiate transcriptional activation.

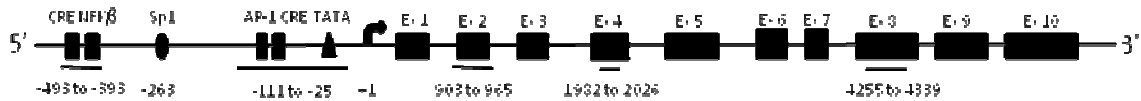
4.7 RAS-MAPK-induced MSK1 recruitment and H3 modifications at the regulatory regions of IE genes in parental and *Hras*-transformed mouse fibroblasts

Treatment of quiescent 10T1/2 cells with the phorbol ester TPA initiates the RAS-MAPK signaling pathway and triggers the downstream MSK-mediated nucleosomal response, which is associated with gene activation (Soloaga et al., 2003). Among the genes that are induced by RAS-MAPK signaling are those coding for IE genes, such as cyclooxygenase-2 (*Cox-2*) and members of the AP-1 family of transcription factors [*Fos*, *Jun*, FOS-like antigen 1 (*Fosl1*), also known as FOS-related antigen 1 (*Fra-1*)], all of which have roles in tumorigenesis and synaptic signaling (Verde et al., 2007; Yang and Chen, 2008). Figure 20 shows the genomic structure and regulatory regions of murine *Jun*, *Cox-2* and *Fosl1* genes.

Jun



Cox-2



Fos1

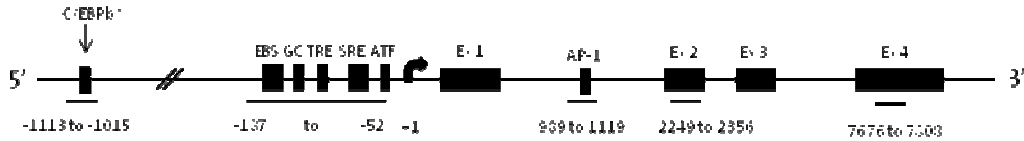


Figure 20: Genomic structures of murine *Jun*, *Cox-2* and *Fos1* genes.

The black bars underneath the gene maps indicate regions amplified in the ChIP assays. Each region is labeled according to the 5' position of the forward primer relative to the transcription start site. The exons are represented by boxes and the binding sites of relevant transcription factors located in the amplified regions are displayed. Abbreviations are: CTF, CCAAT-box-binding protein (also known as NF1, nuclear factor 1); CRE, cyclic-AMP responsive element; EBS, Ets binding site; GC, GC box which is a binding site for the Sp family transcription factors; TRE, TPA-responsive element; SRE, serum-responsive element. AP-1 constitutes a combination of dimers formed of members of the JUN, FOS and ATF families of transcription factors. *Potential protein binding sites. Gene maps are not to scale.

Mouse fibroblast 10T1/2 and Ciras-3 cell lines were stimulated with TPA for 0, 15 and 30 minutes, and the distribution of MSK1 along the regulatory and coding regions of the three IE genes was determined, using a high resolution ChIP assay. In this assay the nuclei isolated from formaldehyde-crosslinked cells were digested with micrococcal nuclease (MNase), such that the chromatin fragments were processed down to mononucleosomal length (Figure 21).

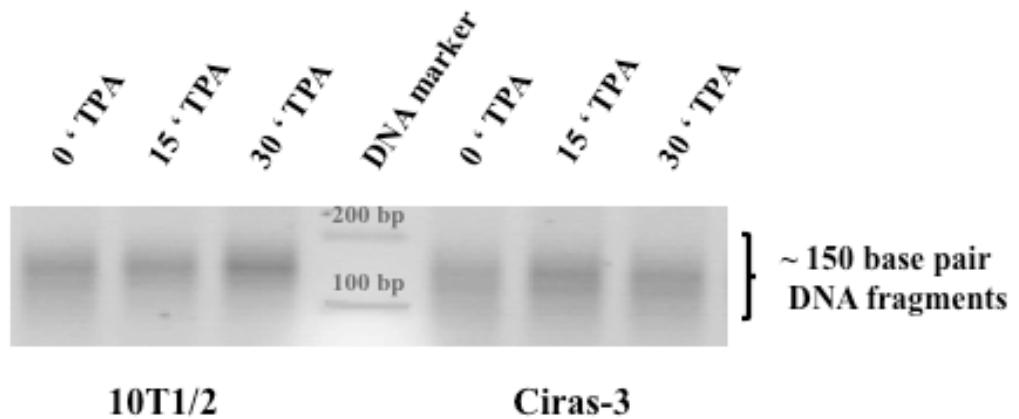


Figure 21: The MNase-generated chromatin fragments are predominantly mononucleosomal.

After heat reversal of crosslinks, purified DNA from MNase-treated 10T1/2 and Ciras-3 inputs were run on a 1.8% agarose TBE gel for comparison.

The regions chosen for real time PCR analysis are displayed in Figure 20. MSK1 association in 10T1/2 and Ciras-3 cells occurred within 15 and 30 minutes of TPA treatment with both upstream regions of *Jun*; the 5' distal region (-711) containing a putative binding site for the ELK-1 transcription factor and the 5' proximal region (-146) with binding sites for several transcription factors, including JUN (Figure 22). There was no significant TPA-induced association of MSK1 with the *Jun* coding regions (+129, +1115 and +2953). Also, Figure 22 shows that 15 and 30 minute TPA stimulation of 10T1/2 and Ciras-3 cells increased the binding of MSK1 to the 5' distal (-493) and 5' proximal (-111) upstream regions of the *Cox-2* gene, but not to its coding regions (+903, +1982 and +4255).

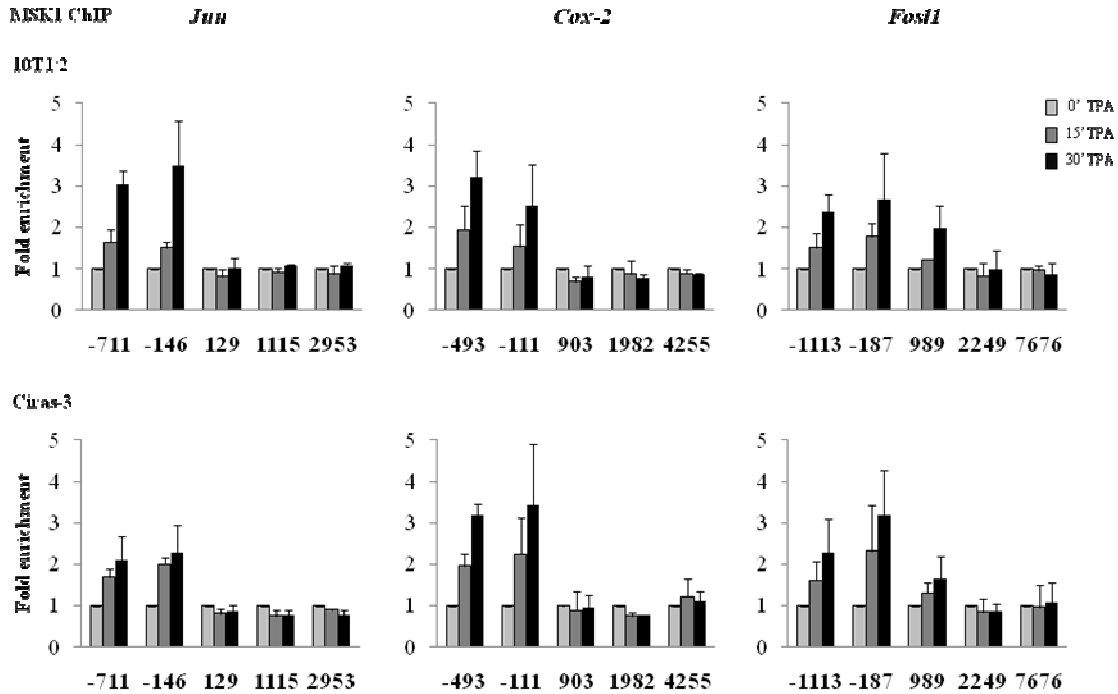


Figure 22: TPA-induced MSK1 recruitment at the *Jun*, *Cox-2* and *FosII* regulatory regions in parental and *Hras*-transformed mouse fibroblasts.

ChIP experiments were performed using antibodies against MSK1 on formaldehyde-crosslinked mononucleosomes prepared from serum-starved 10T1/2 and Ciras-3 cells treated with TPA for 0, 15 and 30 min. Equal amounts of input and immunoprecipitated DNA were quantified by real-time quantitative PCR. The enrichment values of each sequence in ChIP DNA samples relative to input DNA were calculated as described in Materials and Methods, and were normalized to time 0 values. Enrichment values are the mean of three independent experiments, and the error bars represent the standard deviation.

Furthermore, TPA treatment of 10T1/2 and Ciras-3 cells increased the occupancy of MSK1 after 15 and 30 minutes on three *FosII* gene regions: the 5' distal region (-1113) containing a putative binding site for C/EBP β protein, the 5' proximal region (-187) with multiple responsive elements, and the region (+989) located in intron 1 which contains an AP-1 binding site (Figure 20). The TPA-induced MSK1 binding at the regulatory regions of IE genes was strongest at 30 minutes. Therefore, in response to RAS-MAPK signaling, MSK1 is recruited to the regulatory regions of IE genes in parental and *Hras*-transformed mouse fibroblast cell lines. The recruitment of MSK1 to specific regulatory regions of

responsive genes is most likely mediated by particular transcription factors, such as Elk-1, NFκB and AP-1 (Espino et al., 2006; Vermeulen et al., 2003; Zhang et al., 2008).

Various H3 modifications have been reported to occur at the nucleosomes of inducible genes (Cerutti and Casas-Mollano, 2009). However, distribution of phospho-H3 along IE genes responding to RAS-MAPK signaling has not been elucidated. Since the RAS-MAPK-activated MSK1 targets S10 and S28 within the N-terminal domain of H3, antibodies against H3S10ph and H3S28ph were used to immunoprecipitate formaldehyde-crosslinked mononucleosomes from serum starved 10T1/2 and Ciras-3 cells treated with TPA for 0, 15 and 30 minutes. As seen in Figure 23A, the levels of H3S10ph and H3S28ph at the regulatory regions of *Jun*, *Cox-2* and *Fos11* increase with the TPA time-course, peaking at 30 minutes in 10T1/2 cell line. The same trend was observed for Ciras-3 cells (Figure 23B). Further, Figure 23 demonstrates that the distribution of H3S10ph and H3S28ph along upstream IE regulatory regions and in the first *Fos11* intron mirrors that of MSK1, suggesting that these phospho-H3 marks contribute to promoter remodeling and transcriptional initiation, but not elongation. On the other hand, distribution of H3 acetylation (H3K9acK14ac) extended from the regulatory regions of IE genes into the coding regions, although with progressively decreasing levels (Figure 24A).

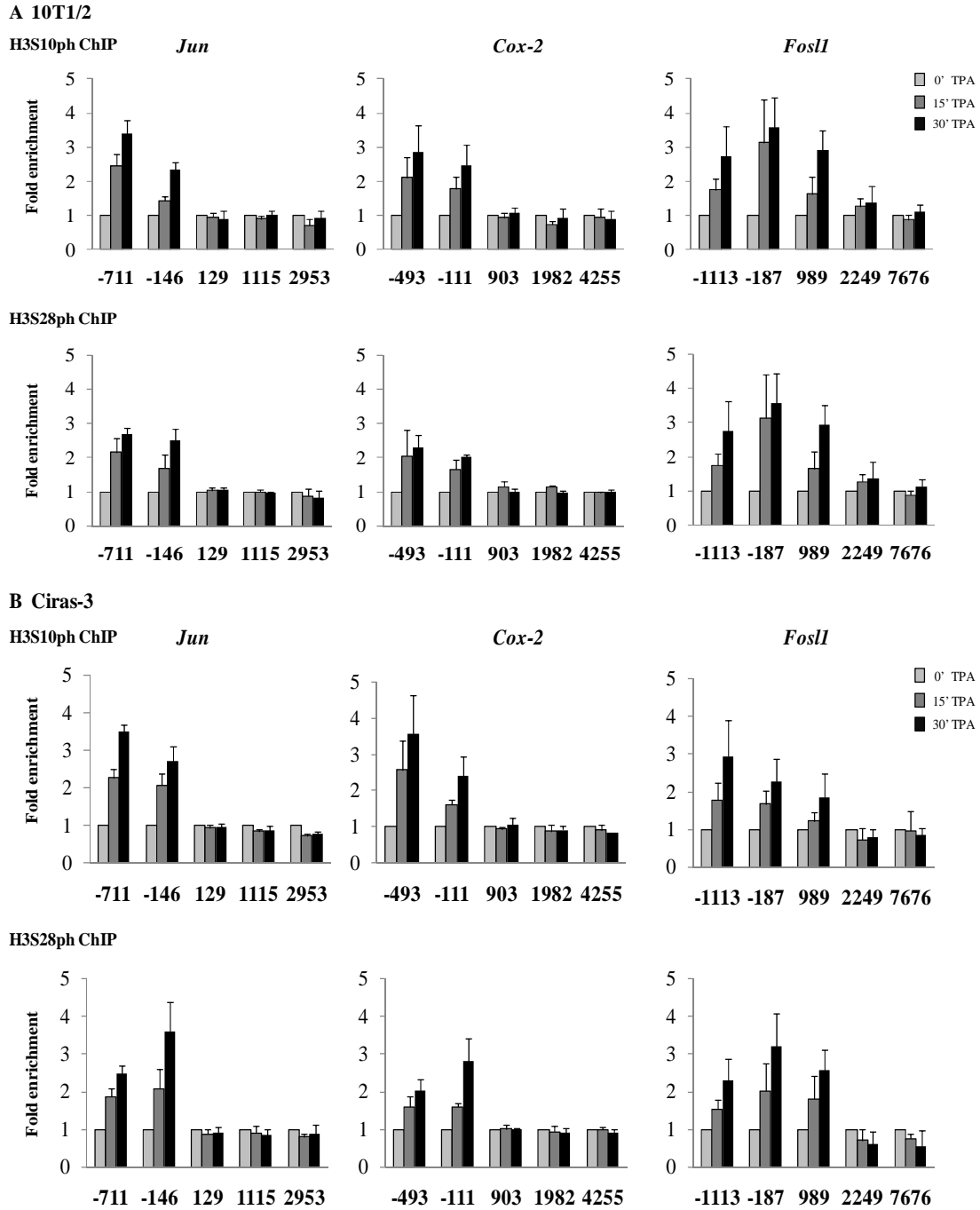
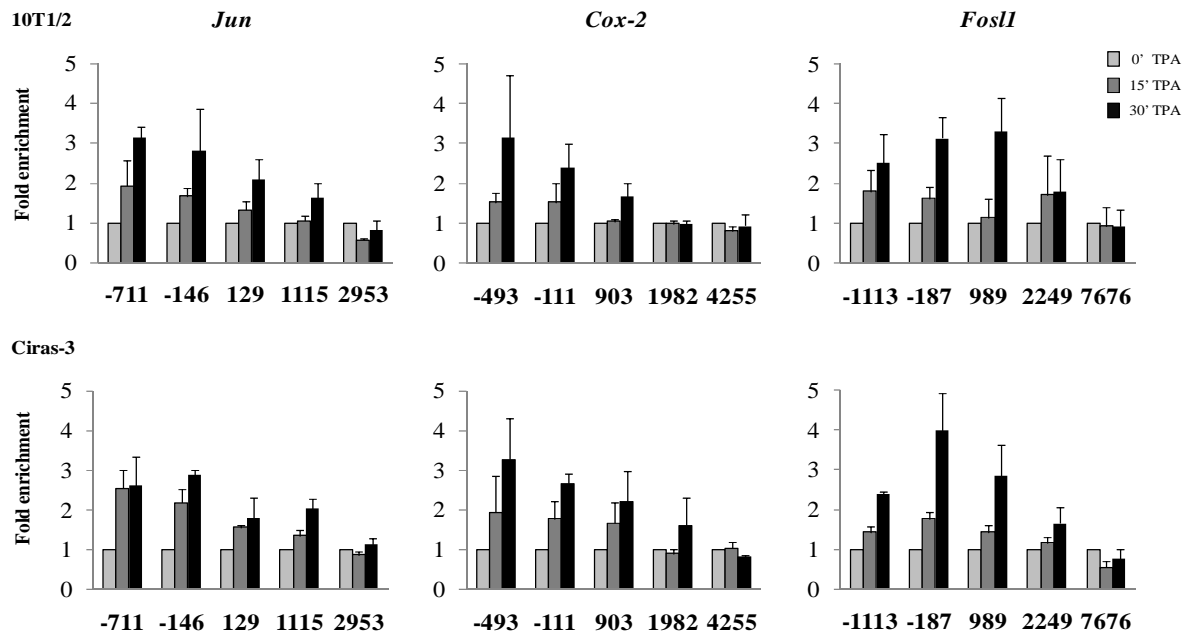


Figure 23: TPA-induced phosphorylation of H3 at Ser10 and Ser28 at the regulatory regions of *Jun*, *Cox-2* and *FosII* in parental and *Hras*-transformed mouse fibroblasts.

ChIP experiments were performed using antibodies against H3S10ph and H3S28ph on formaldehyde-crosslinked mononucleosomes prepared from serum-starved 10T1/2 (A) and Ciras-3 (B) cells treated with TPA for 0, 15 and 30 min. Enrichment values, obtained as described in Figure 22 are the mean of three independent experiments, and the error bars represent the standard deviation.

A H3K9acK14ac ChIP



B H3K4me3 ChIP

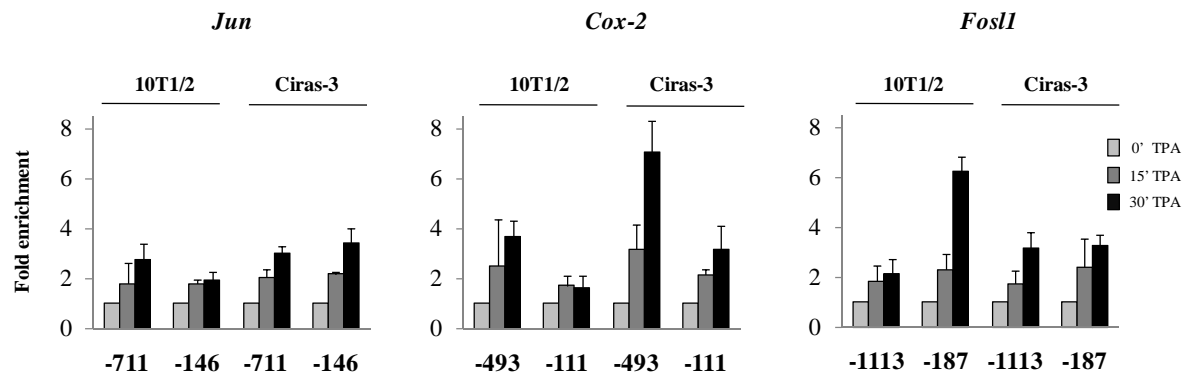


Figure 24: TPA-induced H3 acetylation and methylation along *Jun*, *Cox-2* and *FosII* genes in parental and *Hras*-transformed mouse fibroblasts.

ChIP experiments were performed using antibodies against H3K9acK14ac (A) and H3K4me3 (B) on formaldehyde-crosslinked mononucleosomes prepared from serum-starved 10T1/2 and Ciras-3 cells treated with TPA for 0, 15 and 30 min. Enrichment values, obtained as described in Figure 22 are the mean of three independent experiments, and the error bars represent the standard deviation.

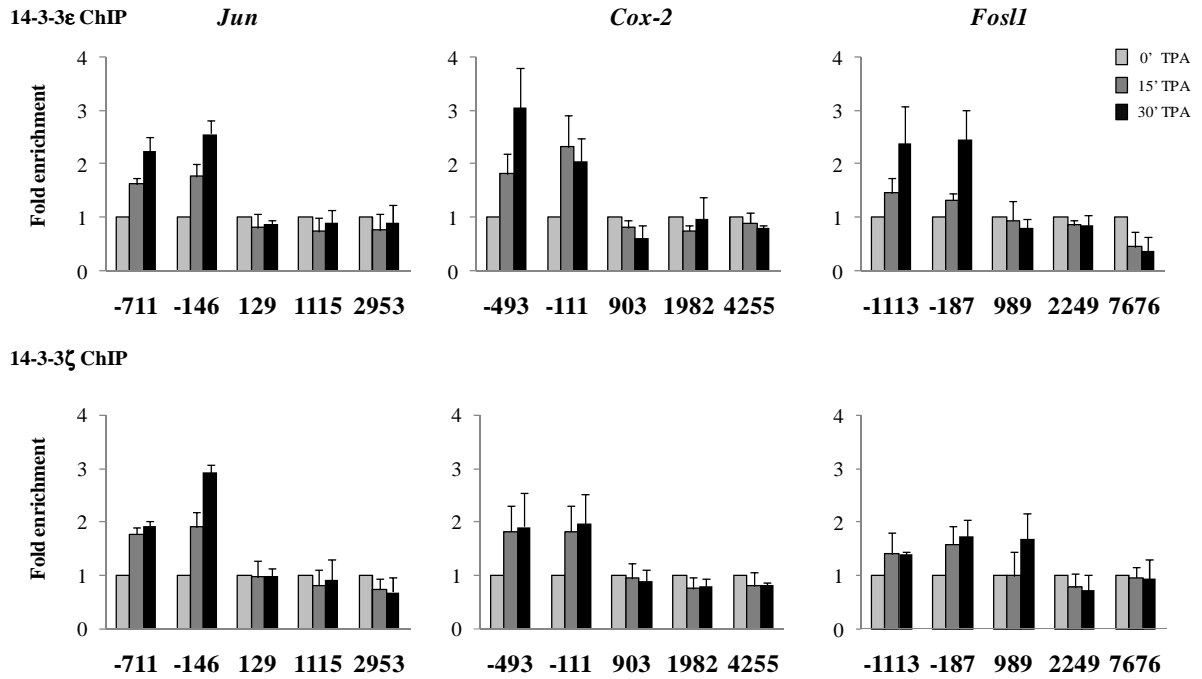
Trimethylation of H3K4 is a hallmark of transcriptional activation (Ruthenburg et al., 2007). Therefore, ChIP experiments with antibodies raised against H3K4me3 were performed in order to investigate the transcriptional state of IE genes in response to RAS-

MAPK signaling. Figure 24B shows that H3K4me3 levels increased in response to TPA at the regulatory regions of *Jun*, *Cox-2* and *Fos11* in parental and *Hras*-transformed cells. It is noteworthy to mention that the basal level (time 0) of H4K4me3 at the regulatory regions of IE genes was higher than that of other H3 modifications, such as H3S10ph, H3S28ph or H3K9acK14ac, in both 10T1/2 and Ciras-3 cells.

4.8 Recruitment of phospho-H3 binding proteins and chromatin remodeling/modifying enzymes to regulatory regions of IE genes in response to RAS-MAPK signaling

Since 14-3-3 isoforms act as effectors of H3 phosphorylation at inducible genes (Macdonald et al., 2005), ChIP assays were performed to determine the distribution of 14-3-3 isoforms (ϵ and ζ) along *Jun*, *Cox-2* and *Fos11* genes in TPA-treated 10T1/2 and Ciras-3 cells. Upon TPA-stimulation of serum-starved 10T1/2 and Ciras-3 cells, 14-3-3 ϵ and 14-3-3 ζ associated with the same regulatory regions of *Jun*, *Cox-2* and *Fos11* as did H3S10ph and H3S28ph (Figure 25). Furthermore, recruitment of the SWI/SNF2 ATPase, BRG1 and the H3 KAT, PCAF increased in response to TPA stimulation at the same regulatory regions (Figure 26A/B). In the case of the *Cox-2* gene in 10T1/2 cells, BRG1 and PCAF, to a lesser extent, associated with the 5' distal regions (-493) upon TPA stimulation, while the TPA-induced binding of BRG1 with the 5' proximal region (-111) was weaker, and TPA-induced association of PCAF was negligible (Figure 26). However, TPA-induced H3 acetylation was observed at both of the *Cox-2* regulatory regions (-493 and -111) as seen in Figure 24A.

A 10T1/2



B Ciras-3

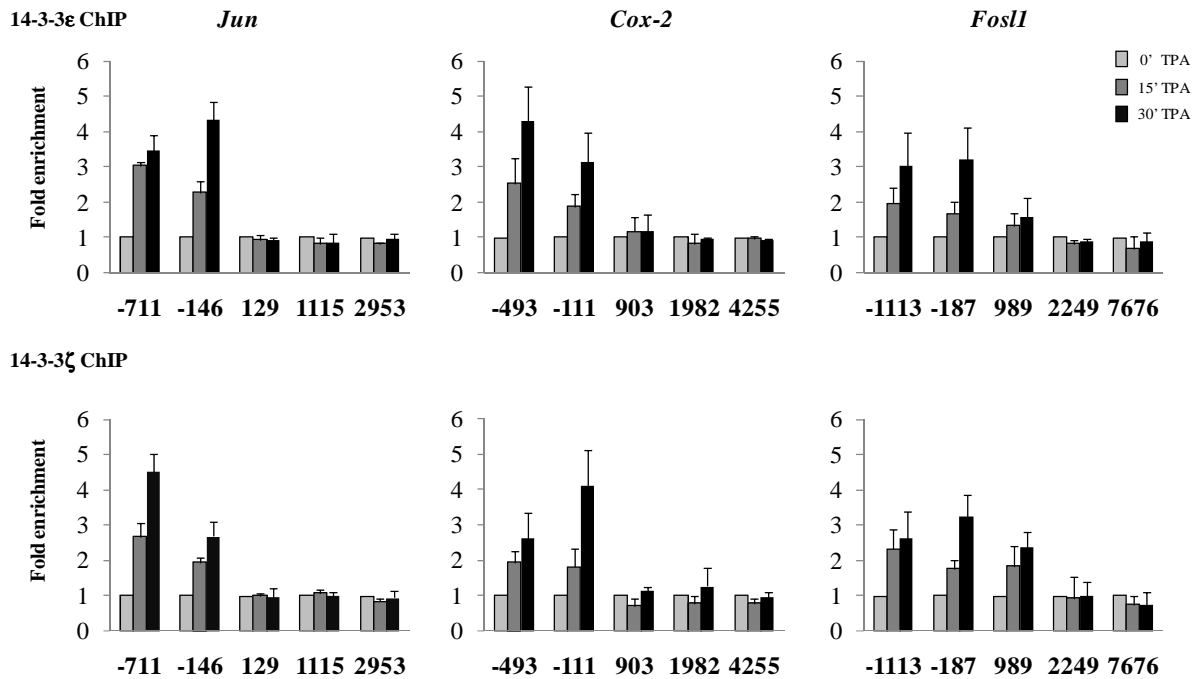
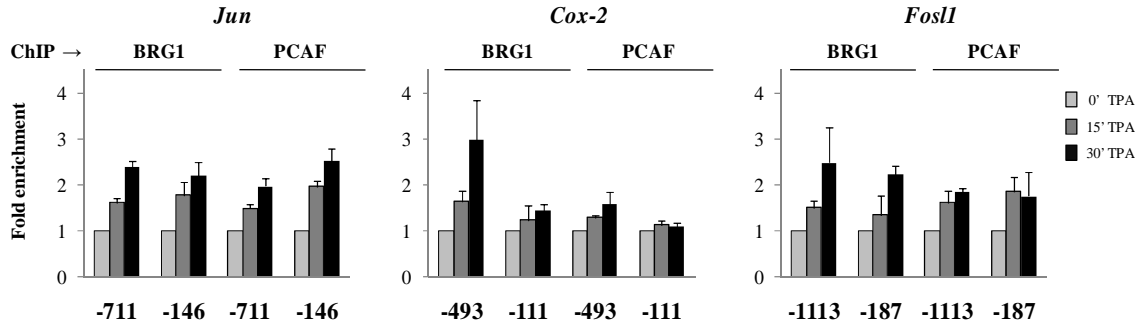


Figure 25: TPA-induced recruitment of 14-3-3 proteins to regulatory regions of *Jun*, *Cox-2* and *FosII* in parental and *Hras*-transformed mouse fibroblasts.

ChIP experiments were performed using antibodies against 14-3-3 ϵ and 14-3-3 ζ on formaldehyde-crosslinked mononucleosomes prepared from serum-starved 10T1/2 (A) and Ciras-3 (B) cells treated with TPA for 0, 15 and 30 minutes. n= 3.

A 10T1/2



B Ciras-3

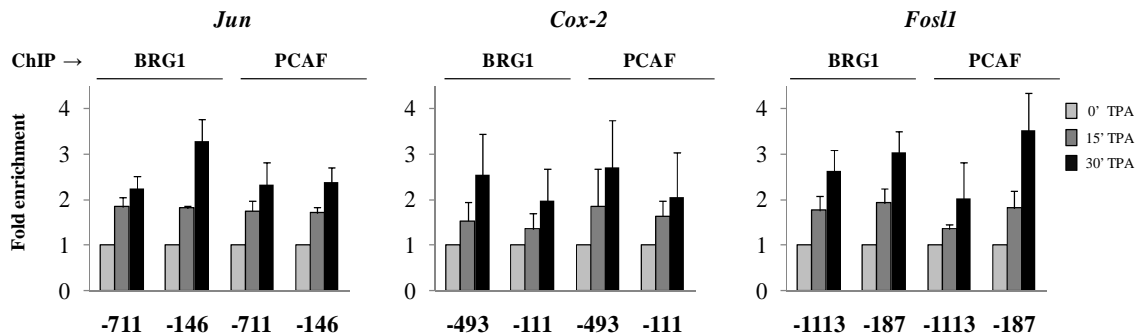


Figure 26: TPA-induced recruitment of chromatin remodelers/modifiers to regulatory regions of *Jun*, *Cox-2* and *FosII* in parental and *Hras*-transformed mouse fibroblasts.

ChIP experiments were performed using antibodies against BRG1 and PCAF on formaldehyde-crosslinked mononucleosomes prepared from serum-starved 10T1/2 (A) and Ciras-3 (B) cells treated with TPA for 0, 15 and 30 min. Enrichment values, obtained as described in Figure 22 are the mean of three independent experiments, and the error bars represent the standard deviation.

4.9 RAS-MAPK-induced formation of multi-protein complexes at the promoter regions of IE genes

Figure 19 shows that a ternary complex between MSK1, 14-3-3 ζ and BRG1 forms in response to RAS-MAPK signaling. To determine if these interactions occur at the nucleosomes of IE gene promoters, re-ChIP assays were performed. Formaldehyde-crosslinked mononucleosomes from serum-starved and 30 minute TPA-treated 10T1/2 cells were subjected to the ChIP procedure with MSK1 antibodies and the resulting

eluted MSK1-bound ChIP fragments were again immunoprecipitated with antibodies against H3S10ph. Figure 27 shows that the MSK1-H3S10ph re-ChIP assay resulted in a marked increase in DNA precipitation of *Jun*, *Cox-2* and *Fosll* proximal-promoter regulatory regions, validating the fidelity of the re-ChIP assay. On the contrary, the H3S10ph-H3S28ph re-ChIP assay did not yield any significant TPA-induced immunoprecipitation of the proximal-promoter regions from *Jun*, *Cox-2* and *Fosll* genes (Figure 27). These observations demonstrate that, upon TPA stimulation, MSK1 and H3S10ph are found on the same proximal IE gene regulatory regions, while H3S10ph and H3S28ph marks are not localized together at the nucleosomes of proximal-promoter IE gene regions. In order to investigate the formation of multi-protein complexes at the regulatory regions of inducible IE genes, re-ChIP assays were performed with MSK1 antibodies, followed by sequential immunoprecipitations with antibodies against 14-3-3 ζ , BRG1 and PCAF. Figure 27 shows that 30 minute TPA stimulation of 10T1/2 cells increases co-occupancy of MSK1 with 14-3-3 ζ , BRG1 and PCAF. Also, simultaneous occupancy of 14-3-3 ζ and BRG1 at the proximal regulatory regions of *Jun*, *Cox-2* and *Fosll* increases in response to TPA (Figure 27). Moreover, since 14-3-3 isoforms can form homo- or heterodimers, re-ChIP assays were performed with antibodies against 14-3-3 ζ , followed by sequential immunoprecipitations with 14-3-3 ϵ antibodies to determine if both of the 14-3-3 isoforms occupy the same regulatory regions of IE genes. Figure 27 demonstrates the TPA-induced increase in co-occupancy of 14-3-3 ζ and 14-3-3 ϵ at the proximal-promoter regions of *Jun* and *Fosll* genes, but not for the *Cox-2* gene. Thus, these observations suggest that the 14-3-3 heterodimer composition at the regulatory regions may be gene specific.

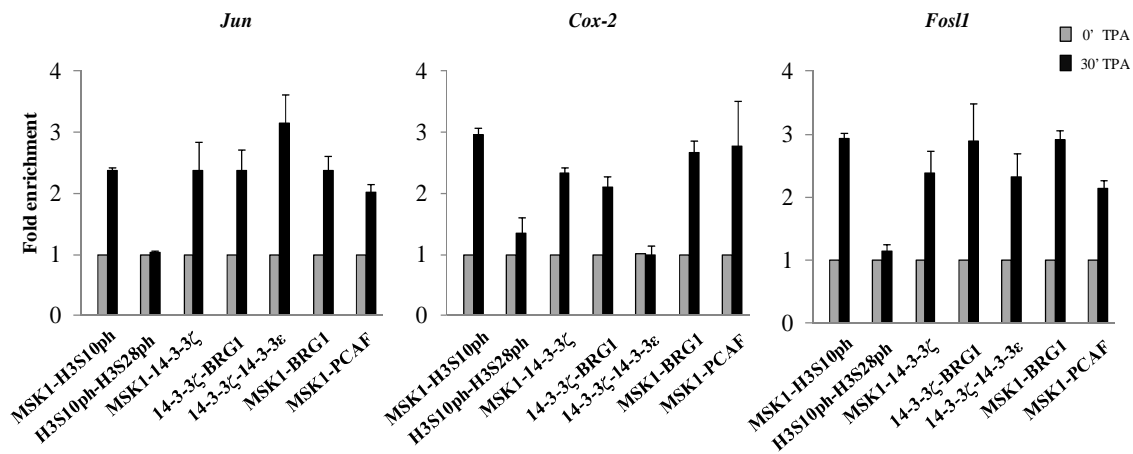


Figure 27: TPA-induced co-occupancy of MSK1, 14-3-3 proteins and chromatin remodelers/modifiers at the proximal regulatory regions of *Jun*, *Cox-2* and *FosII*.

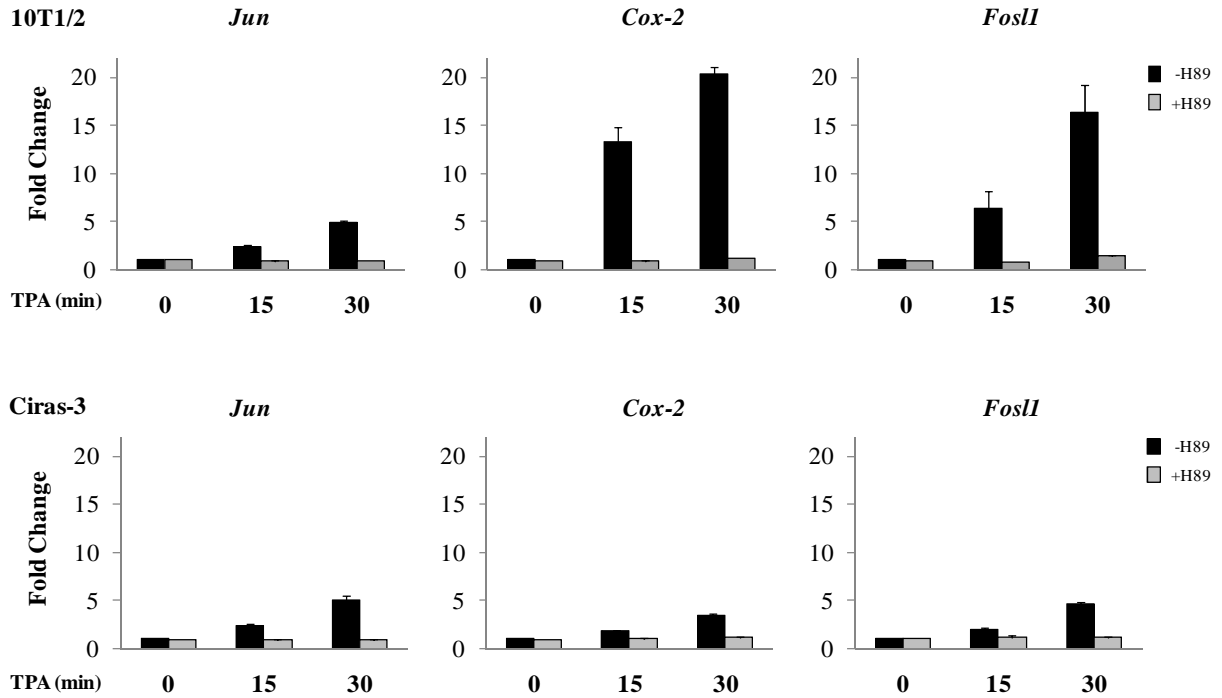
Re-ChIP experiments were performed on formaldehyde-crosslinked mononucleosomes prepared from serum-starved 10T1/2 cells treated with TPA for 0 and 30 min. The antibodies were used as indicated. Enrichment values, obtained as described in Figure 22, are the mean of three independent experiments, and the error bars represent the standard deviation.

4.10 The effect of MSK1 inhibition on IE gene transcriptional induction in response to RAS-MAPK signaling

MSK1 is selectively inhibited by H89 at a concentration of 10 μ M. H89-mediated inhibition of MSK activity also abolishes the nucleosomal response (Thomson et al., 1999). To evaluate the effect of MSK1 inhibition on the expression of *Jun*, *Cox-2* and *FosII* in response to RAS-MAPK signaling, serum-starved 10T1/2 and Ciras-3 cells were pre-treated with H89 prior to TPA treatment. Figure 28A shows the TPA-induced expression of *Jun*, *Cox-2* and *FosII* in 10T1/2 and Ciras-3 cells. The induction of *Cox-2* and *FosII* genes was more pronounced in 10T1/2 cells. It is noteworthy to mention that the expression level of *Cox-2* and *FosII* was higher at time 0 in Ciras-3, which might reflect the more pronounced induction of these two genes in 10T1/2 cells. Further, in the presence of H89, the TPA-induced IE gene expression was abolished in both cell lines

(Figure 28A). Since H89 is able to inhibit another potential H3 kinase, protein kinase A (PKA) *in vitro* (Davies et al., 2000), the effects of a specific PKA inhibitor (Rp-cAMP) on the induction of IE genes was analyzed by exposing serum-starved 10T1/2 cells to Rp-cAMP prior to TPA stimulation. Figure 28B shows that the exposure of quiescent 10T1/2 cells to Rp-cAMP did not affect the TPA-induced transcription of *Jun*, *Cox-2* and *Fos11*, demonstrating that the effects of H89 were due to the inhibition of MSK. Furthermore, TPA treatment of serum-starved 10T1/2 and Ciras-3 cells increased the association of RNA polymerase II phosphorylated at serine 5 (RNAPII S5ph) at the promoter regions of *Jun*, *Cox-2* and *Fos11*, whereas in the presence of H89, TPA-induced RNAPII S5ph association with the promoter regions of IE genes was severely reduced (Figure 29). RNAPII S5ph is an initiation-engaged form of RNAPII (Xie et al., 2006); therefore, these ChIP results imply that the formation of an initiation complex at the 5' end of IE genes requires a chromatin remodeling event that is dependent on the MSK-mediated nucleosomal response. Treatment of 10T1/2 and Ciras-3 cells with H89 prior to the addition of TPA did not reduce total levels of RNAPII S5ph (Figure 30).

A



B

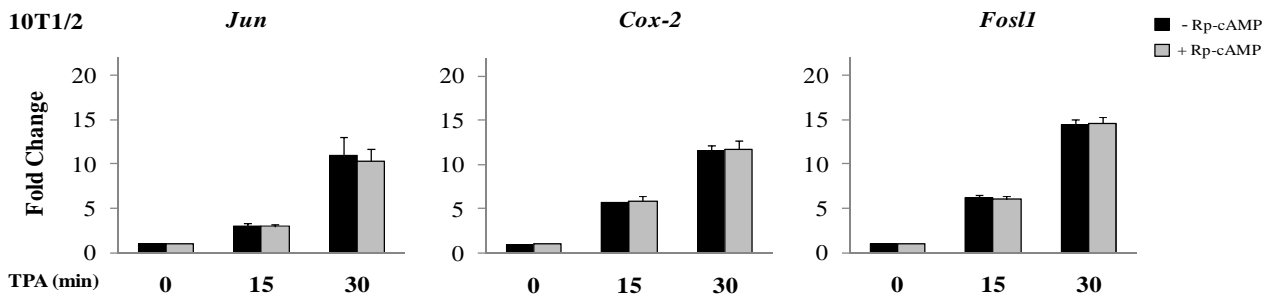


Figure 28: H89 inhibits the TPA-induced expression of *Jun*, *Cox-2* and *FosII* genes in parental and *Hras*-transformed mouse fibroblasts.

A) Serum-starved 10T1/2 cells and Ciras-3 were pre-treated or not with H89 prior to TPA stimulation for 0, 15 or 30 min. Total RNA was isolated and quantified by real time RT-PCR. Fold change values were normalized to GAPDH levels and time 0 values. n = 3; B) Serum-starved 10T1/2 cells were pre-treated or not with Rp-cAMP prior to TPA stimulation for 0, 15 or 30 min. Fold change values were normalized to GAPDH levels and time 0 values. n = 3, error bars represent the standard deviation.

RNAPII S5ph ChIP

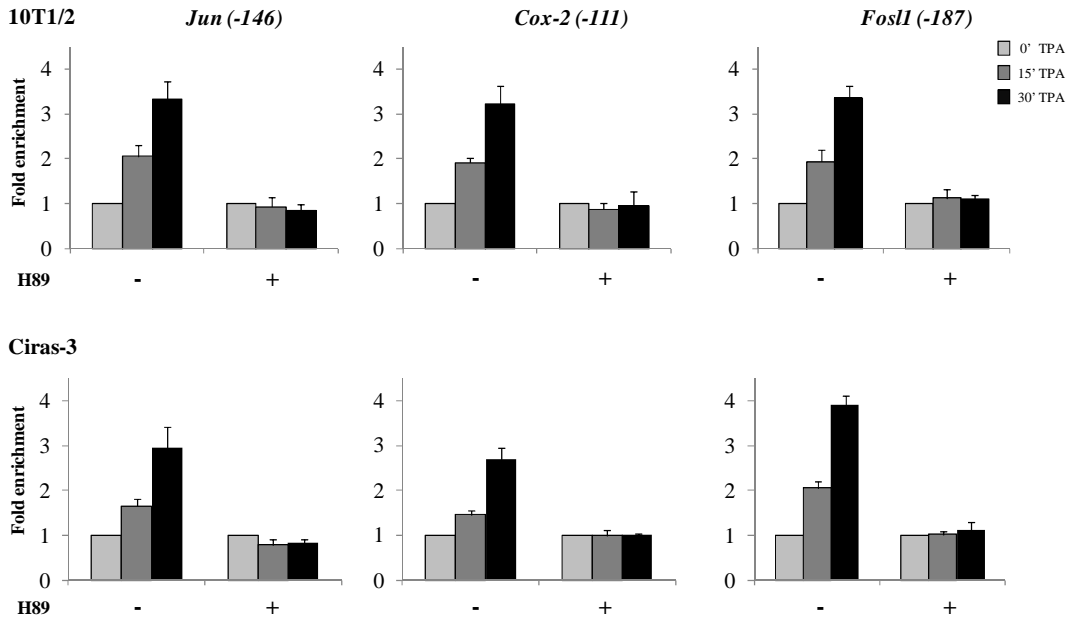


Figure 29: H89 reduces the levels of TPA-induced RNAPII S5ph at proximal promoters of *Jun*, *Cox-2* and *FosI1* in parental and *Hras*-transformed mouse fibroblasts.

10T1/2 and Ciras-3 formaldehyde-crosslinked mononucleosomes were prepared and used in ChIP assays with anti-RNAPII S5ph antibodies. Equal amounts of input and immunoprecipitated DNA were quantified by real-time quantitative PCR. Enrichment values are the mean of three independent experiments and the error bars represent the standard deviation.

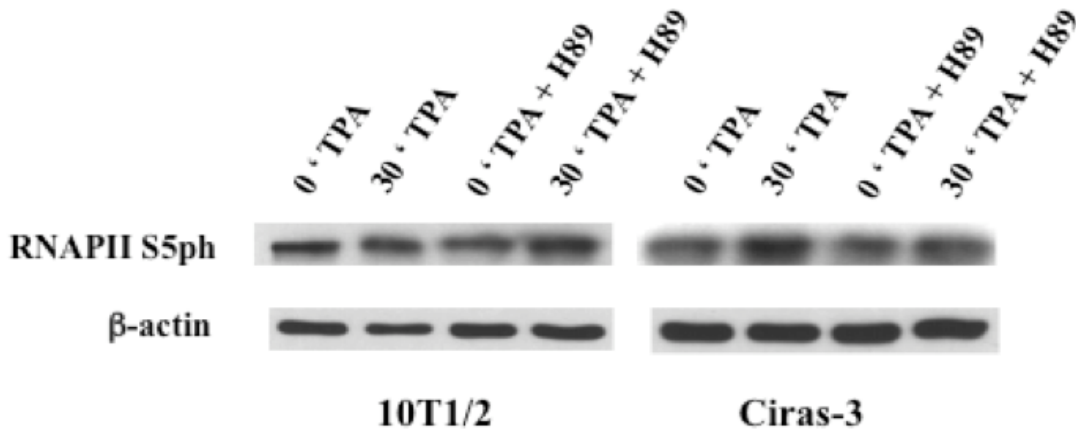


Figure 30: H89 has no effect on the levels of RNAPII S5ph in 10T1/2 and Ciras-3 cells.

Cell extracts (20 μg) isolated from TPA-treated 10T1/2 and Ciras-3 cells treated or not with H89 were resolved on a SDS-10% polyacrylamide gel, transferred to a membrane and immunochemically stained with anti-RNAPII S5ph and anti-β-actin antibodies.

4.11 The effect of H89 on the recruitment of MSK1, 14-3-3 isoforms, chromatin remodelers/modifiers, the resulting H3 modifications and transcription factors at the regulatory regions of IE genes

In order to evaluate the consequence of MSK1 inhibition on the initiation of promoter remodeling at inducible IE genes, ChIP assays were performed with formaldehyde-crosslinked lysates from 10T1/2 and Ciras-3 cells that were pre-treated with H89. Figures 31 and 32 show that H89 abolished TPA-induced MSK1 recruitment and the ensuing H3S10ph and H3S28ph levels at the proximal 5' regions of *Jun* (-146), *Cox-2* (-111) and *FosII* (-187) in 10T1/2 and Ciras-3 cells. Correspondingly, TPA-induced binding of 14-3-3 ϵ , 14-3-3 ζ , BRG1 and PCAF at the same 5' regulatory regions of the three IE genes was severely reduced in both cell lines (Figures 31 and 32). Furthermore, TPA-induced H3 acetylation and methylation levels were markedly reduced at the proximal-promoter regions of *Jun* (-146), *Cox-2* (-111) and *FosII* (-187) in the presence of H89 (Figures 31, 32 and 33). The reduction of TPA-induced H3 acetylation and methylation by H89 was more severe in *Hras*-transformed Ciras-3 cells (Figure 33). The analysis of the immunoprecipitated DNA for the 5' distal regulatory regions of *Jun* (-711), *Cox-2* (-493) and *FosII* (-1113) demonstrated that TPA-induced MSK1 recruitment, H3 phosphoacetylation and binding of 14-3-3 ϵ , 14-3-3 ζ , BRG1 and PCAF were similarly affected at these upstream regions of the three IE genes by H89 pre-treatment of 10T1/2 and Ciras-3 cells (Figures 34 and 35). The lack of MSK1 recruitment to the promoter regions of IE genes following H89 pretreatment of cells suggests that the recruitment of MSK1 is dependent on its kinase activity, which is required to activate the complex such that it is recruited to the IE gene promoter regions. An alternative

explanation could be that H89 interferes with the formation of the MSK1-14-3-3-SWI/SNF complex. To explore this latter possibility, we tested the ability of anti-MSK1 antibodies to co-immunoprecipitate 14-3-3 ζ or BRG1 when quiescent 10T1/2 cells were exposed to H89 prior to TPA treatment. Figure 37 shows that BRG1 and 14-3-3 ζ formed complexes with MSK1 in 10T1/2 cells pre-treated with H89 and TPA-stimulated for 0 or 30 min. Thus, H89 did not prevent the formation of MSK1 complexes, and its negative effect on promoter region remodeling and IE gene induction is most likely due to the inhibition of MSK1 kinase activity.

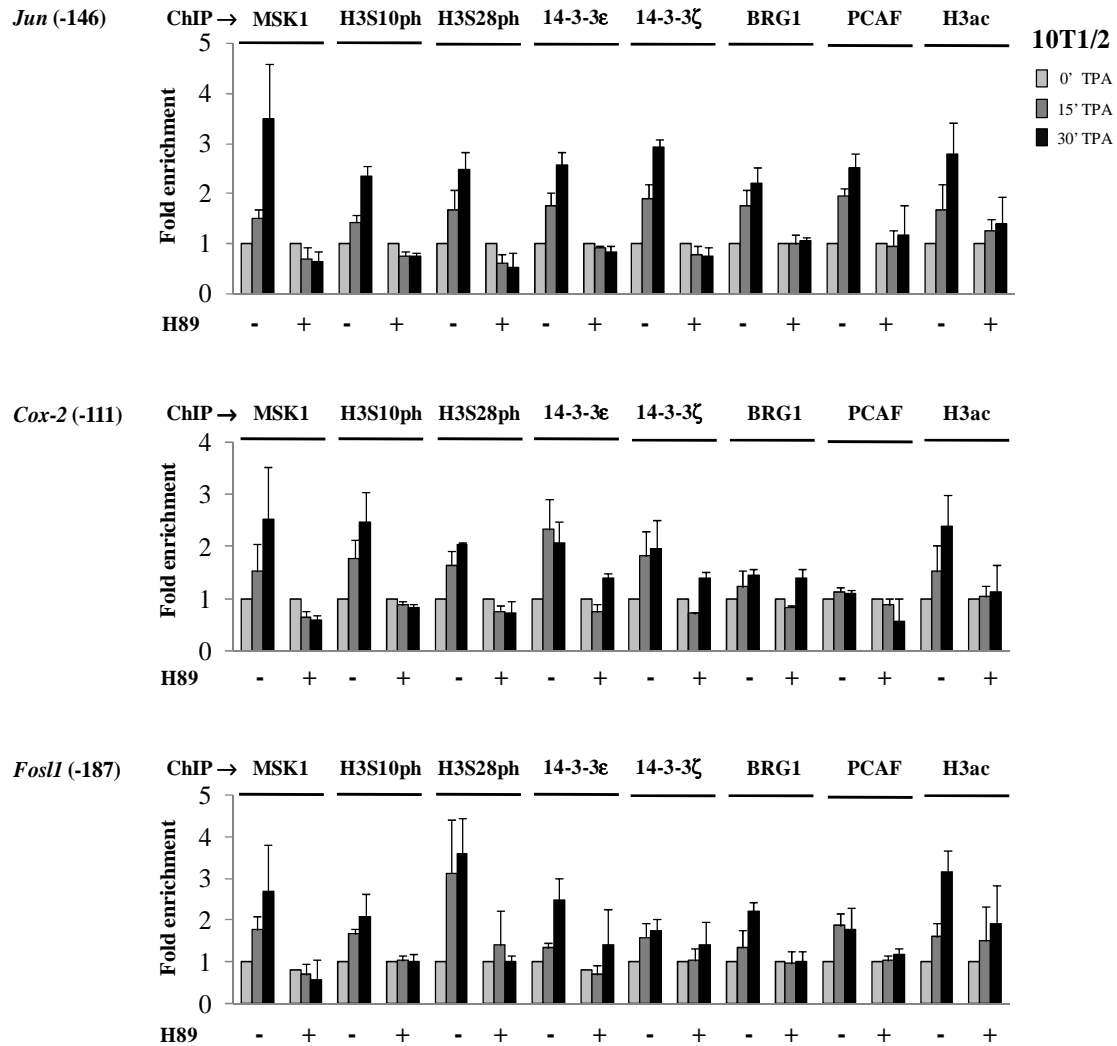


Figure 31: H89 inhibits TPA-induced nucleosomal response and chromatin remodeler/modifier recruitment to 5' proximal regulatory regions of *Jun*, *Cox-2* and *FosII* in parental mouse fibroblasts.

Serum-starved 10T1/2 cells were pre-treated or not with H89 prior to TPA stimulation for 0, 15 or 30 min. Formaldehyde crosslinked mononucleosomes were prepared and used in ChIP assays with antibodies against MSK1, H3S10ph, H3S28ph, 14-3-3ε, 14-3-3ζ, BRG1, PCAF or H3K9acK14ac. Enrichment values, obtained as described in Figure 22 are the mean of three independent experiments, and the error bars represent the standard deviation.

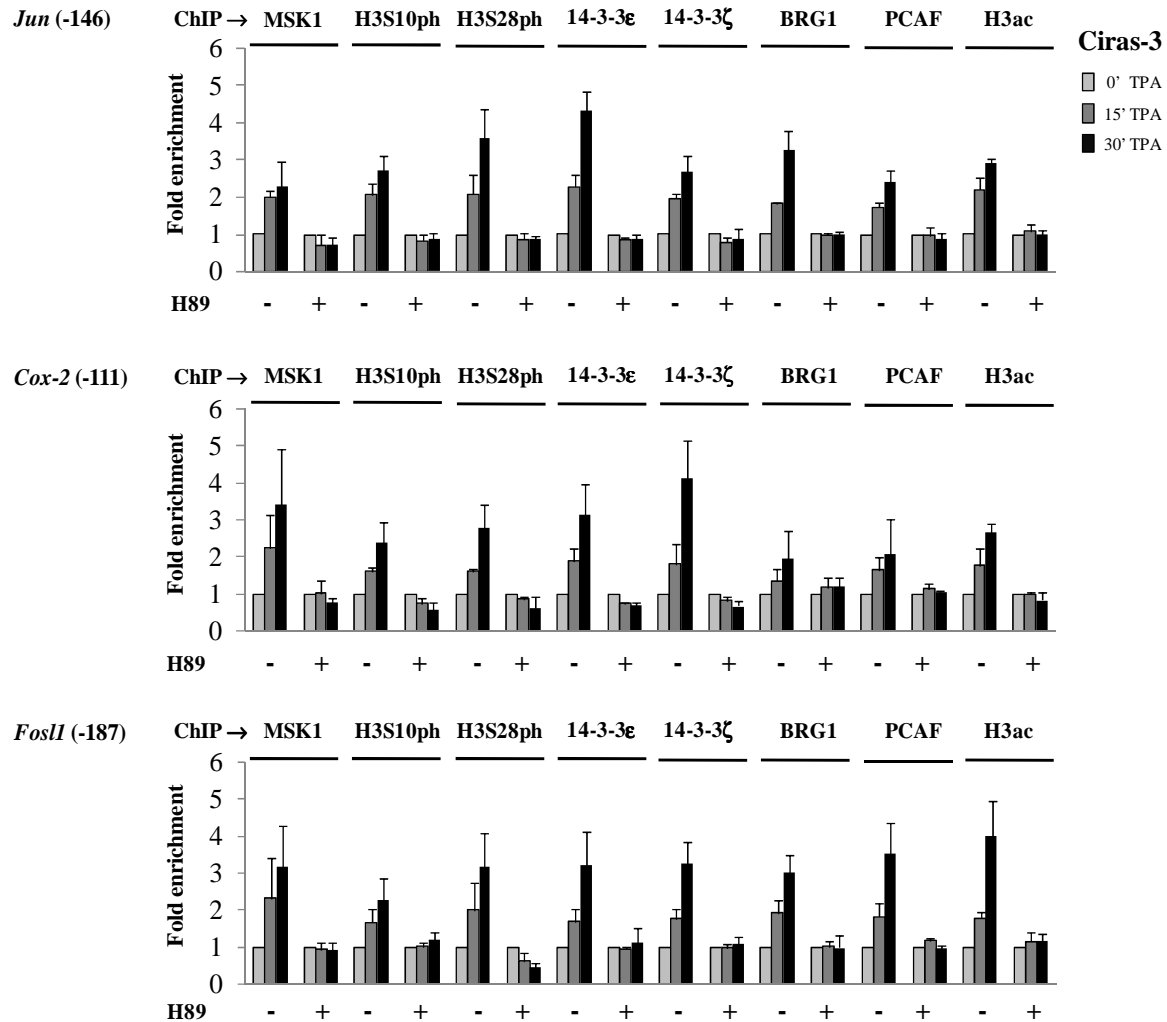


Figure 32: H89 inhibits TPA-induced nucleosomal response and chromatin remodeler/modifier recruitment to 5' proximal regulatory regions of *Jun*, *Cox-2* and *FosII* in *Hras*-transformed mouse fibroblasts.

Serum-starved Ciras-3 cells were pre-treated or not with H89 prior to TPA stimulation for 0, 15 or 30 min. Formaldehyde crosslinked mononucleosomes were prepared and used in ChIP assays with antibodies against MSK1, H3S10ph, H3S28ph, 14-3-3ε, 14-3-3ζ, BRG1, PCAF or H3K9acK14ac. Enrichment values, obtained as described in Figure 22 are the mean of three independent experiments, and the error bars represent the standard deviation.

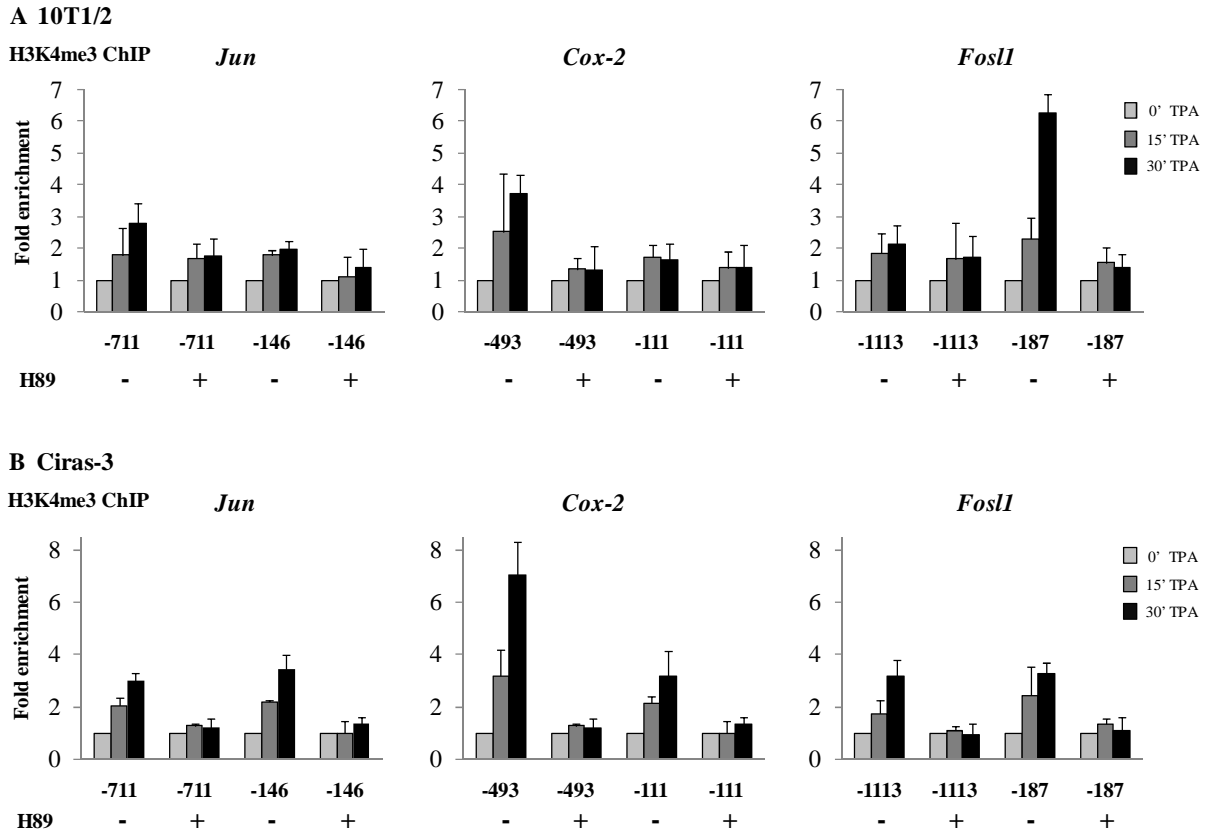


Figure 33: H89 reduces TPA-induced H3 methylation at regulatory regions of *Jun*, *Cox-2* and *FosII* in parental and *Hras*-transformed mouse fibroblasts.

Serum-starved 10T1/2 (A) and Ciras-3 (B) cells were pre-treated or not with H89 prior to TPA stimulation for 0, 15 or 30 min. Formaldehyde crosslinked mononucleosomes were prepared and used in ChIP assays with anti-H3K4me3 antibodies. Enrichment values, obtained as described in Figure 22 are the mean of three independent experiments, and the error bars represent the standard deviation.

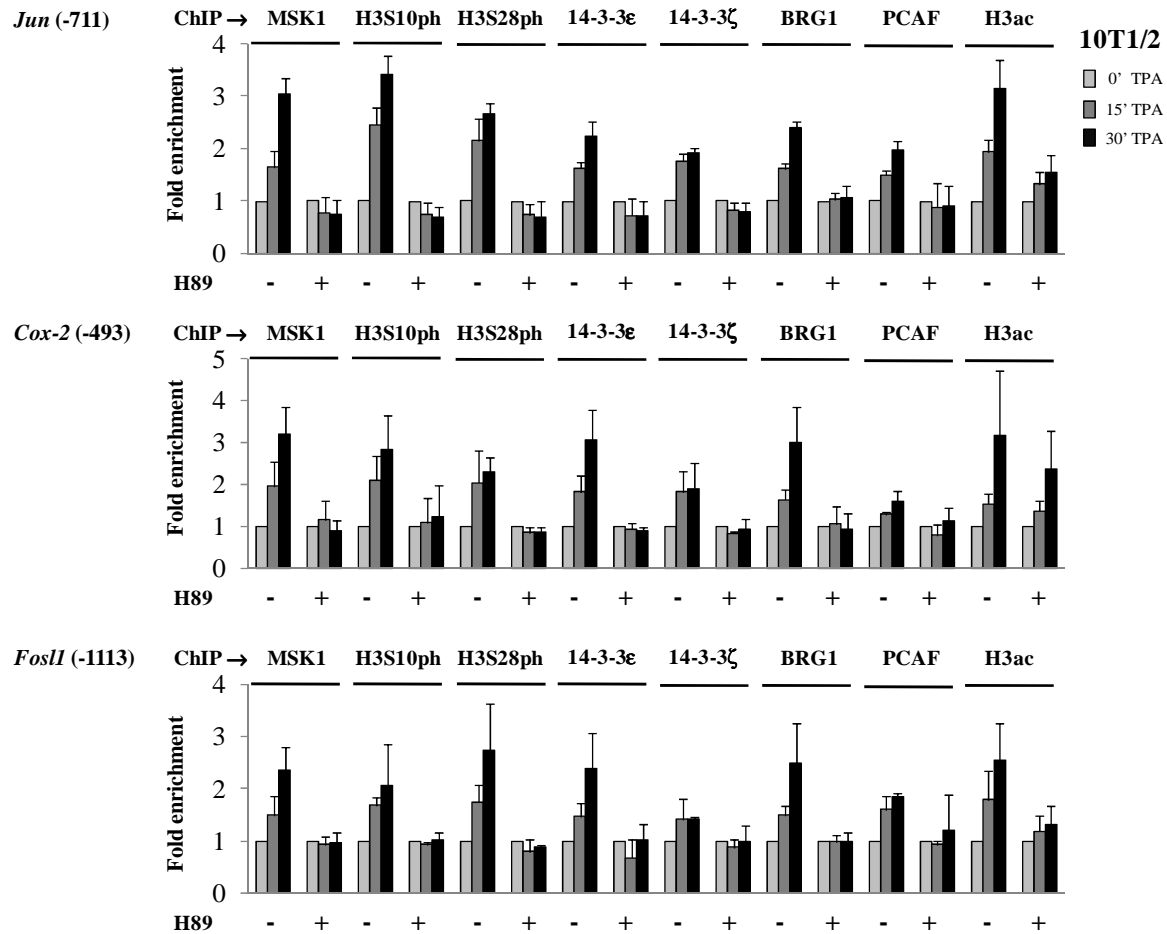


Figure 34: H89 inhibits TPA-induced nucleosomal response and chromatin remodeler/modifier recruitment to 5' distal regulatory regions of *Jun*, *Cox-2* and *FosII* in parental mouse fibroblasts.

Serum-starved 10T1/2 cells were pre-treated or not with H89 prior to TPA stimulation for 0, 15 or 30 min. Formaldehyde crosslinked mononucleosomes were prepared and used in ChIP assays with antibodies against MSK1, H3S10ph, H3S28ph, 14-3-3ε, 14-3-3ζ, BRG1, PCAF or H3K9acK14ac. Enrichment values, obtained as described in Figure 22 are the mean of three independent experiments, and the error bars represent the standard deviation.

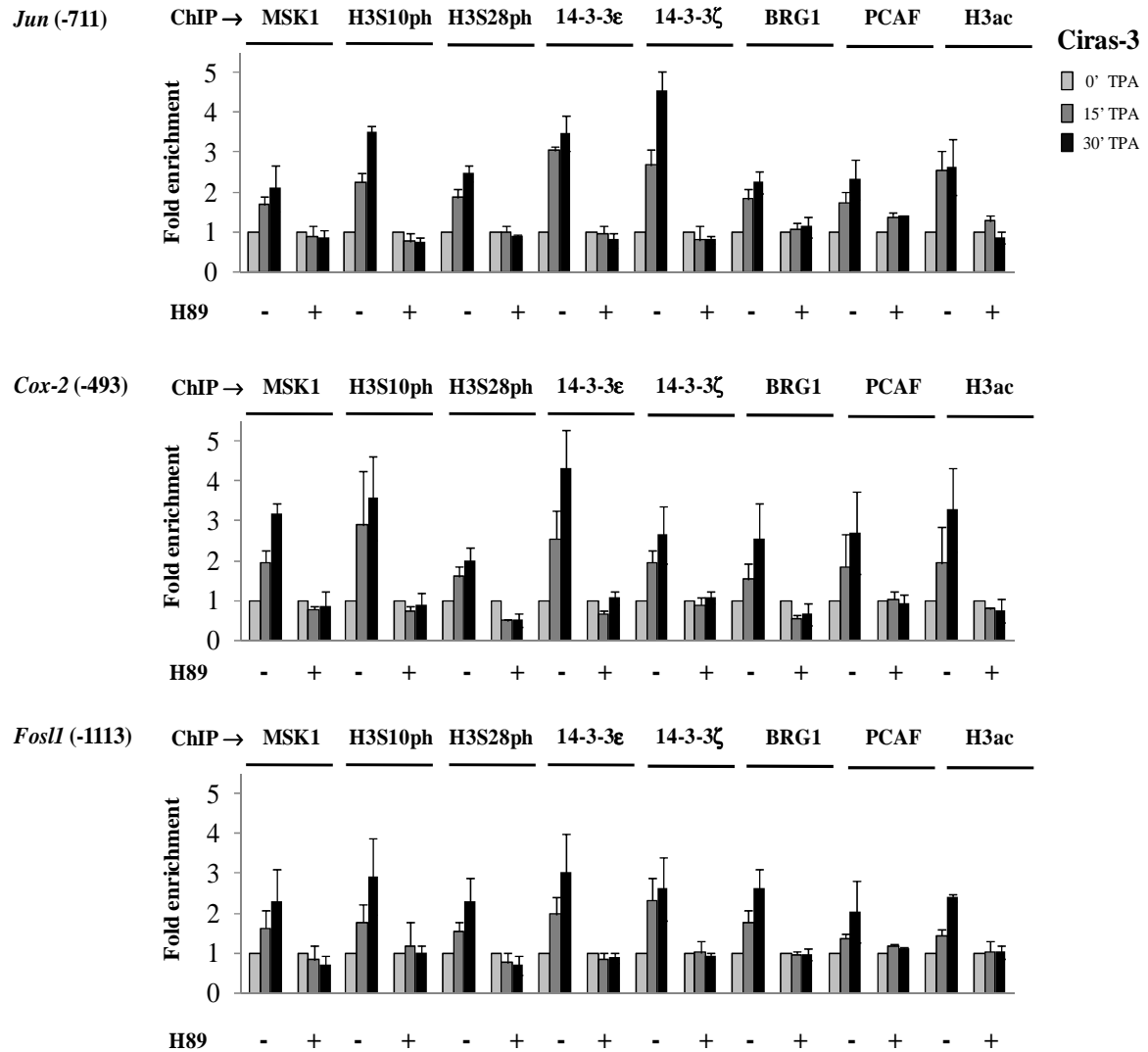


Figure 35: H89 inhibits TPA-induced nucleosomal response and chromatin remodeler/modifier recruitment to 5' distal regulatory regions of *Jun*, *Cox-2* and *FosII* in *Hras*-transformed mouse fibroblasts.

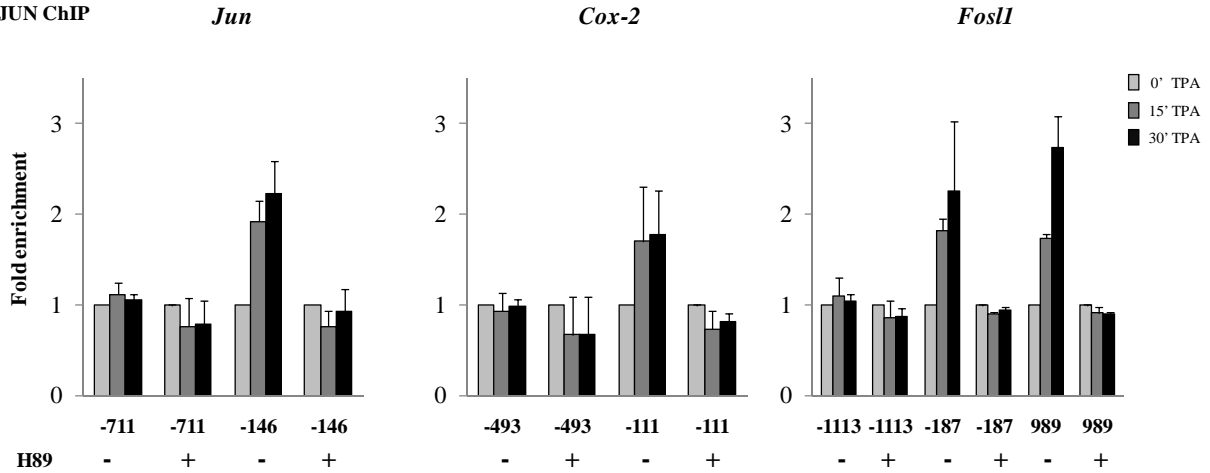
Serum-starved Ciras-3 cells were pre-treated or not with H89 prior to TPA stimulation for 0, 15 or 30 min. Formaldehyde crosslinked mononucleosomes were prepared and used in ChIP assays with antibodies against MSK1, H3S10ph, H3S28ph, 14-3-3ε, 14-3-3ζ, BRG1, PCAF or H3K9acK14ac. Enrichment values, obtained as described in Figure 22 are the mean of three independent experiments, and the error bars represent the standard deviation.

The AP-1 transcription factor, a homo- or heterodimer consisting of proteins belonging to JUN, FOS (including FRA) and ATF families, is involved in the regulation of IE genes, including genes coding for its components. The TPA-induced association of JUN with

the regulatory regions of *Jun*, *Cox-2* and *FosII* was investigated by ChIP assay. Figure 36 shows that TPA stimulation of serum-starved 10T1/2 and Ciras-3 cells increases JUN binding at the 5' proximal, but not distal, regulatory regions of *Jun*, *Cox-2* and *FosII*, as well as at the regulatory region located in the first intron of *FosII* (+989).

A 10T1/2

JUN ChIP



B Ciras-3

JUN ChIP

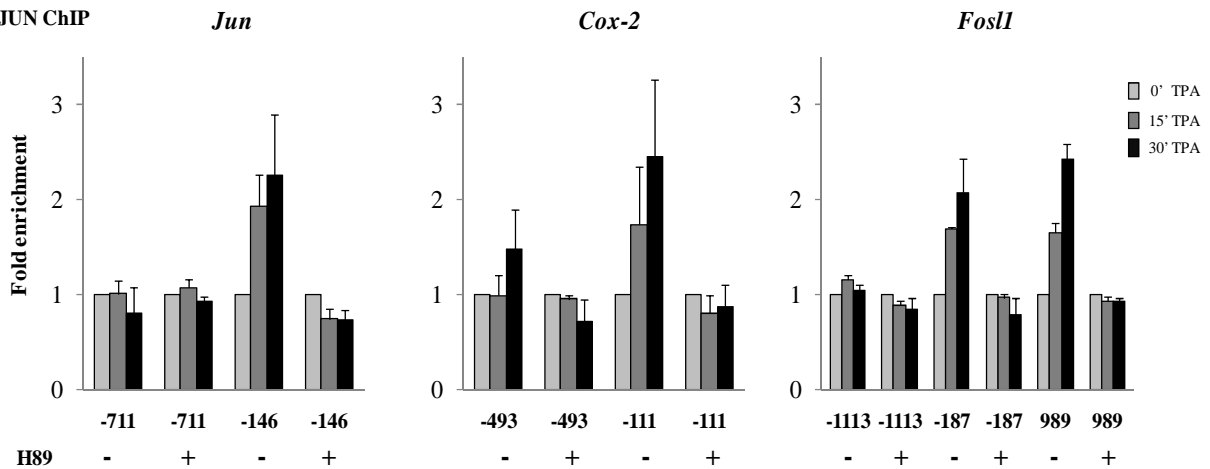


Figure 36: H89 abolishes TPA-induced recruitment of JUN to regulatory regions of *Jun*, *Cox-2* and *FosII* in parental and *Hras*-transformed mouse fibroblasts.

Serum-starved 10T1/2 (A) and Ciras-3 (B) cells were pre-treated or not with H89 prior to TPA stimulation for 0, 15 or 30 min. Formaldehyde crosslinked mononucleosomes were prepared and used in ChIP assays with anti-JUN antibodies. Enrichment values are the mean of three independent experiments, and the error bars represent the standard deviation.

These results are in agreement with the mapping of known JUN, and AP-1 binding sites and TPA-responsive element (TRE). Additionally, when serum-starved 10T1/2 and Ciras-3 cells were treated with H89 prior to TPA stimulation, JUN binding with its DNA binding sites was abolished for each of the three IE genes (Figure 36). These results indicate that the binding of JUN to its cognate DNA sequences in the three investigated IE genes is dependent on the TPA-induced and MSK-mediated nucleosomal response.

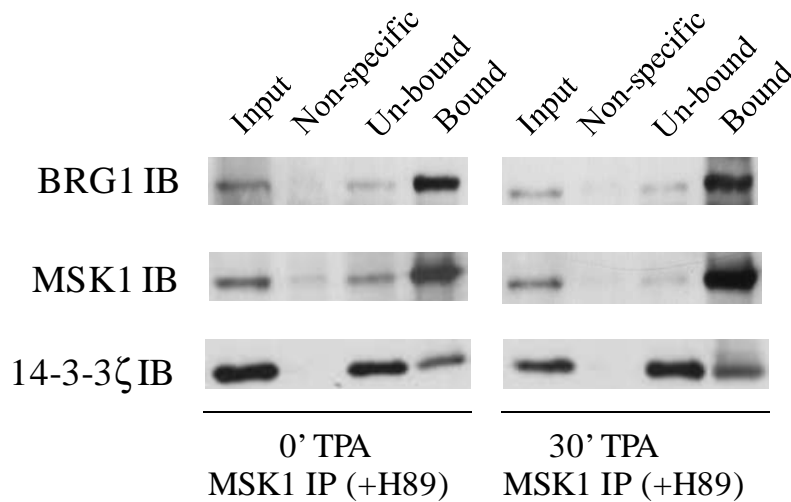


Figure 37: H89 has no effect on MSK1 association with BRG1 and 14-3-3ζ.

Serum-starved 10T1/2 cells were pre-treated or not with H89 prior to TPA stimulation for 0 or 30 min. Aliquots of 1 mg total cell extract were incubated with anti-MSK1 antibodies. The whole “Bound” and “Non-specific” fractions and equivalent volumes of “Input” and “Un-bound” fractions, corresponding to 25 μg of total cell extracts were resolved on SDS-10%-PAGE and immunoblotted with indicated antibodies.

4.12 MSK1 regulates TPA-induced expression of *Jun*, *Cox-2* and *Fosll*

Recent studies have reported the involvement of MSK1 in regulation of immediate-early and NF κ B-dependent genes (Arthur, 2008). Stably transduced parental and *Hras*-transformed mouse fibroblasts with the MSK1 shRNA (MSK1 KD) were used to directly assess the extent of MSK1 regulation in TPA-induced expression of *Jun*, *Cox-2* and *Fosll*. Figure 38 shows that approximately 74% and 90% knockdown of MSK1 were achieved with stable transductions of MSK1 shRNA in 10T1/2 and Ciras-3 cells, respectively.

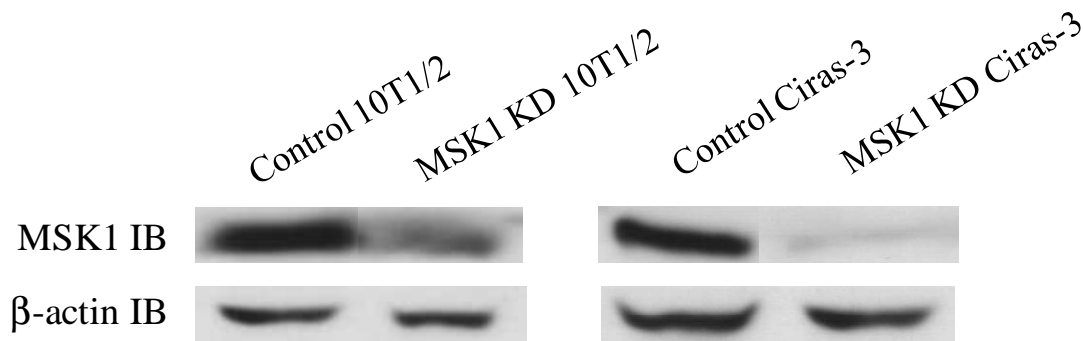


Figure 38: MSK1 knockdown in parental and *Hras*-transformed mouse fibroblasts.

20 μ g of control (empty lentiviral vector control) and MSK1 knockdown (MSK1 shRNA, KD) 10T1/2 and Ciras-3 cell lysates were run on SDS-10%-PAGE. Membranes were immunoblotted with anti-MSK1 and anti- β -actin antibodies. 74% and 90% of MSK1 knock down was observed in 10T1/2 and Ciras-3 cells transduced with MSK1 shRNA, respectively. Percentage of MSK1 knock down was determined by measuring densitometric values from anti-MSK1 controls and normalizing these values with densitometric values of anti- β -actin.

Serum-starved 10T1/2 and Ciras-3 control and MSK1 KD cells were left untreated or treated with TPA for 30 minutes. Real time PCR analysis was performed to assess TPA-induced expression of IE genes in MSK1 knockdown 10T1/2 and Ciras-3 cells as compared to control 10T1/2 and Ciras-3 cells. Figure 39 shows that TPA induced the expression of *Jun*, *Cox-2* and *Fosll* in control 10T1/2 and Ciras-3 cells. On the other

hand, TPA-induced expression of *Jun*, *Cox-2* and *Fos11* was significantly reduced in 10T1/2 and Ciras-3 cells with diminished MSK1 protein levels.

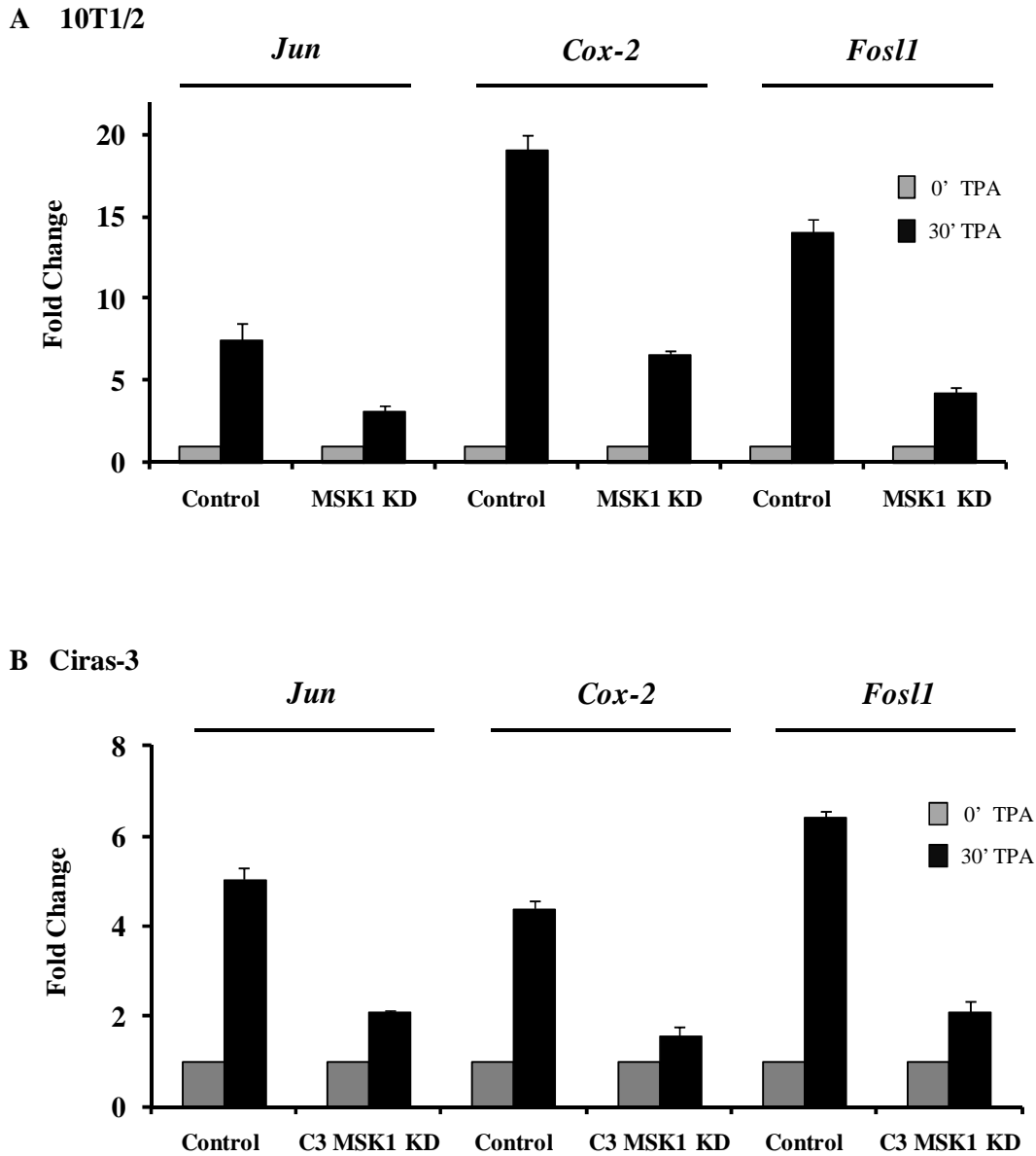


Figure 39: MSK1 knockdown reduces TPA-induced expression of *Jun*, *Cox-2* and *Fos11* in parental and *Hras*-transformed mouse fibroblasts. Serum-starved control and MSK1 KD 10T1/2 (A) and Ciras-3 (B) cells were left untreated or treated with TPA for 30 minutes. Total RNA was isolated and quantified by real time RT-PCR. Fold change values were normalized to GAPDH levels and time 0 values. n = 3.

MSK1 knockdown in parental 10T1/2 cells reduced the TPA-induced expression of *Jun*, *Cox-2* and *Fos11* by 59%, 66% and 70%, respectively. Furthermore, in *Hras*-transformed cells, MSK1 knockdown reduced the TPA-induced expression of *Fos11* by 67%, *Cox-2* by 64% and *Jun* by 58% (Figure 39). These results show that MSK1 has a significant role in mediating the expression of IE genes in response to RAS-MAPK signaling. Furthermore, we show that upregulated RAS-MAPK signaling contributes to increased protein expression (Figure 40). The upregulation of JUN (8-fold), FRA-1 (4-fold) and COX-2 (6-fold) protein levels, was observed in *Hras*-transformed mouse fibroblasts (Figure 40). We showed that MSK1 regulates the expression of IE genes (Figure 38), and that MSK1 activity is enhanced in *Hras*-transformed cells; therefore, the observed increases of JUN, FRA-1 and COX-2 protein levels in oncogene-transformed cells complement our data.

A

	G ₀ /G ₁	G ₂ /GM	S-phase
10T1/2	70%	12%	18%
Ciras-3	65%	14%	21%

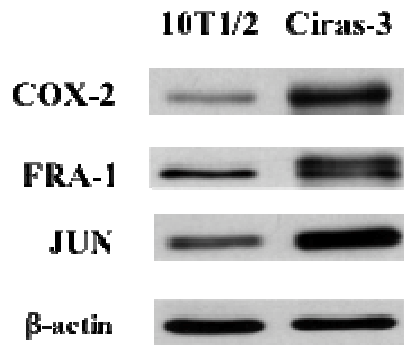
B

Figure 40: Protein levels of COX-2, FRA-1 and JUN are elevated in *Hras*-transformed mouse fibroblasts.

A) Cell cycle distribution of 10T1/2 and Ciras-3 cells as determined by FACS analysis.

B) 20 μ g of cell-cycle matched 10T1/2 and Ciras-3 cell lysates were resolved on SDS-10%-PAGE. Membranes were immunochemically stained with anti-COX-2, anti-FRA-1, anti-JUN and anti- β -actin antibodies.

In order to determine the consequences of MSK1 knockdown on molecular events that occur at the nucleosomes of IE genes, we performed our high resolution ChIP experiments on quiescent control and MSK1 knockdown 10T1/2 cells that were either not stimulated or stimulated with TPA for 30 min, using antibodies against H3S10ph, H3S28ph, 14-3-3 ϵ , 14-3-3 ζ , BRG1 or JUN. Figure 41A shows that the association of all these proteins with the *Jun*, *Cox-2* and *Fos11* 5' proximal regulatory regions was reduced by half in MSK1 knockdown cells compared to control cells. A similar reduction in the association of 14-3-3 ζ and BRG1 to the three gene proximal regulatory regions was observed in re-ChIP experiments performed on mononucleosomes from quiescent control

and MSK1 knockdown 10T1/2 cells that were either not stimulated or stimulated with TPA for 30 min (Figure 41B). Thus, MSK1 is required for the TPA-induced nucleosomal response and chromatin remodeling that takes place at the promoter regions of IE genes.

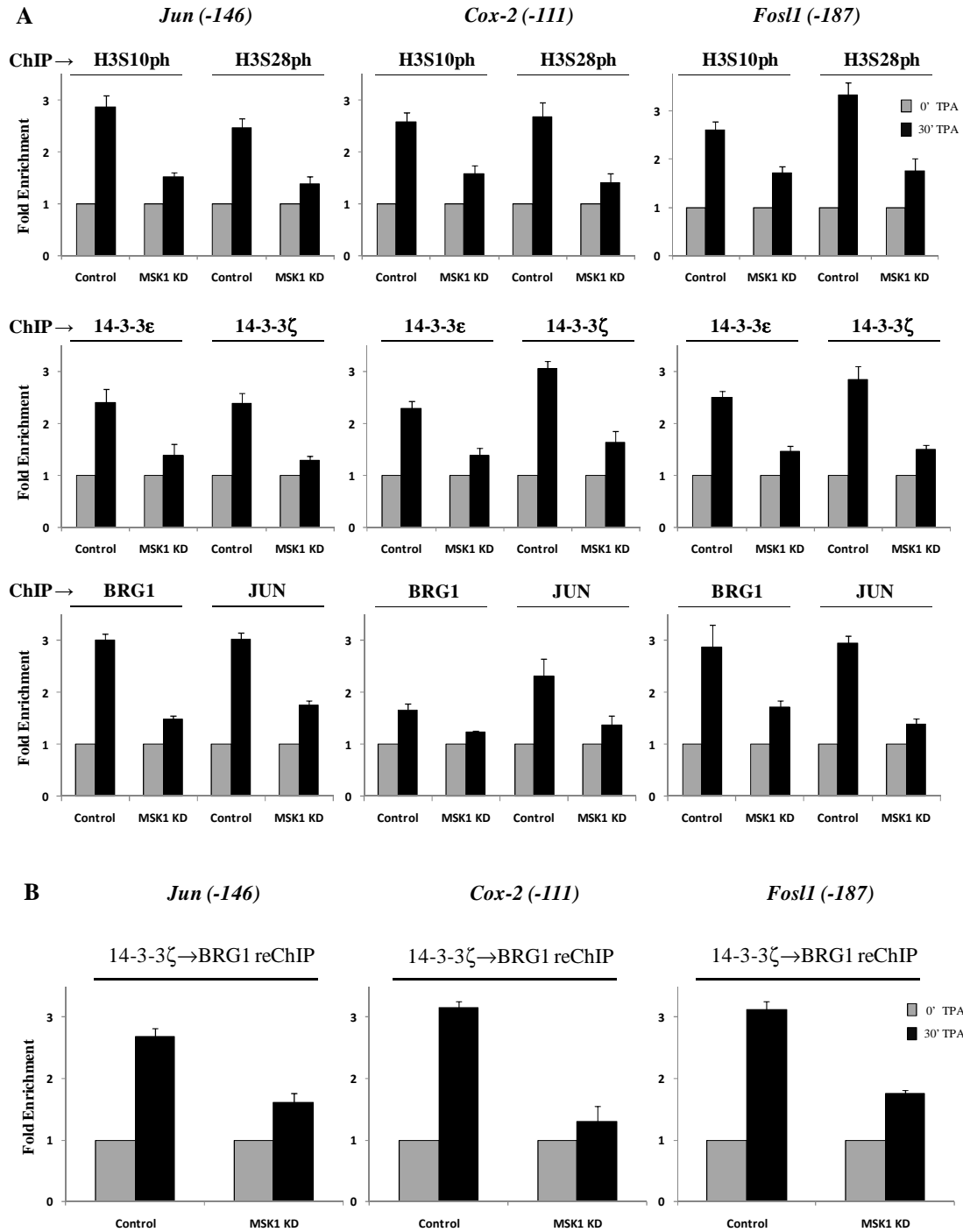


Figure 41: MSK1 is required for the TPA-induced nucleosomal response.

ChIP experiments using antibodies against H3S10ph, H3S28ph, 14-3-3ε, 14-3-3ζ, BRG1 or JUN (A) and re-ChIP experiments using antibodies as indicated (B) were performed on formaldehyde-crosslinked mononucleosomes prepared from serum-starved control and MSK1 knockdown 10T1/2 cells (MSK1 KD) treated with TPA for 30 min. Equal amounts of input and ChIP DNA were quantified by real-time quantitative PCR. The enrichment values of the 5' proximal sequences of *Jun* (-146), *Cox-2* (-111) and *FosI1* (-187) genes are the mean of three independent experiments, and the error bars represent the standard deviation.

5.0 DISCUSSION

5.1 The activity of MSK1 is upregulated in *Hras*-transformed mouse fibroblasts

Constitutive activation of the RAS-RAF-ERK pathway in *Hras*-transformed mouse fibroblasts increases the steady-state level of phosphorylated Ser10 and Ser28 of H3 (Chadee et al., 1999; Dunn et al., 2009). Our results show that the activity of a downstream target of this signal transduction pathway, the H3 kinase MSK1, is increased in the *Hras*-transformed cells, due to the upregulation of MSK1 activating kinases, ERK1/2. Furthermore, constitutive activation of the RAS-MAPK pathway did not alter the protein level of MSK1 or the subcellular distribution of the enzyme. Since the level of the H3 phosphatase is not altered in *Hras*-transformed cells (Chadee et al., 1999), the net result of this constitutively activated pathway is an increase in the steady-state level of phosphorylated H3. In the kinase assays with H3 and H4 and immunoprecipitated MSK1, we observed a low level of H4 radiolabeling. There was the possibility that immunoprecipitated MSK1 was associated with another kinase that phosphorylated H4. However, it was observed that purified MSK1, when incubated with H3 and H4, would also weakly label H4, with H3 being the preferred substrate (Drobic et al., 2004). MSK1 phosphorylates H3 at the site RKS. H4 has the sequence RIS47, which may be the site phosphorylated albeit weakly by MSK1. Because this portion of the H4 molecule is in the histone fold, localized to the interior of the nucleosome, it is likely that H4 Ser47 is inaccessible to MSK1 in chromatin, unless MSK1 is associated with necessary enzymatic activities that would further alter the nucleosome structure to allow access to Ser47 of H4. This phospho-modification of H4 has been detected *in vivo* (Cosgrove et al., 2004). However, the steady-state level of H4S47ph in transformed cells is not known. Moreover,

it could be hypothesized that the levels of this H4 modification would also be elevated in transformed cells that have an upregulated RAS-RAF-ERK pathway.

Phosphorylated H3 in cycling Ciras-3 cells and in TPA- or EGF-stimulated 10T1/2 mouse fibroblasts is associated with relaxed chromatin regions that are located in specific nuclear locations (Chadee et al., 1999). Chromatin immunoprecipitation assays have provided direct evidence that the induced phosphorylated Ser10 of H3 is bound to the promoter regions of the immediate-early genes *Fos*, *c-Myc*, and *Jun* (Chadee et al., 1999; Cheung et al., 2000; Clayton et al., 2000). Pre-treatment of Ciras-3 and 10T1/2 cells with the potent MSK1 inhibitor H89 reduced or prevented the transiently TPA-induced expression of immediate-early genes such as *Fos* and urokinase plasminogen activator (*uPA*), suggesting that phosphorylation of H3 contributed to the induced transcription of these genes (Strelkov and Davie, 2002). Similar results were obtained with MSK1/2 knock out mouse primary embryonic fibroblasts (Soloaga et al., 2003). The elevated activity of MSK1 in *Hras*-transformed cells may be one of several deregulated chromatin modifying enzymes that through their action of remodeling the chromatin lead to aberrant expression of genes in the transformed cells.

MSK1 is located primarily in the nucleus and to a lesser extent in the cytoplasm of Ciras-3 and 10T1/2 mouse fibroblasts. Our results show that, most, if not all, MSK1 is extracted from the nuclei with 0.5% Triton X-100. Thus, the majority of MSK1 is loosely bound to chromatin and other nuclear substructures. This observation suggests that MSK1 is not associated with the nuclear matrix, a conclusion that was confirmed by demonstrating that nuclear matrices did not retain MSK1. The sub-nuclear location of MSK1 is in contrast with other chromatin modifying enzymes, such as lysine

acetyltransferases (CBP and PCAF) and histone deacetylases (HDAC1 and HDAC2), which are tightly bound in the nucleus and associated with the nuclear matrix (Sun et al., 2001).

Mutations in *RAS* are found at a high frequency in different types of cancer including adenocarcinomas of the pancreas, colon, and lung (Malumbres and Barbacid, 2003). Additional mutations or over-expression of EGF receptors and HER-2/neu receptors that signal through RAS to elevate the activity of the RAS-MAPK pathway are relatively common in breast cancer (Murphy and Modi, 2009). Mutations such as those in the *BRAF* gene and oncoproteins (e.g. *c-SRC*) observed in melanoma and breast cancer also activate the RAS-MAPK pathway (Dhomen and Marais, 2009). The wide-spread involvement of the RAS-MAPK pathway in multiple cancer sites suggests that the activation of the H3 kinase MSK1 may be a frequent alteration in neoplasia and considering the enzyme's role in chromatin remodeling, may be a worthy target for therapeutic intervention.

5.2 MSK1 associates with transcription factors, phospho-H3 binding proteins and chromatin modifying/remodeling enzymes

It is well established that the MSK enzymes are involved in regulating the MAPK-mediated nucleosomal response (Arthur, 2008). However, the mode of MSK recruitment to H3 tails within chromatin is not clearly elucidated. Chromatin modifying and remodeling enzymes are known to associate together and be recruited to the same chromatin regions (Peterson, 2001). We were interested in deciphering possible interactions of MSK1 with other chromatin modifying and remodeling enzymes. Initially, we showed that exogenously expressed MSK1 associates with PCAF and BRG1, the two

enzymes that covalently and physically remodel the chromatin, respectively. Further, our co-immunoprecipitation results showed that endogenous MSK1 associates with these two enzymes in human (HEK293) and mouse (10T1/2) cells. In further experiments, we demonstrated that MSK1 associates with the transcription factor NFκB p65 as previously reported (Vermeulen et al., 2003), but not with transcriptional repressor, HDAC1. Interestingly, we are the first to show that MSK1 associates with 14-3-3 proteins that recognize and bind H3 tails containing phosphorylated Ser10 or Ser28. An interesting observation from our co-immunoprecipitations is that MSK1 immunoblotting of BRG1, NFκB p65 and 14-3-3 IP fractions revealed an electrophoretic retardation of the MSK1 band, suggesting possible post-translational modifications of MSK1. Indeed, MSK1 is known to be phosphorylated on 13 residues in response to MAPK signaling in order to render the enzyme fully active towards its substrates (McCoy et al., 2007). Further, it has been shown that in response to EGF and TPA, the molecular weight of MSK1 was electrophoretically shifted (Dyson et al., 2005). It may be that the MSK1 band-shift, observed in BRG1, NFκB p65 and 14-3-3 IP fractions, represents a fully phosphorylated MSK1 protein, implying that only fully activated MSK1 can associate with these proteins. On the other hand, MSK1 may be additionally modified via ubiquitination, SUMOylation or glycosylation. However, other than phosphorylation of MSK1, none of the other PTMs have been reported.

Immunoblotting of PCAF IP fractions with anti-MSK1 antibodies displays the apparent MSK1 molecular weight, which is in contrast with BRG1, NFκB p65 and 14-3-3 IP fractions. This suggests that MSK1 may exist in more than one complex; unmodified MSK1 may be associating with a complex containing PCAF, whereas modified MSK1

enzyme may be interacting with another multi-protein complex containing either BRG1, NFκB p65 and/or 14-3-3 proteins. We showed that the MSK1 complex is able to incorporate acetyl groups into core histone proteins, indicating the presence of KATs other than PCAF within the immunoprecipitated MSK1 complex. Indeed, we show that a specific CBP/p300 inhibitor, curcumin, compromises the KAT activity within the MSK1 complex. Furthermore, previous studies have shown that MSK1 directly interacts with CBP/p300 (Janknecht, 2003). Therefore, it is conceivable that MSK1 interacts with a number of different KATs in order to mediate specific functions.

Our low-stringency co-immunoprecipitations do not discriminate the nature of MSK1's association with the above-mentioned proteins. The interactions of the H3 kinase with other proteins may be direct or indirect, through another neighbouring complex. However, our sequential co-immunoprecipitation results from TPA-treated 10T1/2 cells that were pre-treated with a protein-to-protein crosslinker, DTBP, show that MSK1 is within a ternary complex that contains BRG1 and the 14-3-3ζ isoform.

Thus, our results suggest that MSK1 may be recruited to chromatin via association with transcription factors and/or enzymes that modify/remodel the chromatin. Once MSK1 is recruited to a specific chromatin location, phosphorylation of H3S10 or H3S28 would take place. The 14-3-3 isoforms can recognize this phospho-H3 mark and bind the H3 tails. We favor the model that the binding of 14-3-3 proteins to H3S10ph/S28ph may recruit other co-activators or chromatin remodelers that are required for transcriptional gene activation. The binding of 14-3-3 isoforms to phospho-H3 marks may stabilize the recruited complex at the nucleosome; therefore, 14-3-3 isoforms could function as scaffolds. Since 14-3-3 proteins bind their targets as homo- or

heterodimers, one 14-3-3 isoform could bind the phosphorylated H3 tail while the other isoform may bind a subunit within a chromatin remodeling complex, tethering the recruited enzymatic activities at the nucleosome. Our co-immunoprecipitation results also suggest that MSK1 has a role in the transcriptional activation of genes, due to association of MSK1 with transcriptional factors (NFκB p65) and enzymatic activities (PCAF and BRG1) that have been reported to enhance transcriptional gene activation (Berger, 2007; Vermeulen et al., 2003). Indeed, MSK1 knock out studies have revealed that MSK1 regulates a number of immediate-early and NFκB-dependent genes (Arthur, 2008).

5.3 TPA-induced MSK1 recruitment is crucial for establishment of H3 modifications at regulatory regions of immediate-early genes

ChIP assays have demonstrated that both the EGF- or TPA-induced H3S10ph and the TPA-induced H3S28ph are associated with the promoter regions of IE genes, such as *Fos*, *Jun* and *c-Myc* (Chadee et al., 1999; Cheung et al., 2000; Clayton et al., 2000; Dunn et al., 2009). Inhibition of MEK activity with UO126 prevented TPA-induced expression of these genes. Further, pre-treatment of cells with MSK inhibitor, H89, prevented the TPA-induced H3S10ph and H3S28ph and attenuated IE gene expression but did not diminish ERK phosphorylation (Strelkov and Davie, 2002; Thomson et al., 1999). Also, various studies have shown that an increase in the steady state of acetylated H3 is bound to transcribed chromatin of *Jun* and *Fos* after stimulation of the MAPK signaling pathway (Cheung et al., 2000; Thomson et al., 1999). With the use of a high resolution ChIP assay, which provides resolution at the nucleosomal level (Edmunds and Mahadevan, 2004; Edmunds et al., 2008), we found that TPA triggers MSK1 recruitment to the upstream regulatory regions of *Jun*, *Cox-2* and *Fos11*, followed by phosphorylation

of H3 at S10 or S28 at the nucleosomes of the same IE gene regions. For the first time, we demonstrated that MSK1 and the ensuing H3S10ph and H3S28ph are confined to nucleosomes located in the promoter regions of *Jun*, *Cox-2* and *Fos11*. Thus, the distribution of H3S10ph and H3S28ph is similar to that of the active mark, H3K4me3 (Shilatifard, 2006). We also showed that TPA treatment of parental and *Hras*-transformed mouse fibroblasts caused an increase in the levels of H3K4me3 at the promoter nucleosomes of IE genes. On the other hand, H3 acetylation levels increased in response to TPA at the promoter regions of IE genes, but also extended further into the coding regions, albeit with progressively decreasing levels. Therefore, TPA-induced H3 acetylation was detectable throughout the IE genes, whereas H3 phosphorylation only localized at the 5' end of these genes. This suggests that the TPA-induced MSK1 establishment of the H3 phosphorylation mark at the proximal regulatory IE gene regions is involved in promoter remodeling that may be required for initiation of transcription. Indeed, previous studies have shown that TPA-induced H3 phosphorylated at serine 10 and 28 were co-localized with the transcriptionally initiated form of RNA polymerase II in parental and *Hras*-transformed mouse fibroblasts (Dunn et al., 2009). On the other hand, H3 acetylation has been implicated in transcriptional initiation as well as elongation (Choi and Howe, 2009), and our results support this, as TPA-induced H3 acetylation is present at the IE gene promoters, as well as throughout the gene coding regions.

Additionally, we showed that pre-treatment of cells with MSK inhibitor, H89 abolished recruitment of MSK1 to the regulatory regions of *Jun*, *Cox-2* and *Fos11*, suggesting that the activity of MSK1 may be an important feature for recruitment to

specific chromatin locations. As expected, we showed that H89 prevents TPA-induced H3S10ph and H3S28ph at the regulatory regions of *Jun*, *Cox-2* and *Fos11*. Previous studies have shown that H89 compromises IE gene expression (Strelkov and Davie, 2002), implicating MSK-mediated H3 phosphorylation in the expression of these genes. Further, we showed that H89 affects H3 acetylation and methylation at the regulatory regions of IE genes. These two H3 modifications have been implicated in the transcriptional activation of numerous genes (Kouzarides, 2007). Therefore, MSK may directly or indirectly mediate recruitment of KATs and KHMTases to promoters of IE genes. Interestingly, we show that H3 acetylation and methylation at the regulatory IE gene regions was affected more severely by H89 in *Hras*-transformed mouse fibroblasts than in parental mouse fibroblasts. Oncogene-transformed cells with upregulated RAS-MAPK signaling are more sensitive to H89 inhibition of TPA-induced expression of IE genes (Strelkov and Davie, 2002). We showed that H89 has a more profound effect on the levels of H3K9acK14ac and H3K4me3 at the regulatory regions of IE genes in *Hras*-transformed cells; therefore, collective abolishment of TPA-induced H3 modifications, including H3 phosphorylation, acetylation and methylation, at the regulatory IE gene regions, might explain why H89 is a more potent inhibitor of IE gene expression when compared to parental cells. Since oncogene-transformed cells are “addicted” to upregulated RAS-MAPK signaling, the role of MSK in relaying the signal may be more profound in the transformed cells.

With our ChIP assays, we showed that MSK1 is exclusively recruited to nucleosomes of the regulatory IE gene regions in response to RAS-MAPK signaling, where the H3 kinase phosphorylates H3 at S10 and S28. The existing question is whether

the two phospho-H3 marks exist on the same H3 tail. Previous studies have shown that inducible phosphorylation H3S10 or S28 is independently targeted within the nucleus of mouse fibroblasts (Dunn et al., 2005; Dyson et al., 2005). We are the first to show that TPA-induced phosphorylation of H3 at S10 and S28 does not occur on the same nucleosome at the proximal-promoter regions of *Jun*, *Cox-2* and *Fos11*. In our ReChIP experiments, we showed that TPA does not induce a significant co-existence of the two phospho-H3 marks on the same H3 tail, suggesting that MSK preferentially phosphorylates one of these two serine residues. Several scenarios may explain this observation. It is conceivable that a pre-existing histone H3 tail, as well as other histone tail modifications, may determine which of the two serines is available for phosphorylation. For example, the existence of H3K9 methylation provides a tag for HP1 protein binding (Fischer et al., 2009) and may occlude H3S10 and make the S28 residue more available for phosphorylation at the time of MSK recruitment. Also, pre-existing H3K9 or H3K14 acetylation events may influence H3S10 phosphorylation (Clayton et al., 2006). On the other hand, H3K27 methylation or acetylation act as platforms for specific protein binding and may occlude H3S28 phosphorylation (Hansen et al., 2008; Tie et al., 2009). Furthermore, H3P31 isomerization may influence the ability of MSK to phosphorylate H3S28 (Nelson et al., 2006). Thus, depending on the biochemical environment surrounding S10 and S28 of H3 and the proteins that recognize and bind those biochemical signatures (“readers”), the preference of MSK for H3 S10 or S28 may be determined. Also, association of MSK with different proteins within complexes may provide substrate site-specificity. The ability of associated accessory proteins to modulate the activity and site-specificity of histone-modifying enzymes has been well established.

Incorporation into multi-subunit complexes promotes nucleosome-specific KAT or KHMTase activities of GCN5 and E(Z), respectively (Grant et al., 1997; Muller et al., 2002), whereas association of ESET with the mAM protein specifically enhances its ability to trimethylate H3K9 (Wang et al., 2003). Furthermore, in chromatin, KHMTase activity of EZH2 is directed towards either H3K27 or H1K26, depending upon which isoform of the EED protein with which it is associated (Kuzmichev et al., 2004). Modulation of MSK activity by interactions within different complexes may provide an attractive mechanism to target site-specific H3 modifications within particular chromatin locations. It is also plausible that MSK site-specificity is determined via counteracting histone H3 phosphatases. In *Drosophila*, targeting of heat shock-induced H3 phosphorylation to responsive loci was partly mediated by inhibiting PP2A phosphatase at responsive loci (Nowak et al., 2003). Also, there is evidence that the temporal differences in H3S10 and H3S28 phosphorylation during entry into mitosis are caused by PP1 phosphatase acting on S28 (but not S10) during late G2 phase (Goto et al., 2002). S28 later becomes stably phosphorylated at the onset of M-phase owing to inactivation of PP1 by Cdc2 kinase (Goto et al., 2002). Furthermore, the inability of MSK1 over-expression to deregulate H3 phosphorylation might be due to a dominant nuclear phosphatase activity directed towards H3 (Dyson et al., 2005). Thus, the opposing phosphatase activity may determine which of the two H3 serine residues becomes phosphorylated.

Initially, the independent targeting of H3S10ph and H3S28ph within mouse nucleus suggested that these two phospho-H3 marks are located on different chromatin fragments; therefore, H3S10ph and H3S28ph could associate with promoters of distinct

genes. Further, preliminary results from our lab showed that the independent targeting of H3S10ph and H3S28ph also occurs in the nuclei of normal human fibroblasts (unpublished lab data). However, our ChIP results show that both the H3S10ph and the H3S28ph occur at the regulatory regions of *Jun*, *Cox-2* and *Fos11* in response to RAS-MAPK signaling. On the other hand, we showed with ReChIP assays that these two phospho-H3 marks were not present at the nucleosomes of regulatory IE gene regions at the same time. The underlying question is how both of the H3 modifications are found at the same regulatory regions of IE genes, but not together on the nucleosomal H3 tail. It may be possible that H3S10ph and H3S28ph display specific allele distribution within the same cell. With the use of immuno-DNA FISH, preliminary data from our lab suggests that H3S10ph and H3S28ph differentially localize to *Jun* alleles in mouse fibroblasts (unpublished lab data). The ChIP assay is an averaging technique, so if both H3 modifications occur in the same cell but on different alleles, ChIP analysis would reveal the presence of both, the H3S10ph and the H3S28ph on the same gene regions. Furthermore, allele-specific histone PTMs and differential allelic expression appear to be a common occurrence (Palacios et al., 2009; Serre et al., 2008; Verona et al., 2008). Therefore, individual or combinatorial scenarios involving the pre-existing histone tail modifications, the presence of histone PTM “readers”, different MSK complex(s) recruitment and the counteracting H3 phosphatase activity, may determine the allele-specific distribution of H3S10ph and H3S28ph. Functionally, histone modifications are dependent on the transcriptional status of imprinted alleles and different histone marks illuminate epigenetic mechanisms of genomic imprinting (Verona et al., 2008). Furthermore, allele-specific gene expression appears to be an important factor in human

phenotypic variability and as a consequence, for the development of complex traits and diseases (Palacios et al., 2009). Therefore, the establishment of H3S10ph and H3S28ph by MSK, as well as other histone modifications, at specific gene alleles may contribute to regulation of various biological outcomes.

5.4 “Readers” of H3 phosphorylation marks are recruited to regulatory regions of IE genes in response to RAS-MAPK signaling

There are seven characterized 14-3-3 isoforms, existing as homo- and/or heterodimers (Aitken, 2006). Interestingly, the 14-3-3 proteins are often over-expressed in cancer cells (Bridges and Moorhead, 2004; Li et al., 2008). Recent studies have identified 14-3-3 proteins as phospho-H3 binding proteins or the “readers” of this H3 modification (Macdonald et al., 2005; Winter et al., 2008). The 14-3-3 ϵ and 14-3-3 ζ isoforms bind to H3S10ph and H3S28ph, with the affinity being strongest for S28ph, followed by S10phK14ac and S10ph signatures (Winter et al., 2008). Previous studies have shown that 14-3-3 proteins are recruited to promoter regions of inducible genes and that the knock down of 14-3-3 ζ expression compromises the expression of specific genes (Macdonald et al, 2005; Winter et al, 2008). With our ChIP assays, we demonstrated that TPA-induced recruitment of 14-3-3 ϵ and 14-3-3 ζ to the regulatory regions of *Jun*, *Cox-2* and *FosII* mirrors that of MSK1, H3S10ph and H3S28ph. Further, we showed that H89 compromised the recruitment of 14-3-3 ϵ and 14-3-3 ζ to the regulatory regions of IE genes. Thus, MSK-mediated establishment of H3 phosphorylation regulates the recruitment of 14-3-3 proteins to the regulatory regions of IE genes. Indeed, our ReChIP results showed that TPA induces simultaneous co-occupancy of MSK1 and 14-3-3 ζ at the proximal promoter regions of *Jun*, *Cox-2* and *FosII*. As previously mentioned, 14-3-3

proteins can form homo- and heterodimers. It is not clear in what dimer combination the 14-3-3 proteins are recruited to promoter regions of specific genes. Interestingly, we showed that TPA induces co-occupancy of 14-3-3 ζ and 14-3-3 ϵ at the promoters of *Jun* and *FosII*, but not *Cox-2*. These results suggest that the 14-3-3-dimer composition may be gene specific. It is plausible that different multi-protein complexes that are recruited to promoters of *Jun*, *Cox-2* and *FosII* determine which 14-3-3 dimers are localized to the chromatin. Also, pre-existing histone modifications might determine which 14-3-3 dimers are binding the phospho-H3 mark. It has been shown that H3K14ac enhances binding of 14-3-3 to S10ph (Winter et al., 2008). Other H3 modifications, such as K9ac, K27ac or K27me, may pre-exist on the specific H3 tail that could enhance or prevent specific 14-3-3 isoforms to bind to H3S10/S28ph.

The role of 14-3-3 proteins in IE gene expression is currently unknown. In our co-immunoprecipitations we showed that 14-3-3 proteins associated with a SWI/SNF chromatin remodeler, BRG1. Further, with the use of ReChIP assays, we showed that TPA induced co-occupancy of 14-3-3 ζ and BRG1 at the proximal promoters of IE genes. We favor the model that 14-3-3 proteins could recruit or stabilize the recruited SWI/SNF chromatin-remodeling complex at the promoter regions of specific genes. In this scenario, one 14-3-3 isoform binds the H3S10ph/S28ph, while the other isoform binds to a particular subunit within the chromatin-remodeling complex. The 14-3-3-mediated stabilization of the chromatin-remodeling complex at the promoters may promote localized nucleosome remodeling, thus enabling binding of transcription factors and RNA polymerase II. Consistent with this scenario is the observation that SWI/SNF-mediated remodeling of the MMTV promoter occurs after the recruitment of MSK1 and

the establishment of the H3S10ph mark (Vicent et al., 2008). Furthermore, 14-3-3 isoforms may increase the residency time of transcription factors during the “active” state of a given promoter, therefore controlling the onset of transcription (Hager et al., 2006). In addition, the binding of 14-3-3 isoforms to phosphorylated H3 may protect the phospho-H3 signatures from the action of phosphatases.

5.5 Chromatin modifying and remodeling enzymes are recruited to regulatory regions of IE genes in response to RAS-MAPK signaling

In line with the concept that 14-3-3 proteins recruit the chromatin modifying and remodeling activities to the promoters of IE genes, ChIP assays with anti-PCAF and anti-BRG1 antibodies were performed. We showed that TPA induces recruitment of PCAF and BRG1 at the regulatory regions of *Jun*, *Cox-2* and *Fos11*. Interestingly, TPA-induced recruitment of PCAF to distal and proximal promoter regions of *Cox-2* was minimal, while H3 acetylation was induced with TPA at the same *Cox-2* regions. It may be possible that other KATs are more predominantly recruited to this *Cox-2* promoter location. Surprisingly, our ReChIP results showed that TPA significantly increased co-occupancy of MSK1 and PCAF at the *Cox-2* proximal promoter region, which is a conflicting result. The ReChIP technique is a more sensitive method in detecting enrichment of DNA sequences, since two consecutive rounds of immunoprecipitations are performed and co-occupancy of two proteins is examined at a specific chromatin region. It is plausible that TPA induced minimal PCAF binding, but this event is exclusively mediated via MSK1, since we see a significant enrichment with our ReChIP assay. This assumption would imply that minimal protein binding revealed by the ChIP assay might still be significant. We observed reduction in PCAF binding and H3

acetylation levels at the proximal promoter region of *Cox-2* in the presence of H89, suggesting that MSK mediates the recruitment of PCAF and the ensuing H3 acetylation. Furthermore, H3 acetylation at the *Cox-2* proximal-promoter nucleosome in parental cells may arise from associating factors within the recruited RNAP II holoenzyme that harbor H3-specific KAT activities (Sternier and Berger, 2000).

Furthermore, BRG1 recruitment to proximal promoter regions of *Cox-2* was less when compared to the distal region. The transcription factors that are co-recruited to distal (NF κ B p65) and proximal (AP-1 factors) regions of *Cox-2* and the corresponding recruitment of multi-protein complexes, may determine the extent of chromatin remodeling that takes place at these two promoter regions of *Cox-2*. Also, in line with our scenario of 14-3-3-mediated SWI/SNF complex recruitment, different 14-3-3 dimers may bind the phospho-H3 marks with different affinities, therefore affecting the dynamics of tethering the recruited SWI/SNF complex at the distal and promoter regions of *Cox-2*. In our ReChIP assays, we did not observe TPA-induced 14-3-3 ϵ and 14-3-3 ζ co-occupancy at the proximal promoter region of *Cox-2*, suggesting that this 14-3-3-dimer composition was not present at the *Cox-2* proximal regulatory region. The TPA-induced co-occupancy of 14-3-3 ϵ and 14-3-3 ζ at the distal promoter region of *Cox-2* has not been examined. It may be possible that the difference in 14-3-3-dimer composition at the distal and proximal *Cox-2* promoter regions determines the extent of SWI/SNF complex stabilization, which might have significant effects on the rate of transcriptional initiation. We showed that H89 decreased binding of BRG1 at distal and proximal promoter regions of IE genes, implying that MSK mediated the recruitment of chromatin-remodeling activities to these regulatory gene regions. Consistent with our observations, it has been

previously shown that H89 prevented inducible recruitment of BRG1 to the MMTV promoter (Vicent et al., 2006).

Another interesting result from our CHIP assays is the observation that TPA-induced PCAF and BRG1 binding at the proximal promoter of *Cox-2* was significantly increased in *Hras*-transformed mouse fibroblasts when compared to the parental cell line. Due to upregulated RAS-MAPK signaling in *Hras*-transformed cells, enhanced recruitment of KATs and SWI/SNF to gene promoters may occur. However, we showed that the levels of H3 acetylation at the regulatory regions of IE genes were similar in parental and *Hras*-transformed cells. Further, previous studies from our lab have shown that *Hras*-transformed cells have a more relaxed chromatin structure than the parental cells (Chadee et al., 1999). The more open chromatin state in *Hras*-transformed cells may have unforeseen effects on nucleosome positioning at the promoter regions of *Cox-2*, which might allow for enhanced KAT and SWI/SNF recruitment.

5.6 Recruitment of JUN transcription factor to regulatory regions of IE genes increases in response to RAS-MAPK signaling

AP-1 is an important transcription factor, existing as a homo- or heterodimer. AP-1 dimers are composed of proteins in the JUN (c-JUN, JUN B and JUN D), FOS (c-FOS, FOS B, FRA-1 and FRA-2) and ATF (ATF2 and ATF3) families (Verde et al., 2007; Zenz et al., 2008). AP-1 has been implicated in regulation of genes involved in cell proliferation, apoptosis, oncogene-induced transformation and cancer cell invasion (Mariani et al., 2007; Shen et al., 2008). Furthermore, alterations in the expression of *JUN* and *FOSL1* can cause cell transformation *in vivo* (Mariani et al., 2007; Verde et al., 2007). AP-1 is recruited to its cognate binding sites within promoters of AP-1-regulated

genes, such as *Jun*, *Cox-2* and *FosII* (Looby et al., 2009; Verde et al., 2007). We show that TPA stimulation increases binding of JUN to its AP-1 binding elements within the proximal promoters of *Jun*, *Cox-2* and *FosII*, as well as in the first intron of *FosII* which contains an AP-1 binding site. Furthermore, we showed that H89 abolished the recruitment of JUN to AP-1 sites within the regulatory regions of IE genes. Thus, recruitment of JUN to its binding elements may be dependent on MSK. We showed that H89 decreased binding of BRG1 at the regulatory regions of IE genes; therefore, reduced nucleosome remodeling at the promoters might consequently reduce JUN binding. Also, it is possible that MSK1 and JUN exist in the same complex; however, in the presence of H89, conformational changes in MSK1 protein might prevent both the AP-1 transcription factor and MSK1 from being recruited to AP-1 sites within specific promoters. On the other hand, it has been shown that the transcription factor Elk-1 mediates mitogen-induced recruitment of MSK1 to *FOS* and *EGR-1* promoters (Zhang et al., 2008). Therefore, MSK1 recruitment might be dependent on which transcription factor is recruited and then activated at a specific promoter. ELK-1 is pre-loaded at the *FOS* promoter and then phosphorylated via ERK after mitogen stimulation (Zhang et al., 2008). Transactivation of ELK-1 at the *FOS* promoter may promote MSK1 recruitment. Therefore, MSK1 recruitment to the promoter regions of *Jun*, *Cox-2* and *FosII* may depend on the first-wave of transcription factor-recruitment to distinct cognate binding sites. Recruitment of MSK1 would cause the establishment of phospho-H3 mark at these specific promoter regions. Recognition and binding of phospho-H3 mark by 14-3-3 proteins would recruit the SWI/SNF nucleosome-remodeling complex, which would locally alter chromatin structure to allow binding of other transcription factors, such as

AP-1. For example, the first-wave of transcription factor-recruitment, such as ELK-1 and/or NF1 at the *Jun* promoter, NFκB p65 at the *Cox-2* promoter and C/EBPβ at the *Fos11* promoter may initially recruit the H3 kinase. This recruitment may trigger MSK-mediated promoter remodeling, via recruited chromatin modifying and remodeling activities that allow for the second-wave of transcription factor binding.

5.7 MSK1 is important for the expression of IE genes in response to RAS-MAPK signaling

MSK knock out mice and specific inhibitor studies have shown that MSK is involved in the expression of a number of IE genes (Arthur, 2008). We showed that H89 prevented recruitment of MSK1 and the ensuing H3 phosphorylation at the regulatory regions of IE genes. Further, we showed that H89 decreased binding of 14-3-3 isoforms, as well as recruitment of PCAF, BRG1 and JUN at the promoter regions of these genes. Also, H3 acetylation and methylation levels at the nucleosomes of IE gene promoters were significantly reduced in the presence of H89. Therefore, we wanted to investigate the functional consequence of inhibiting MSK-mediated promoter remodeling of IE genes. We demonstrated that TPA stimulation of parental and *Hras*-transformed mouse fibroblasts induced the expression of *Jun*, *Cox-2* and *Fos11* genes, although the TPA induction of *Cox-2* and *Fos11* genes was more pronounced in the parental cell line. We consistently observed elevated expression levels of *Cox-2* (3-fold) and *Fos11* (4-fold) in serum-starved *Hras*-transformed cells when compared to serum-starved parental cells, which may account for the differences in TPA-induced gene expression. The increase in the expression of *Cox-2* and *Fos11* in *Hras*-transformed cells might be due to inefficient synchronization of cells by serum-starvation, which is common for oncogene-

transformed cells. Also, there is evidence that oncogene-transformed cells over-express *Cox-2* and *Fos11* (Kwon et al., 2007; Verde et al., 2007). We showed that the steady-state protein levels of JUN, FRA-1 and COX-2 were increased in *Hras*-transformed cells, which supported the observations of upregulated IE gene expression in the transformed cells.

With the use of high resolution ChIP assays, we demonstrated that TPA-induced MSK1 mediated remodeling of IE gene promoters. Also, we demonstrated that TPA induced association of RNAPII S5ph, the initiated form of RNAPII, at the proximal promoters of IE genes. We showed that in the presence of H89, TPA-induced expression of *Jun*, *Cox-2* and *Fos11* is ablated in parental and *Hras*-transformed cells, due to reduction in RNAPII S5ph levels at the IE gene promoters. Further, we showed that MSK1 knockdown in parental and *Hras*-transformed mouse fibroblasts significantly reduced TPA-induced expression of *Jun*, *Cox-2* and *Fos11*, demonstrating a direct role of MSK1 in the expression of IE genes. Consistent with the notion that MSK1 regulates the molecular events at the nucleosomes of IE genes, we showed that reduction of MSK1 protein levels in parental mouse fibroblasts decreased the H3S10/28ph levels and the subsequent binding of 14-3-3 isoforms, BRG1 and JUN at the proximal regulatory regions of IE genes in response to TPA stimulation. These observations provide direct evidence that MSK-mediated nucleosomal response controls the expression of IE genes in response to RAS-MAPK signaling. The gene products of *JUN*, *COX-2* and *FOSL1* have been implicated in mediating carcinogenesis and metastasis (Young and Colburn, 2006). Both, the inhibition of MSK activity with H89 and the stable knockdown of MSK1 severely compromise anchorage-independent growth of *Hras*-transformed cells

(unpublished lab data). These results emphasize the importance of MSK-regulated gene expression that may be exploited by cancerous cells with abnormal MAPK signaling.

6.0 CONCLUSIONS

Experimental results presented in this thesis support our hypothesis that MSK1 activity has a role in mediating downstream effects of RAS-MAPK signaling. We demonstrated that upregulated activities of ERKs, but not p38, are responsible for enhanced MSK1 activity that was observed in oncogene-transformed cells. Analyses of the subcellular distribution of MSK1 showed that the H3 kinase was similarly distributed in parental and oncogene-transformed cells, with most MSK1 being present in the nucleus. In contrast to many other chromatin modifying enzymes, MSK1 was loosely bound in the nucleus and was not a component of the nuclear matrix. Collectively, these results provided insights into the dynamics of MSK1 activation.

Furthermore, we provided evidence that the MSK1-mediated nucleosomal response plays a crucial role in the chromatin remodeling and transcriptional initiation of IE genes in response to RAS-MAPK signaling. We demonstrated the exclusive positioning of H3S10ph or H3S28ph at the regulatory regions of IE genes, which indicates that these H3 post-translational modifications have functions primarily in promoter remodeling and transcriptional initiation, but not in elongation. Based on our results we propose a model (Figure 42) in which the activation of the ERK and p38 MAPK pathways activates MSK1. The active MSK1 within a multiprotein complex is then recruited to the regulatory regions of IE genes by transcription factors such as ELK-1, NF κ B or C/EBP β . MSK1 phosphorylates either H3 S10 or H3 S28 and the recognition and binding of phospho-H3 marks by 14-3-3 proteins mediates the recruitment of the chromatin remodeler SWI/SNF, with BRG1 serving as the ATPase subunit. The ensuing remodeling of promoter nucleosomes allows the access of transcription factors such AP-1

to the promoter target sequences. The H3-specific KAT, PCAF, is also recruited as a component of the MSK1 complex. Moreover, PCAF may be recruited to regulatory regions, for example by AP-1, through its association with p300/CBP. Initiation of transcription follows, as is made apparent by the presence of RNAPII S5ph. Thus, MSK-mediated H3 phosphorylation may work in conjunction with other histone modifications to recruit necessary factors that would induce accessible chromatin structure and in turn promote transcriptional initiation.

Collectively, the work presented in this thesis provided a detailed picture of the events taking place at IE gene promoter regions following stimulation of the signal transduction pathway. These events lead to the activation of IE gene expression and subsequent gene expression programming events involved in wound healing, metastasis, stress-related memory response, and food reward-driven learning and cocaine addiction. Although MSK1/2 knockout mice are viable, upon closer inspection, these animals were found to be defective in stress-related learning and memory processes, with the NMDA-R-mediated H3S10ph and associated *Fos* gene induction abolished in the dentate granule neurons (Chandramohan et al., 2008). Interestingly, the molecular defect in a mouse model for Huntington's disease, a neurodegenerative disease, was a deficiency in MSK1 expression resulting in the lack of induced H3S10ph and down-regulation of *Fos* transcription in the striatum (Roze et al., 2008). MSK1 is also involved in the regulation of clock gene expression in the suprachiasmatic nucleus (Butcher et al., 2005) and in the regulation of inflammatory genes, including interleukin-1, interleukin-8 and *COX-2* (Beck et al., 2008; Joo and Jetten, 2008). It is likely that the MSK-mediated nucleosomal

response plays a role in chromatin remodeling and transcriptional reprogramming in many physiological and disease processes.

Furthermore, the constitutive activation of RAS-MAPK signaling in cancer cells is a frequent phenomenon. Altered chromatin structure due to abnormal signal transduction and activation of kinases, such as MSK1, might allow aberrant expression of genes, such as IE genes, thus initiating the steps towards malignant transformation. Therefore, modulation of MSK activity in cancers with upregulated RAS-MAPK signaling may be a novel targeted therapy.

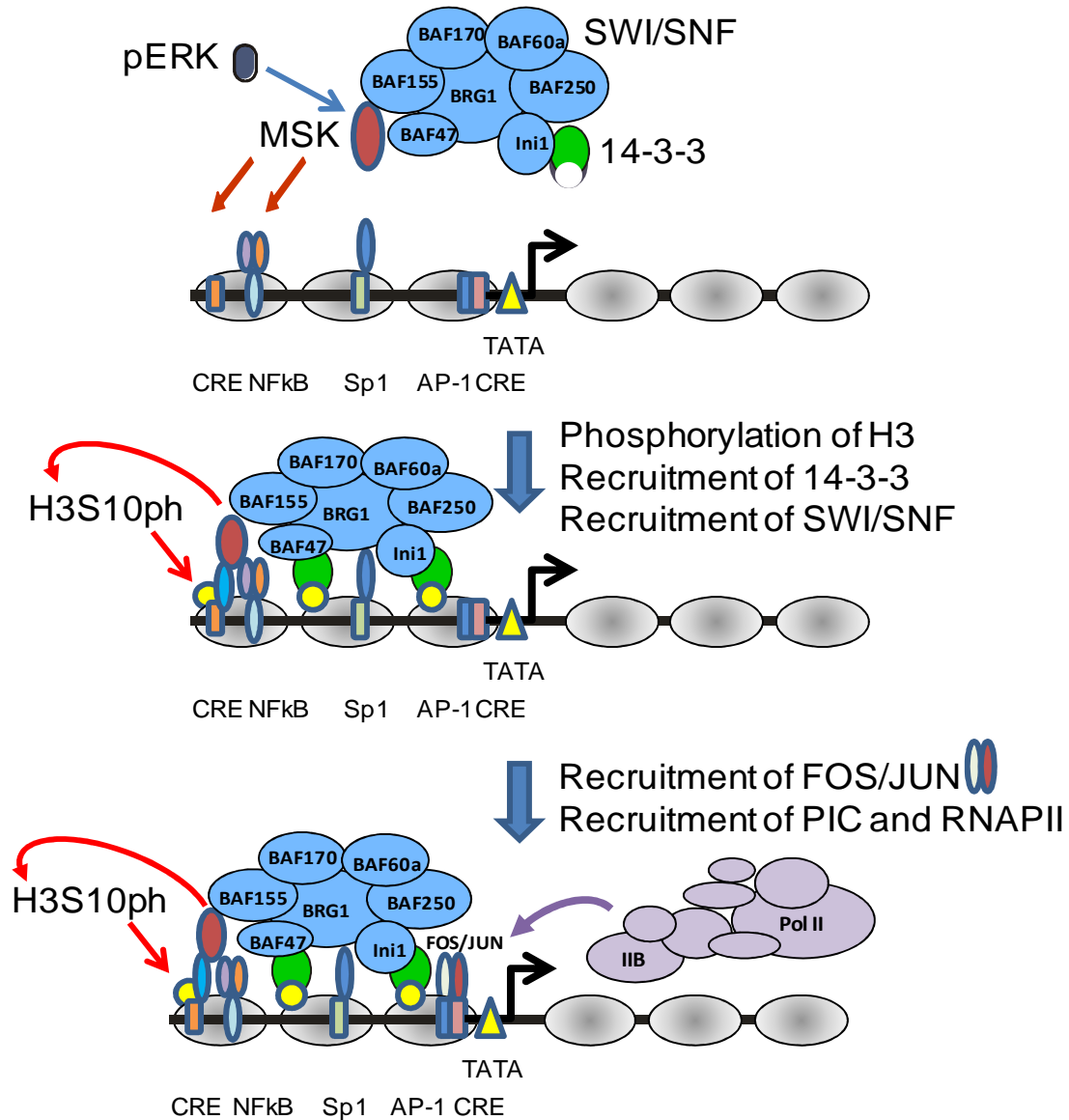


Figure 42: Schematic model representing the role of MSK1 and 14-3-3 in IE gene remodeling and induction in response to MAPK signaling.

MSK (shown as a large red oval) and 14-3-3 (green partial oval) are in a complex with the SWI/SNF chromatin remodeler. The grey ovals along the DNA represent nucleosomes, the NFκB transcription factor (p65/p50 dimer) is shown as a purple/orange pair of ovals binding to the NFκB binding site (blue oval). In response to the activation of the ERK and p38 MAPK pathways, the MSK1 multiprotein complex is recruited to the regulatory regions of IE genes by transcription factors such as Elk1, NF-κB or C/EBPβ. MSK1 phosphorylates either H3 S10 or H3 S28, with H3S10ph being shown (yellow circles). H3S10ph and H3S28ph recruit 14-3-3 proteins, which mediate the recruitment of the chromatin remodeler SWI/SNF, with BRG1 being the ATPase subunit. The ensuing remodeling of promoter nucleosomes allows the access of transcription factors such as AP-1 to the promoter target sequences. The pre-initiation complex (PIC) is recruited at the TATA box (yellow triangle), and initiation of transcription follows, as is made apparent by the presence of RNAPIIS5ph.

7.0 FUTURE DIRECTIONS

In contrast to numerous studies exploring the role of H3S10ph in gene expression (Perez-Cadahia et al., 2009), much less is known about the role of H3S28ph in gene expression. Furthermore, the genomic distribution of either H3 PTM has not been conclusively elucidated. The data presented in this thesis demonstrate that H3S10ph and H3S28ph are located primarily at IE gene promoters, similar to H3K4me3 (Shilatifard, 2006). Positioning H3S10ph and H3S28ph solely at the promoter of genes provides compelling evidence that these H3 PTMs have functions in promoter remodeling and transcription initiation. It will be of interest to test if there is differential allelic association of H3S10ph and H3S28ph with a subset of gene promoters. Immunofluorescence combined with fluorescence *in situ* hybridization (DNA immunofluorescence) can be used to determine the relative location of the phosphorylated H3 and IE gene alleles at the single cell level. The genes that are bound to both H3S10ph and H3S28ph should be investigated, as well as the genes that are bound to one or the other of the H3 PTMs. The former genes would be candidates for differential H3 PTM allelic association. CHIP-sequencing can be used in order to obtain the DNA sequences associated with H3S10ph and H3S28ph. The results of these analyses will inform us as to whether the DNA sequences associated with H3S10ph and H3S28ph differ in 10T1/2 and Ciras-3 cells which would provide evidence that epigenetic programming was altered in the *Hras* -transformed cells.

The expression of RAS oncoproteins is known to alter epigenetic processes (e.g. DNA methylation) and alter the expression of transcription factors such AP-1 family members (Watanabe et al., 2008). We would expect to identify several promoters associated with H3S10ph and/or H3S128ph in Ciras-3 but not in 10T1/2 cells and vice

versa. It would be difficult to predict the number of genes that are associated with both H3S10ph and H3S28ph and potentially exhibit differential allelic expression; however, based on the data presented in this thesis for *Fos*, *Jun* and *Fos11*, all promoters regulating the expression of AP-1 family members will be associated with both H3 PTMs.

Different studies have demonstrated a direct role of MSK1 in cellular transformation (Kim et al., 2008). Knockdown of MSK1 drastically reduced ability of Ciras-3 cells to form colonies in soft agar but had little impact on proliferation rates when cultured on plastic dishes (unpublished lab data). Furthermore, determining whether MSK2, which is expressed in both 10T1/2 and Ciras-3 cells, also impairs the anchorage-independent growth of Ciras-3 cells will be of interest.

The results from this thesis demonstrate that without MSK recruitment and activity, H3 phosphorylation, 14-3-3 recruitment and IE gene promoter remodeling does not occur. It will be intriguing to test the hypothesis that 14-3-3 isoforms are required to recruit the SWI/SNF complex to the promoter nucleosome containing H3S10ph or H3S28ph (see model in Fig. 42). The remodeling of these nucleosomes enables the association of transcription factors such as Jun/Fos (AP-1) to their binding sites (e.g. in the *Cox-2* promoter). These events lead to the recruitment of the pre-initiation complex (PIC) and RNAPII and the onset of transcription. If this notion is correct, then in the absence of 14-3-3 isoforms, the remodeling of the IE gene promoter and the loading of transcription factors will be compromised.

8.0 REFERENCES

Ahn, S.H., Cheung, W.L., Hsu, J.Y., Diaz, R.L., Smith, M.M., and Allis, C.D. (2005). Sterile 20 kinase phosphorylates histone H2B at serine 10 during hydrogen peroxide-induced apoptosis in *S. cerevisiae*. *Cell* *120*, 25-36.

Aitken, A. (2006). 14-3-3 proteins: a historic overview. *Semin Cancer Biol* *16*, 162-172.

Alen, C., Kent, N.A., Jones, H.S., O'Sullivan, J., Aranda, A., and Proudfoot, N.J. (2002). A role for chromatin remodeling in transcriptional termination by RNA polymerase II. *Mol Cell* *10*, 1441-1452.

Amati, B., Frank, S.R., Donjerkovic, D., and Taubert, S. (2001). Function of the c-Myc oncoprotein in chromatin remodeling and transcription. *Biochim Biophys Acta* *1471*, M135-145.

Ananieva, O., Darragh, J., Johansen, C., Carr, J.M., McIlrath, J., Park, J.M., Wingate, A., Monk, C.E., Toth, R., Santos, S.G., *et al.* (2008). The kinases MSK1 and MSK2 act as negative regulators of Toll-like receptor signaling. *Nat Immunol* *9*, 1028-1036.

Anest, V., Cogswell, P.C., and Baldwin, A.S., Jr. (2004). I κ B kinase alpha and p65/RelA contribute to optimal epidermal growth factor-induced c-fos gene expression independent of I κ Balpha degradation. *J Biol Chem* *279*, 31183-31189.

Aoki, Y., Niihori, T., Kawame, H., Kurosawa, K., Ohashi, H., Tanaka, Y., Filocamo, M., Kato, K., Suzuki, Y., Kure, S., and Matsubara, Y. (2005). Germline mutations in HRAS proto-oncogene cause Costello syndrome. *Nat Genet* *37*, 1038-1040.

Aoki, Y., Niihori, T., Narumi, Y., Kure, S., and Matsubara, Y. (2008). The RAS/MAPK syndromes: novel roles of the RAS pathway in human genetic disorders. *Hum Mutat* *29*, 992-1006.

Arthur, J.S. (2008). MSK activation and physiological roles. *Front Biosci* *13*, 5866-5879.

Arthur, J.S., Fong, A.L., Dwyer, J.M., Davare, M., Reese, E., Obrietan, K., and Impey, S. (2004). Mitogen- and stress-activated protein kinase 1 mediates cAMP response element-binding protein phosphorylation and activation by neurotrophins. *J Neurosci* *24*, 4324-4332.

Beck, I.M., Vanden Berghe, W., Vermeulen, L., Bougarne, N., Vander Cruyssen, B., Haegeman, G., and De Bosscher, K. (2008). Altered subcellular distribution of MSK1 induced by glucocorticoids contributes to NF- κ B inhibition. *EMBO J* *27*, 1682-1693.

Becker, P.B., and Horz, W. (2002). ATP-dependent nucleosome remodeling. *Annu Rev Biochem* *71*, 247-273.

Berger, S.L. (2007). The complex language of chromatin regulation during transcription. *Nature* 447, 407-412.

Bhaumik, S.R., Smith, E., and Shilatifard, A. (2007). Covalent modifications of histones during development and disease pathogenesis. *Nat Struct Mol Biol* 14, 1008-1016.

Brami-Cherrier, K., Valjent, E., Herve, D., Darragh, J., Corvol, J.C., Pages, C., Arthur, S.J., Girault, J.A., and Caboche, J. (2005). Parsing molecular and behavioral effects of cocaine in mitogen- and stress-activated protein kinase-1-deficient mice. *J Neurosci* 25, 11444-11454.

Bridges, D., and Moorhead, G.B. (2004). 14-3-3 proteins: a number of functions for a numbered protein. *Sci STKE* 2004, re10.

Brose, M.S., Volpe, P., Feldman, M., Kumar, M., Rishi, I., Gerrero, R., Einhorn, E., Herlyn, M., Minna, J., Nicholson, A., *et al.* (2002). BRAF and RAS mutations in human lung cancer and melanoma. *Cancer Res* 62, 6997-7000.

Butcher, G.Q., Lee, B., Cheng, H.Y., and Obrietan, K. (2005). Light stimulates MSK1 activation in the suprachiasmatic nucleus via a PACAP-ERK/MAP kinase-dependent mechanism. *J Neurosci* 25, 5305-5313.

Calipel, A., Lefevre, G., Pouponnot, C., Mouriaux, F., Eychene, A., and Mascarelli, F. (2003). Mutation of B-Raf in human choroidal melanoma cells mediates cell proliferation and transformation through the MEK/ERK pathway. *J Biol Chem* 278, 42409-42418.

Cerutti, H., and Casas-Mollano, J.A. (2009). Histone H3 phosphorylation: universal code or lineage specific dialects? *Epigenetics* 4, 71-75.

Chadee, D.N., Hendzel, M.J., Tylicski, C.P., Allis, C.D., Bazett-Jones, D.P., Wright, J.A., and Davie, J.R. (1999). Increased Ser-10 phosphorylation of histone H3 in mitogen-stimulated and oncogene-transformed mouse fibroblasts. *J Biol Chem* 274, 24914-24920.

Chandramohan, Y., Droste, S.K., Arthur, J.S., and Reul, J.M. (2008). The forced swimming-induced behavioural immobility response involves histone H3 phosphoacetylation and c-Fos induction in dentate gyrus granule neurons via activation of the N-methyl-D-aspartate/extracellular signal-regulated kinase/mitogen- and stress-activated kinase signalling pathway. *Eur J Neurosci* 27, 2701-2713.

Cheung, P., Tanner, K.G., Cheung, W.L., Sassone-Corsi, P., Denu, J.M., and Allis, C.D. (2000). Synergistic coupling of histone H3 phosphorylation and acetylation in response to epidermal growth factor stimulation. *Mol Cell* 5, 905-915.

Choi, H.S., Choi, B.Y., Cho, Y.Y., Mizuno, H., Kang, B.S., Bode, A.M., and Dong, Z. (2005). Phosphorylation of histone H3 at serine 10 is indispensable for neoplastic cell transformation. *Cancer Res* 65, 5818-5827.

Choi, J.K., and Howe, L.J. (2009). Histone acetylation: truth of consequences? *Biochem Cell Biol* 87, 139-150.

Chwang, W.B., Arthur, J.S., Schumacher, A., and Sweatt, J.D. (2007). The nuclear kinase mitogen- and stress-activated protein kinase 1 regulates hippocampal chromatin remodeling in memory formation. *J Neurosci* 27, 12732-12742.

Chwang, W.B., O'Riordan, K.J., Levenson, J.M., and Sweatt, J.D. (2006). ERK/MAPK regulates hippocampal histone phosphorylation following contextual fear conditioning. *Learn Mem* 13, 322-328.

Clayton, A.L., Hazzalin, C.A., and Mahadevan, L.C. (2006). Enhanced histone acetylation and transcription: a dynamic perspective. *Mol Cell* 23, 289-296.

Clayton, A.L., Rose, S., Barratt, M.J., and Mahadevan, L.C. (2000). Phosphoacetylation of histone H3 on c-fos- and c-jun-associated nucleosomes upon gene activation. *EMBO J* 19, 3714-3726.

Cosgrove, M.S., Boeke, J.D., and Wolberger, C. (2004). Regulated nucleosome mobility and the histone code. *Nat Struct Mol Biol* 11, 1037-1043.

Cote, J., Peterson, C.L., and Workman, J.L. (1998). Perturbation of nucleosome core structure by the SWI/SNF complex persists after its detachment, enhancing subsequent transcription factor binding. *Proc Natl Acad Sci U S A* 95, 4947-4952.

Davey, C.A., Sargent, D.F., Luger, K., Maeder, A.W., and Richmond, T.J. (2002). Solvent mediated interactions in the structure of the nucleosome core particle at 1.9 Å resolution. *J Mol Biol* 319, 1097-1113.

Davie, J.R. (2003). MSK1 and MSK2 mediate mitogen- and stress-induced phosphorylation of histone H3: a controversy resolved. *Sci STKE* 2003, PE33.

Davie, J.R., He, S., Li, L., Sekhavat, A., Espino, P., Drohic, B., Dunn, K.L., Sun, J.M., Chen, H.Y., Yu, J., *et al.* (2008). Nuclear organization and chromatin dynamics--Sp1, Sp3 and histone deacetylases. *Adv Enzyme Regul* 48, 189-208.

Davie, J.R., Samuel, S.K., Spencer, V.A., Holth, L.T., Chadee, D.N., Peltier, C.P., Sun, J.M., Chen, H.Y., and Wright, J.A. (1999). Organization of chromatin in cancer cells: role of signalling pathways. *Biochem Cell Biol* 77, 265-275.

Davie, J.R., and Spencer, V.A. (2001). Signal transduction pathways and the modification of chromatin structure. *Prog Nucleic Acid Res Mol Biol* 65, 299-340.

Davies, S.P., Reddy, H., Caivano, M., and Cohen, P. (2000). Specificity and mechanism of action of some commonly used protein kinase inhibitors. *Biochem J* 351, 95-105.

Denayer, E., de Ravel, T., and Legius, E. (2008). Clinical and molecular aspects of RAS related disorders. *J Med Genet* 45, 695-703.

Deng, Q., Liao, R., Wu, B.L., and Sun, P. (2004). High intensity ras signaling induces premature senescence by activating p38 pathway in primary human fibroblasts. *J Biol Chem* 279, 1050-1059.

Dhomen, N., and Marais, R. (2009). BRAF signaling and targeted therapies in melanoma. *Hematol Oncol Clin North Am* 23, 529-545, ix.

Dimitri, P., Caizzi, R., Giordano, E., Carmela Accardo, M., Lattanzi, G., and Biamonti, G. (2009). Constitutive heterochromatin: a surprising variety of expressed sequences. *Chromosoma* 118, 419-435.

Dirscherl, S.S., and Krebs, J.E. (2004). Functional diversity of ISWI complexes. *Biochem Cell Biol* 82, 482-489.

Downward, J. (2003). Targeting RAS signalling pathways in cancer therapy. *Nat Rev Cancer* 3, 11-22.

Drobic, B., Dunn, K.L., Espino, P.S., and Davie, J.R. (2006). Abnormalities of chromatin in tumor cells. *EXS*, 25-47.

Drobic, B., Espino, P.S., and Davie, J.R. (2004). Mitogen- and stress-activated protein kinase 1 activity and histone h3 phosphorylation in oncogene-transformed mouse fibroblasts. *Cancer Res* 64, 9076-9079.

Dunn, K.L., Espino, P.S., Drobic, B., He, S., and Davie, J.R. (2005). The Ras-MAPK signal transduction pathway, cancer and chromatin remodeling. *Biochem Cell Biol* 83, 1-14.

Dunn, K.L., He, S., Wark, L., Delcuve, G.P., Sun, J.M., Yu Chen, H., Mai, S., and Davie, J.R. (2009). Increased genomic instability and altered chromosomal protein phosphorylation timing in HRAS-transformed mouse fibroblasts. *Genes Chromosomes Cancer* 48, 397-409.

Dyson, M.H., Thomson, S., Inagaki, M., Goto, H., Arthur, S.J., Nightingale, K., Iborra, F.J., and Mahadevan, L.C. (2005). MAP kinase-mediated phosphorylation of distinct pools of histone H3 at S10 or S28 via mitogen- and stress-activated kinase 1/2. *J Cell Sci* 118, 2247-2259.

Edmunds, J.W., and Mahadevan, L.C. (2004). MAP kinases as structural adaptors and enzymatic activators in transcription complexes. *J Cell Sci* 117, 3715-3723.

Edmunds, J.W., Mahadevan, L.C., and Clayton, A.L. (2008). Dynamic histone H3 methylation during gene induction: HYPB/Setd2 mediates all H3K36 trimethylation. *EMBO J* 27, 406-420.

Egan, S.E., McClarty, G.A., Jarolim, L., Wright, J.A., Spiro, I., Hager, G., and Greenberg, A.H. (1987). Expression of H-ras correlates with metastatic potential: evidence for direct regulation of the metastatic phenotype in 10T1/2 and NIH 3T3 cells. *Mol Cell Biol* 7, 830-837.

Espino, P.S., Drohic, B., Dunn, K.L., and Davie, J.R. (2005). Histone modifications as a platform for cancer therapy. *J Cell Biochem* 94, 1088-1102.

Espino, P.S., Li, L., He, S., Yu, J., and Davie, J.R. (2006). Chromatin modification of the trefoil factor 1 gene in human breast cancer cells by the Ras/mitogen-activated protein kinase pathway. *Cancer Res* 66, 4610-4616.

Ferreira, H., Flaus, A., and Owen-Hughes, T. (2007). Histone modifications influence the action of Snf2 family remodelling enzymes by different mechanisms. *J Mol Biol* 374, 563-579.

Fischer, T., Cui, B., Dhakshnamoorthy, J., Zhou, M., Rubin, C., Zofall, M., Veenstra, T.D., and Grewal, S.I. (2009). Diverse roles of HP1 proteins in heterochromatin assembly and functions in fission yeast. *Proc Natl Acad Sci U S A* 106, 8998-9003.

Fry, C.J., and Peterson, C.L. (2001). Chromatin remodeling enzymes: who's on first? *Curr Biol* 11, R185-197.

Fry, C.J., Shogren-Knaak, M.A., and Peterson, C.L. (2004). Histone H3 amino-terminal tail phosphorylation and acetylation: synergistic or independent transcriptional regulatory marks? *Cold Spring Harb Symp Quant Biol* 69, 219-226.

Funding, A.T., Johansen, C., Kragballe, K., and Iversen, L. (2007). Mitogen- and stress-activated protein kinase 2 and cyclic AMP response element binding protein are activated in lesional psoriatic epidermis. *J Invest Dermatol* 127, 2012-2019.

Funding, A.T., Johansen, C., Kragballe, K., Otkjaer, K., Jensen, U.B., Madsen, M.W., Fjording, M.S., Finnemann, J., Skak-Nielsen, T., Paludan, S.R., and Iversen, L. (2006).

Mitogen- and stress-activated protein kinase 1 is activated in lesional psoriatic epidermis and regulates the expression of pro-inflammatory cytokines. *J Invest Dermatol* 126, 1784-1791.

Fyodorov, D.V., and Kadonaga, J.T. (2002). Dynamics of ATP-dependent chromatin assembly by ACF. *Nature* 418, 897-900.

Garcia, B.A., Barber, C.M., Hake, S.B., Ptak, C., Turner, F.B., Busby, S.A., Shabanowitz, J., Moran, R.G., Allis, C.D., and Hunt, D.F. (2005). Modifications of human histone H3 variants during mitosis. *Biochemistry* *44*, 13202-13213.

Garcia-Ramirez, M., Rocchini, C., and Ausio, J. (1995). Modulation of chromatin folding by histone acetylation. *J Biol Chem* *270*, 17923-17928.

Gavin, I., Horn, P.J., and Peterson, C.L. (2001). SWI/SNF chromatin remodeling requires changes in DNA topology. *Mol Cell* *7*, 97-104.

Georgel, P.T., Tsukiyama, T., and Wu, C. (1997). Role of histone tails in nucleosome remodeling by Drosophila NURF. *EMBO J* *16*, 4717-4726.

Gerber, M., and Shilatifard, A. (2003). Transcriptional elongation by RNA polymerase II and histone methylation. *J Biol Chem* *278*, 26303-26306.

Gerits, N., Kostenko, S., Shiryaev, A., Johannessen, M., and Moens, U. (2008). Relations between the mitogen-activated protein kinase and the cAMP-dependent protein kinase pathways: comradeship and hostility. *Cell Signal* *20*, 1592-1607.

Gesser, B., Johansen, C., Rasmussen, M.K., Funding, A.T., Otkjaer, K., Kjellerup, R.B., Kragballe, K., and Iversen, L. (2007). Dimethylfumarate specifically inhibits the mitogen and stress-activated kinases 1 and 2 (MSK1/2): possible role for its anti-psoriatic effect. *J Invest Dermatol* *127*, 2129-2137.

Glover, D.M., Leibowitz, M.H., McLean, D.A., and Parry, H. (1995). Mutations in aurora prevent centrosome separation leading to the formation of monopolar spindles. *Cell* *81*, 95-105.

Goto, H., Tomono, Y., Ajiro, K., Kosako, H., Fujita, M., Sakurai, M., Okawa, K., Iwamatsu, A., Okigaki, T., Takahashi, T., and Inagaki, M. (1999). Identification of a novel phosphorylation site on histone H3 coupled with mitotic chromosome condensation. *J Biol Chem* *274*, 25543-25549.

Goto, H., Yasui, Y., Nigg, E.A., and Inagaki, M. (2002). Aurora-B phosphorylates Histone H3 at serine28 with regard to the mitotic chromosome condensation. *Genes Cells* *7*, 11-17.

Grant, P.A., Duggan, L., Cote, J., Roberts, S.M., Brownell, J.E., Candau, R., Ohba, R., Owen-Hughes, T., Allis, C.D., Winston, F., *et al.* (1997). Yeast Gcn5 functions in two multisubunit complexes to acetylate nucleosomal histones: characterization of an Ada complex and the SAGA (Spt/Ada) complex. *Genes Dev* *11*, 1640-1650.

Grewal, S.I., and Moazed, D. (2003). Heterochromatin and epigenetic control of gene expression. *Science* *301*, 798-802.

Gschwind, A., Fischer, O.M., and Ullrich, A. (2004). The discovery of receptor tyrosine kinases: targets for cancer therapy. *Nat Rev Cancer* 4, 361-370.

Gurley, L.R., D'Anna, J.A., Barham, S.S., Deaven, L.L., and Tobey, R.A. (1978). Histone phosphorylation and chromatin structure during mitosis in Chinese hamster cells. *Eur J Biochem* 84, 1-15.

Hager, G.L., Elbi, C., Johnson, T.A., Voss, T., Nagaich, A.K., Schiltz, R.L., Qiu, Y., and John, S. (2006). Chromatin dynamics and the evolution of alternate promoter states. *Chromosome Res* 14, 107-116.

Hamiche, A., Sandaltzopoulos, R., Gdula, D.A., and Wu, C. (1999). ATP-dependent histone octamer sliding mediated by the chromatin remodeling complex NURF. *Cell* 97, 833-842.

Hansen, J.C. (2002). Conformational dynamics of the chromatin fiber in solution: determinants, mechanisms, and functions. *Annu Rev Biophys Biomol Struct* 31, 361-392.

Hansen, K.H., Bracken, A.P., Pasini, D., Dietrich, N., Gehani, S.S., Monrad, A., Rappsilber, J., Lerdrup, M., and Helin, K. (2008). A model for transmission of the H3K27me3 epigenetic mark. *Nat Cell Biol* 10, 1291-1300.

Hassan, A.H., Neely, K.E., Vignali, M., Reese, J.C., and Workman, J.L. (2001a). Promoter targeting of chromatin-modifying complexes. *Front Biosci* 6, D1054-1064.

Hassan, A.H., Neely, K.E., and Workman, J.L. (2001b). Histone acetyltransferase complexes stabilize swi/snf binding to promoter nucleosomes. *Cell* 104, 817-827.

Hayes, J.J., Clark, D.J., and Wolffe, A.P. (1991). Histone contributions to the structure of DNA in the nucleosome. *Proc Natl Acad Sci U S A* 88, 6829-6833.

Henzel, M.J., Wei, Y., Mancini, M.A., Van Hooser, A., Ranalli, T., Brinkley, B.R., Bazett-Jones, D.P., and Allis, C.D. (1997). Mitosis-specific phosphorylation of histone H3 initiates primarily within pericentromeric heterochromatin during G2 and spreads in an ordered fashion coincident with mitotic chromosome condensation. *Chromosoma* 106, 348-360.

Henry, K.W., Wyce, A., Lo, W.S., Duggan, L.J., Emre, N.C., Kao, C.F., Pillus, L., Shilatifard, A., Osley, M.A., and Berger, S.L. (2003). Transcriptional activation via sequential histone H2B ubiquitylation and deubiquitylation, mediated by SAGA-associated Ubp8. *Genes Dev* 17, 2648-2663.

Herdegen, T., and Leah, J.D. (1998). Inducible and constitutive transcription factors in the mammalian nervous system: control of gene expression by Jun, Fos and Krox, and CREB/ATF proteins. *Brain Res Brain Res Rev* 28, 370-490.

Hirschhorn, J.N., Brown, S.A., Clark, C.D., and Winston, F. (1992). Evidence that SNF2/SWI2 and SNF5 activate transcription in yeast by altering chromatin structure. *Genes Dev* 6, 2288-2298.

Huang, S., Litt, M., and Felsenfeld, G. (2005). Methylation of histone H4 by arginine methyltransferase PRMT1 is essential in vivo for many subsequent histone modifications. *Genes Dev* 19, 1885-1893.

Hublitz, P., Albert, M., and Peters, A.H. (2009). Mechanisms of transcriptional repression by histone lysine methylation. *Int J Dev Biol* 53, 335-354.

Hurley, J.H., and Meyer, T. (2001). Subcellular targeting by membrane lipids. *Curr Opin Cell Biol* 13, 146-152.

Ichinose, H., Garnier, J.M., Chambon, P., and Losson, R. (1997). Ligand-dependent interaction between the estrogen receptor and the human homologues of SWI2/SNF2. *Gene* 188, 95-100.

Janknecht, R. (2003). Regulation of the ER81 transcription factor and its coactivators by mitogen- and stress-activated protein kinase 1 (MSK1). *Oncogene* 22, 746-755.

Jenuwein, T., and Allis, C.D. (2001). Translating the histone code. *Science* 293, 1074-1080.

Joo, J.H., and Jetten, A.M. (2008). NF-kappaB-dependent transcriptional activation in lung carcinoma cells by farnesol involves p65/RelA (Ser276) phosphorylation via the MEK-MSK1 signaling pathway. *J Biol Chem* 283, 16391-16399.

Kaszas, E., and Cande, W.Z. (2000). Phosphorylation of histone H3 is correlated with changes in the maintenance of sister chromatid cohesion during meiosis in maize, rather than the condensation of the chromatin. *J Cell Sci* 113 (Pt 18), 3217-3226.

Kim, H.G., Lee, K.W., Cho, Y.Y., Kang, N.J., Oh, S.M., Bode, A.M., and Dong, Z. (2008). Mitogen- and stress-activated kinase 1-mediated histone H3 phosphorylation is crucial for cell transformation. *Cancer Res* 68, 2538-2547.

Klose, R.J., and Zhang, Y. (2007). Regulation of histone methylation by demethyliminination and demethylation. *Nat Rev Mol Cell Biol* 8, 307-318.

Kouzarides, T. (2007). Chromatin modifications and their function. *Cell* 128, 693-705.

Krishna, M., and Narang, H. (2008). The complexity of mitogen-activated protein kinases (MAPKs) made simple. *Cell Mol Life Sci* 65, 3525-3544.

Kung, S.K., An, D.S., and Chen, I.S. (2000). A murine leukemia virus (MuLV) long terminal repeat derived from rhesus macaques in the context of a lentivirus vector and MuLV gag sequence results in high-level gene expression in human T lymphocytes. *J Virol* 74, 3668-3681.

Kuzmichev, A., Jenuwein, T., Tempst, P., and Reinberg, D. (2004). Different EZH2-containing complexes target methylation of histone H1 or nucleosomal histone H3. *Mol Cell* 14, 183-193.

Kwon, H., Imbalzano, A.N., Khavari, P.A., Kingston, R.E., and Green, M.R. (1994). Nucleosome disruption and enhancement of activator binding by a human SW1/SNF complex. *Nature* 370, 477-481.

Kwon, J.Y., Lee, K.W., Hur, H.J., and Lee, H.J. (2007). Peonidin inhibits phorbol-ester-induced COX-2 expression and transformation in JB6 P+ cells by blocking phosphorylation of ERK-1 and -2. *Ann N Y Acad Sci* 1095, 513-520.

Laemmli, U.K. (1970). Cleavage of structural proteins during the assembly of the head of bacteriophage T4. *Nature* 227, 680-685.

Langst, G., and Becker, P.B. (2004). Nucleosome remodeling: one mechanism, many phenomena? *Biochim Biophys Acta* 1677, 58-63.

Langst, G., Bonte, E.J., Corona, D.F., and Becker, P.B. (1999). Nucleosome movement by CHRAC and ISWI without disruption or trans-displacement of the histone octamer. *Cell* 97, 843-852.

Lee, D.Y., Teyssier, C., Strahl, B.D., and Stallcup, M.R. (2005). Role of protein methylation in regulation of transcription. *Endocr Rev* 26, 147-170.

Legius, E., Marchuk, D.A., Collins, F.S., and Glover, T.W. (1993). Somatic deletion of the neurofibromatosis type 1 gene in a neurofibrosarcoma supports a tumour suppressor gene hypothesis. *Nat Genet* 3, 122-126.

Levenson, J.M., and Sweatt, J.D. (2005). Epigenetic mechanisms in memory formation. *Nat Rev Neurosci* 6, 108-118.

Li, Z., Zhao, J., Du, Y., Park, H.R., Sun, S.Y., Bernal-Mizrachi, L., Aitken, A., Khuri, F.R., and Fu, H. (2008). Down-regulation of 14-3-3zeta suppresses anchorage-independent growth of lung cancer cells through anoikis activation. *Proc Natl Acad Sci U S A* 105, 162-167.

Liu, C.L., Kaplan, T., Kim, M., Buratowski, S., Schreiber, S.L., Friedman, N., and Rando, O.J. (2005). Single-nucleosome mapping of histone modifications in *S. cerevisiae*. *PLoS Biol* 3, e328.

Liu, G., Zhang, Y., Bode, A.M., Ma, W.Y., and Dong, Z. (2002). Phosphorylation of 4E-BP1 is mediated by the p38/MSK1 pathway in response to UVB irradiation. *J Biol Chem* 277, 8810-8816.

Looby, E., Abdel-Latif, M.M., Athie-Morales, V., Duggan, S., Long, A., and Kelleher, D. (2009). Deoxycholate induces COX-2 expression via Erk1/2-, p38-MAPK and AP-1-dependent mechanisms in esophageal cancer cells. *BMC Cancer* 9, 190.

Lorch, Y., Zhang, M., and Kornberg, R.D. (1999). Histone octamer transfer by a chromatin-remodeling complex. *Cell* 96, 389-392.

Lorch, Y., Zhang, M., and Kornberg, R.D. (2001). RSC unravels the nucleosome. *Mol Cell* 7, 89-95.

Luger, K., Mader, A.W., Richmond, R.K., Sargent, D.F., and Richmond, T.J. (1997). Crystal structure of the nucleosome core particle at 2.8 Å resolution. *Nature* 389, 251-260.

Lusser, A., and Kadonaga, J.T. (2003). Chromatin remodeling by ATP-dependent molecular machines. *Bioessays* 25, 1192-1200.

Macdonald, N., Welburn, J.P., Noble, M.E., Nguyen, A., Yaffe, M.B., Clynes, D., Moggs, J.G., Orphanides, G., Thomson, S., Edmunds, J.W., *et al.* (2005). Molecular basis for the recognition of phosphorylated and phosphoacetylated histone h3 by 14-3-3. *Mol Cell* 20, 199-211.

Mahadevan, L.C., Willis, A.C., and Barratt, M.J. (1991). Rapid histone H3 phosphorylation in response to growth factors, phorbol esters, okadaic acid, and protein synthesis inhibitors. *Cell* 65, 775-783.

Malumbres, M., and Barbacid, M. (2003). RAS oncogenes: the first 30 years. *Nat Rev Cancer* 3, 459-465.

Mantamadiotis, T., Lemberger, T., Bleckmann, S.C., Kern, H., Kretz, O., Martin Villalba, A., Tronche, F., Kellendonk, C., Gau, D., Kapfhammer, J., *et al.* (2002). Disruption of CREB function in brain leads to neurodegeneration. *Nat Genet* 31, 47-54.

Marcu, M.G., Jung, Y.J., Lee, S., Chung, E.J., Lee, M.J., Trepel, J., and Neckers, L. (2006). Curcumin is an inhibitor of p300 histone acetyltransferase. *Med Chem* 2, 169-174.

Margueron, R., Trojer, P., and Reinberg, D. (2005). The key to development: interpreting the histone code? *Curr Opin Genet Dev* 15, 163-176.

Mariani, O., Brennetot, C., Coindre, J.M., Gruel, N., Ganem, C., Delattre, O., Stern, M.H., and Aurias, A. (2007). JUN oncogene amplification and overexpression block adipocytic differentiation in highly aggressive sarcomas. *Cancer Cell* *11*, 361-374.

Mayr, B., and Montminy, M. (2001). Transcriptional regulation by the phosphorylation-dependent factor CREB. *Nat Rev Mol Cell Biol* *2*, 599-609.

McCoy, C.E., Macdonald, A., Morrice, N.A., Campbell, D.G., Deak, M., Toth, R., McIlrath, J., and Arthur, J.S. (2007). Identification of novel phosphorylation sites in MSK1 by precursor ion scanning MS. *Biochem J* *402*, 491-501.

Mellor, J. (2005). The dynamics of chromatin remodeling at promoters. *Mol Cell* *19*, 147-157.

Mendelsohn, J., and Baselga, J. (2000). The EGF receptor family as targets for cancer therapy. *Oncogene* *19*, 6550-6565.

Mitin, N., Rossman, K.L., and Der, C.J. (2005). Signaling interplay in Ras superfamily function. *Curr Biol* *15*, R563-574.

Mor, A., and Philips, M.R. (2006). Compartmentalized Ras/MAPK signaling. *Annu Rev Immunol* *24*, 771-800.

Morales, V., and Richard-Foy, H. (2000). Role of histone N-terminal tails and their acetylation in nucleosome dynamics. *Mol Cell Biol* *20*, 7230-7237.

Muller, J., Hart, C.M., Francis, N.J., Vargas, M.L., Sengupta, A., Wild, B., Miller, E.L., O'Connor, M.B., Kingston, R.E., and Simon, J.A. (2002). Histone methyltransferase activity of a Drosophila Polycomb group repressor complex. *Cell* *111*, 197-208.

Murnion, M.E., Adams, R.R., Callister, D.M., Allis, C.D., Earnshaw, W.C., and Swedlow, J.R. (2001). Chromatin-associated protein phosphatase 1 regulates aurora-B and histone H3 phosphorylation. *J Biol Chem* *276*, 26656-26665.

Murphy, C.G., and Modi, S. (2009). HER2 breast cancer therapies: a review. *Biologics* *3*, 289-301.

Nelson, C.J., Santos-Rosa, H., and Kouzarides, T. (2006). Proline isomerization of histone H3 regulates lysine methylation and gene expression. *Cell* *126*, 905-916.

Nowak, S.J., and Corces, V.G. (2000). Phosphorylation of histone H3 correlates with transcriptionally active loci. *Genes Dev* *14*, 3003-3013.

Nowak, S.J., and Corces, V.G. (2004). Phosphorylation of histone H3: a balancing act between chromosome condensation and transcriptional activation. *Trends Genet* 20, 214-220.

Nowak, S.J., Pai, C.Y., and Corces, V.G. (2003). Protein phosphatase 2A activity affects histone H3 phosphorylation and transcription in *Drosophila melanogaster*. *Mol Cell Biol* 23, 6129-6138.

Palacios, R., Gazave, E., Goni, J., Piedrafita, G., Fernando, O., Navarro, A., and Villoslada, P. (2009). Allele-specific gene expression is widespread across the genome and biological processes. *PLoS One* 4, e4150.

Pandit, B., Sarkozy, A., Pennacchio, L.A., Carta, C., Oishi, K., Martinelli, S., Pogna, E.A., Schackwitz, W., Ustaszewska, A., Landstrom, A., *et al.* (2007). Gain-of-function RAF1 mutations cause Noonan and LEOPARD syndromes with hypertrophic cardiomyopathy. *Nat Genet* 39, 1007-1012.

Panigrahi, A.K., Tomar, R.S., and Chaturvedi, M.M. (2003). Mechanism of nucleosome disruption and octamer transfer by the chicken SWI/SNF-like complex. *Biochem Biophys Res Commun* 306, 72-78.

Pearson, G., Robinson, F., Beers Gibson, T., Xu, B.E., Karandikar, M., Berman, K., and Cobb, M.H. (2001). Mitogen-activated protein (MAP) kinase pathways: regulation and physiological functions. *Endocr Rev* 22, 153-183.

Perez-Cadahia, B., Drohic, B., and Davie, J.R. (2009). H3 phosphorylation: dual role in mitosis and interphase. *Biochem Cell Biol* 87, 695-709.

Peterson, C.L. (2001). Chromatin: mysteries solved? *Biochem Cell Biol* 79, 219-225.

Peterson, C.L., Dingwall, A., and Scott, M.P. (1994). Five SWI/SNF gene products are components of a large multisubunit complex required for transcriptional enhancement. *Proc Natl Acad Sci U S A* 91, 2905-2908.

Peterson, C.L., and Logie, C. (2000). Recruitment of chromatin remodeling machines. *J Cell Biochem* 78, 179-185.

Phelan, M.L., Sif, S., Narlikar, G.J., and Kingston, R.E. (1999). Reconstitution of a core chromatin remodeling complex from SWI/SNF subunits. *Mol Cell* 3, 247-253.

Pittenger, C., Huang, Y.Y., Paletzki, R.F., Bourtchouladze, R., Scanlin, H., Vronskaya, S., and Kandel, E.R. (2002). Reversible inhibition of CREB/ATF transcription factors in region CA1 of the dorsal hippocampus disrupts hippocampus-dependent spatial memory. *Neuron* 34, 447-462.

Prigent, C., and Dimitrov, S. (2003). Phosphorylation of serine 10 in histone H3, what for? *J Cell Sci* 116, 3677-3685.

Racki, L.R., and Narlikar, G.J. (2008). ATP-dependent chromatin remodeling enzymes: two heads are not better, just different. *Curr Opin Genet Dev* 18, 137-144.

Rajalingam, K., Schreck, R., Rapp, U.R., and Albert, S. (2007). Ras oncogenes and their downstream targets. *Biochim Biophys Acta* 1773, 1177-1195.

Raman, M., Chen, W., and Cobb, M.H. (2007). Differential regulation and properties of MAPKs. *Oncogene* 26, 3100-3112.

Rando, O.J., and Chang, H.Y. (2009). Genome-wide views of chromatin structure. *Annu Rev Biochem* 78, 245-271.

Rhodes, D. (1997). Chromatin structure. The nucleosome core all wrapped up. *Nature* 389, 231, 233.

Richmond, T.J., and Davey, C.A. (2003). The structure of DNA in the nucleosome core. *Nature* 423, 145-150.

Rieger, P.T. (2004). The biology of cancer genetics. *Semin Oncol Nurs* 20, 145-154.

Rogakou, E.P., Pilch, D.R., Orr, A.H., Ivanova, V.S., and Bonner, W.M. (1998). DNA double-stranded breaks induce histone H2AX phosphorylation on serine 139. *J Biol Chem* 273, 5858-5868.

Roux, P.P., and Blenis, J. (2004). ERK and p38 MAPK-activated protein kinases: a family of protein kinases with diverse biological functions. *Microbiol Mol Biol Rev* 68, 320-344.

Roze, E., Betuing, S., Deyts, C., Marcon, E., Brami-Cherrier, K., Pages, C., Humbert, S., Merienne, K., and Caboche, J. (2008). Mitogen- and stress-activated protein kinase-1 deficiency is involved in expanded-huntingtin-induced transcriptional dysregulation and striatal death. *FASEB J* 22, 1083-1093.

Ruthenburg, A.J., Allis, C.D., and Wysocka, J. (2007). Methylation of lysine 4 on histone H3: intricacy of writing and reading a single epigenetic mark. *Mol Cell* 25, 15-30.

Salvador, L.M., Park, Y., Cottom, J., Maizels, E.T., Jones, J.C., Schillace, R.V., Carr, D.W., Cheung, P., Allis, C.D., Jameson, J.L., and Hunzicker-Dunn, M. (2001). Follicle-stimulating hormone stimulates protein kinase A-mediated histone H3 phosphorylation and acetylation leading to select gene activation in ovarian granulosa cells. *J Biol Chem* 276, 40146-40155.

Schnitzler, G.R., Sif, S., and Kingston, R.E. (1998). A model for chromatin remodeling by the SWI/SNF family. *Cold Spring Harb Symp Quant Biol* 63, 535-543.

Serre, D., Gurd, S., Ge, B., Sladek, R., Sinnett, D., Harmsen, E., Bibikova, M., Chudin, E., Barker, D.L., Dickinson, T., *et al.* (2008). Differential allelic expression in the human genome: a robust approach to identify genetic and epigenetic cis-acting mechanisms regulating gene expression. *PLoS Genet* 4, e1000006.

Shankaranarayana, G.D., Motamedi, M.R., Moazed, D., and Grewal, S.I. (2003). Sir2 regulates histone H3 lysine 9 methylation and heterochromatin assembly in fission yeast. *Curr Biol* 13, 1240-1246.

Shechter, D., Dormann, H.L., Allis, C.D., and Hake, S.B. (2007). Extraction, purification and analysis of histones. *Nat Protoc* 2, 1445-1457.

Shen, Q., Uray, I.P., Li, Y., Krisko, T.I., Strecker, T.E., Kim, H.T., and Brown, P.H. (2008). The AP-1 transcription factor regulates breast cancer cell growth via cyclins and E2F factors. *Oncogene* 27, 366-377.

Shilatifard, A. (2006). Chromatin modifications by methylation and ubiquitination: implications in the regulation of gene expression. *Annu Rev Biochem* 75, 243-269.

Shoemaker, C.B., and Chalkley, R. (1978). An H3 histone-specific kinase isolated from bovine thymus chromatin. *J Biol Chem* 253, 5802-5807.

Simone, C. (2006). SWI/SNF: the crossroads where extracellular signaling pathways meet chromatin. *J Cell Physiol* 207, 309-314.

Sims, R.J., 3rd, and Reinberg, D. (2006). Histone H3 Lys 4 methylation: caught in a bind? *Genes Dev* 20, 2779-2786.

Sindreu, C.B., Scheiner, Z.S., and Storm, D.R. (2007). Ca²⁺-stimulated adenylyl cyclases regulate ERK-dependent activation of MSK1 during fear conditioning. *Neuron* 53, 79-89.

Sng, J.C., Taniura, H., and Yoneda, Y. (2004). A tale of early response genes. *Biol Pharm Bull* 27, 606-612.

Soloaga, A., Thomson, S., Wiggin, G.R., Rampersaud, N., Dyson, M.H., Hazzalin, C.A., Mahadevan, L.C., and Arthur, J.S. (2003). MSK2 and MSK1 mediate the mitogen- and stress-induced phosphorylation of histone H3 and HMG-14. *EMBO J* 22, 2788-2797.

Sterner, D.E., and Berger, S.L. (2000). Acetylation of histones and transcription-related factors. *Microbiol Mol Biol Rev* 64, 435-459.

Steward, M.M., Lee, J.S., O'Donovan, A., Wyatt, M., Bernstein, B.E., and Shilatifard, A. (2006). Molecular regulation of H3K4 trimethylation by ASH2L, a shared subunit of MLL complexes. *Nat Struct Mol Biol* 13, 852-854.

Strahl, B.D., and Allis, C.D. (2000). The language of covalent histone modifications. *Nature* 403, 41-45.

Strelkov, I.S., and Davie, J.R. (2002). Ser-10 phosphorylation of histone H3 and immediate early gene expression in oncogene-transformed mouse fibroblasts. *Cancer Res* 62, 75-78.

Suganuma, T., and Workman, J.L. (2008). Crosstalk among Histone Modifications. *Cell* 135, 604-607.

Sun, J.M., Chen, H.Y., and Davie, J.R. (2001). Effect of estradiol on histone acetylation dynamics in human breast cancer cells. *J Biol Chem* 276, 49435-49442.

Sun, J.M., Chen, H.Y., Espino, P.S., and Davie, J.R. (2007). Phosphorylated serine 28 of histone H3 is associated with destabilized nucleosomes in transcribed chromatin. *Nucleic Acids Res* 35, 6640-6647.

Sweatt, J.D. (2004). Mitogen-activated protein kinases in synaptic plasticity and memory. *Curr Opin Neurobiol* 14, 311-317.

Thomson, S., Clayton, A.L., Hazzalin, C.A., Rose, S., Barratt, M.J., and Mahadevan, L.C. (1999). The nucleosomal response associated with immediate-early gene induction is mediated via alternative MAP kinase cascades: MSK1 as a potential histone H3/HMG-14 kinase. *EMBO J* 18, 4779-4793.

Tie, F., Banerjee, R., Stratton, C.A., Prasad-Sinha, J., Stepanik, V., Zlobin, A., Diaz, M.O., Scacheri, P.C., and Harte, P.J. (2009). CBP-mediated acetylation of histone H3 lysine 27 antagonizes *Drosophila* Polycomb silencing. *Development* 136, 3131-3141.

Toth, K., Brun, N., and Langowski, J. (2006). Chromatin compaction at the mononucleosome level. *Biochemistry* 45, 1591-1598.

Trojer, P., and Reinberg, D. (2007). Facultative heterochromatin: is there a distinctive molecular signature? *Mol Cell* 28, 1-13.

Turjanski, A.G., Vaque, J.P., and Gutkind, J.S. (2007). MAP kinases and the control of nuclear events. *Oncogene* 26, 3240-3253.

Utley, R.T., Cote, J., Owen-Hughes, T., and Workman, J.L. (1997). SWI/SNF stimulates the formation of disparate activator-nucleosome complexes but is partially redundant with cooperative binding. *J Biol Chem* 272, 12642-12649.

Van Hooser, A., Goodrich, D.W., Allis, C.D., Brinkley, B.R., and Mancini, M.A. (1998). Histone H3 phosphorylation is required for the initiation, but not maintenance, of mammalian chromosome condensation. *J Cell Sci* *111* (Pt 23), 3497-3506.

Vaquero, A., Sternglanz, R., and Reinberg, D. (2007). NAD⁺-dependent deacetylation of H4 lysine 16 by class III HDACs. *Oncogene* *26*, 5505-5520.

Verde, P., Casalino, L., Talotta, F., Yaniv, M., and Weitzman, J.B. (2007). Deciphering AP-1 function in tumorigenesis: fra-ternizing on target promoters. *Cell Cycle* *6*, 2633-2639.

Vermeulen, L., De Wilde, G., Van Damme, P., Vanden Berghe, W., and Haegeman, G. (2003). Transcriptional activation of the NF-kappaB p65 subunit by mitogen- and stress-activated protein kinase-1 (MSK1). *EMBO J* *22*, 1313-1324.

Verona, R.I., Thorvaldsen, J.L., Reese, K.J., and Bartolomei, M.S. (2008). The transcriptional status but not the imprinting control region determines allele-specific histone modifications at the imprinted H19 locus. *Mol Cell Biol* *28*, 71-82.

Vicent, G.P., Ballare, C., Nacht, A.S., Clausell, J., Subtil-Rodriguez, A., Quiles, I., Jordan, A., and Beato, M. (2008). Convergence on chromatin of non-genomic and genomic pathways of hormone signaling. *J Steroid Biochem Mol Biol* *109*, 344-349.

Vicent, G.P., Ballare, C., Zaurin, R., Saragueta, P., and Beato, M. (2006). Chromatin remodeling and control of cell proliferation by progestins via cross talk of progesterone receptor with the estrogen receptors and kinase signaling pathways. *Ann N Y Acad Sci* *1089*, 59-72.

Vicent, G.P., Nacht, A.S., Smith, C.L., Peterson, C.L., Dimitrov, S., and Beato, M. (2004). DNA instructed displacement of histones H2A and H2B at an inducible promoter. *Mol Cell* *16*, 439-452.

Vignali, M., Hassan, A.H., Neely, K.E., and Workman, J.L. (2000). ATP-dependent chromatin-remodeling complexes. *Mol Cell Biol* *20*, 1899-1910.

Walter, W., Clynes, D., Tang, Y., Marmorstein, R., Mellor, J., and Berger, S.L. (2008). 14-3-3 interaction with histone H3 involves a dual modification pattern of phosphoacetylation. *Mol Cell Biol* *28*, 2840-2849.

Wang, H., An, W., Cao, R., Xia, L., Erdjument-Bromage, H., Chatton, B., Tempst, P., Roeder, R.G., and Zhang, Y. (2003). mAM facilitates conversion by ESET of dimethyl to trimethyl lysine 9 of histone H3 to cause transcriptional repression. *Mol Cell* *12*, 475-487.

Watanabe, H., Soejima, K., Yasuda, H., Kawada, I., Nakachi, I., Yoda, S., Naoki, K., and Ishizaka, A. (2008). Deregulation of histone lysine methyltransferases contributes to oncogenic transformation of human bronchoepithelial cells. *Cancer Cell Int* 8, 15.

Wei, Y., Yu, L., Bowen, J., Gorovsky, M.A., and Allis, C.D. (1999). Phosphorylation of histone H3 is required for proper chromosome condensation and segregation. *Cell* 97, 99-109.

Whitehouse, I., Flaus, A., Cairns, B.R., White, M.F., Workman, J.L., and Owen-Hughes, T. (1999). Nucleosome mobilization catalysed by the yeast SWI/SNF complex. *Nature* 400, 784-787.

Wierenga, A.T., Vogelzang, I., Eggen, B.J., and Vellenga, E. (2003). Erythropoietin-induced serine 727 phosphorylation of STAT3 in erythroid cells is mediated by a MEK-, ERK-, and MSK1-dependent pathway. *Exp Hematol* 31, 398-405.

Wiggin, G.R., Soloaga, A., Foster, J.M., Murray-Tait, V., Cohen, P., and Arthur, J.S. (2002). MSK1 and MSK2 are required for the mitogen- and stress-induced phosphorylation of CREB and ATF1 in fibroblasts. *Mol Cell Biol* 22, 2871-2881.

Winston, F., and Allis, C.D. (1999). The bromodomain: a chromatin-targeting module? *Nat Struct Biol* 6, 601-604.

Winston, F., and Carlson, M. (1992). Yeast SNF/SWI transcriptional activators and the SPT/SIN chromatin connection. *Trends Genet* 8, 387-391.

Winter, S., Simboeck, E., Fischle, W., Zupkovitz, G., Dohnal, I., Mechtler, K., Ammerer, G., and Seiser, C. (2008). 14-3-3 proteins recognize a histone code at histone H3 and are required for transcriptional activation. *EMBO J* 27, 88-99.

Xie, S.Q., Martin, S., Guillot, P.V., Bentley, D.L., and Pombo, A. (2006). Splicing speckles are not reservoirs of RNA polymerase II, but contain an inactive form, phosphorylated on serine2 residues of the C-terminal domain. *Mol Biol Cell* 17, 1723-1733.

Yang, H., and Chen, C. (2008). Cyclooxygenase-2 in synaptic signaling. *Curr Pharm Des* 14, 1443-1451.

Young, M.R., and Colburn, N.H. (2006). Fra-1 a target for cancer prevention or intervention. *Gene* 379, 1-11.

Zenz, R., Eferl, R., Scheinecker, C., Redlich, K., Smolen, J., Schonhaler, H.B., Kenner, L., Tschachler, E., and Wagner, E.F. (2008). Activator protein 1 (Fos/Jun) functions in inflammatory bone and skin disease. *Arthritis Res Ther* 10, 201.

Zhang, H.M., Li, L., Papadopoulou, N., Hodgson, G., Evans, E., Galbraith, M., Dear, M., Vouquier, S., Saxton, J., and Shaw, P.E. (2008). Mitogen-induced recruitment of ERK and MSK to SRE promoter complexes by ternary complex factor Elk-1. *Nucleic Acids Res* 36, 2594-2607.

Zhang, Y., Liu, G., and Dong, Z. (2001). MSK1 and JNKs mediate phosphorylation of STAT3 in UVA-irradiated mouse epidermal JB6 cells. *J Biol Chem* 276, 42534-42542.

Zhong, S., Jansen, C., She, Q.B., Goto, H., Inagaki, M., Bode, A.M., Ma, W.Y., and Dong, Z. (2001). Ultraviolet B-induced phosphorylation of histone H3 at serine 28 is mediated by MSK1. *J Biol Chem* 276, 33213-33219.

Zippo, A., De Robertis, A., Serafini, R., and Oliviero, S. (2007). PIM1-dependent phosphorylation of histone H3 at serine 10 is required for MYC-dependent transcriptional activation and oncogenic transformation. *Nat Cell Biol* 9, 932-944.